Villanova University

The Graduate School

Department of Civil and Environmental Engineering

AN INFILTRATION MODEL OF AN UNDERGROUND ROCK STORAGE BED INFILTRATION BMP

A Thesis in

Civil Engineering

By

Megan C. Vanacore

Submitted in partial fulfillment

of the requirements

for the degree of

Master of Science

January 2007

AN INFILTRATION MODEL OF AN UNDERGROUND ROCK STORAGE BED INFILTRATION BMP

By

Megan C. Vanacore

January 2007

Robert G. Traver, Ph.D., P.E. Associate Professor of Civil and Environmental Engineering	Date
Andrea Welker, Ph.D., P.E. Associate Professor of Civil and Environmental Engineering	Date
Ronald A. Chadderton, Ph.D., P.E. Chairman, Department of Civil and Environmental Engineering	Date
Gary A. Gabriele, Ph.D., P.E. Dean, College of Engineering	Date

Acknowledgements

First of all, I would like to thank Dr. Robert Traver for this wonderful opportunity, I am so thankful to have had this experience. Thank you for all of your leadership and instruction over the last two years. To Dr. Ronald Chadderton, thank you for your wisdom and guidance in this process. To Dr. Andrea Welker, thank you so much for all of your help making sense of all of these equations. Thank you to Linda DeAngelis for all the help that she gives us day to day and organizing all of the wonderful workshops and seminars we've had. You always keep everything running smoothly. Bill Heasom, thank you for your help with the Green and Ampt spreadsheet, I'd still be sitting in the office trying to figure this stuff out. Dr. Michael Horst and Clay Emerson, thank you for your help with my research and all of the help that you give us all out in the field. To Erica Dean, Gregg Woodruff, and Tom Batroney, thank you for all of your help and for making the last two years so much fun. I'll miss those early mornings in the rain. To Erika Tokarz and Andrea Braga, thanks so much for all the great times, it wouldn't have been the same without you. To my parents, thank you for all of your love and support in everything. I am so lucky to have you behind me every step of the way. Thank you to all of my family for always believing in me and never forgetting to ask how my paper was going. Last, but certainly not least, thank you to my wonderful husband Jon. You are definitely the best thing to come out of my time at Villanova and I never could have finished this without your help. I look forward to a lifetime of adventures with you.

Abstract

Stormwater management has increasingly come to the forefront of issues facing development today. While stormwater management used to mean capturing and conveying runoff from the site as soon as possible, we now know the effects that this practice has on the watershed. The previous focus of peak flow rate on a site by site basis has neglected the effects of development on groundwater recharge, stream flows and the health of the watershed as a whole. It is now recognized that controlling the volume of runoff is equally important to maintain the pre-development hydrology of the site.

To reduce the increased volume of runoff, which is produced as a result of increased impervious area, infiltration best management practices (BMPs) can be used to infiltrate runoff back into the ground. One such BMP is an underground infiltration bed, which temporarily stores runoff that slowly percolates it into the underlying soil. While these BMPs can be extremely useful, especially in areas where there is no room for traditional detention basins, modeling the system to predict the anticipated infiltration can be difficult.

A common method used to calculate infiltration is the Green and Ampt Equation. This physically based approach uses hydraulic conductivity, suction and depth of the wetting front to calculate the rate of infiltration. The problem is that soil properties vary from site to site and even within a site. Infiltration rates are affected by temperature and moisture content and depth of ponded water. Much research has been done to determine the relationships between infiltration rate and these parameters. Variations of the Green and Ampt equation have also been developed to account for some of these parameters.

This paper created a model to adjust the factors in the Green and Ampt equation for both temperature of the water and the moisture content of the soil. This allows the user to look at the underground infiltration bed's performance under a variety of field conditions. This provides a more realistic estimate of the infiltration rather than use an overly conservative model, which results in the design of a larger, more expensive facility.

This model was verified using three years of data collected from the Porous Concrete Infiltration BMP at Villanova University. The initial conditions for each modeled storm were used as input parameters for the model and the resulting graph of ponded depth versus time was compared to the recorded data. For comparison, the standard Green and Ampt model was also run. The developed model showed up to a 99.53% improvement over the standard model in predicting the infiltration from the subsurface infiltration bed. Various sensitivity analyses were performed as well as statistical analyses of the results.

Table of Contents

List of Figures

List of Tables

Chapter 1: Project Overview

1.1 Project Statement

The purpose of this research is to model the infiltration rate of a large underground rock storage bed to predict performance and create design guidelines for subsurface BMPs. The research is based on recorded field data collected from the porous concrete infiltration BMP located at Villanova University. A mathematical model was created using moisture meter, rain-gage, and pressure transducer monitoring data collected over a three year period. The results of the developed model were compared to the results of a standard Green and Ampt model and found to be up to 99.53% more accurate in predicting the infiltration rate from a subsurface infiltration bed.

1.2 Introduction

The effects of urbanization on our natural water systems have become a growing concern over the past few decades. Increasing development and the associated impervious surfaces and compacted soils has caused an increase in the rate and volume of stormwater runoff, pollution and a decrease in groundwater recharge. This reduction in groundwater recharge, caused by the loss of infiltration, decreases the baseflow in streams which has negative impacts on the aquatic life as well as recreational uses (Final Draft PA SWM Manual, April 2006). In addition, grading practices during construction eliminate the natural depressions in the land which capture runoff and allow water to infiltrate or evaporate, further contributing to the increased runoff volumes.

Impervious surfaces and storm sewer systems also convey water to streams at a much faster rate than natural overland flow paths. The increase in the velocity and quantity of water entering streams during storm events causes stream bank erosion which

results in sediment deposits farther downstream in the system. This also causes an increase in the frequency with which the streams flow at bank-full or overflow conditions.

Along with the increase in the quantity of runoff, there is also an associated decrease in the water quality of streams caused by stormwater entering the streams. This overabundance of stormwater has increased levels of sediments, suspended and dissolved solids, metals and nutrients and other pollutants in streams. In an undisturbed system, these pollutants are often removed by the soil during infiltration before the water enters the ground water flow. When water is no longer infiltrating but is being added directly to surface waters, these pollutants are also added, which has negative impacts on the health of these systems. Also, as runoff travels across heated impervious surfaces, the water increases in temperature, this results in the thermal pollution of streams. Thermal pollution can cause a decrease in diversity of the organisms in surface waters as well as an overall decrease in the number of organisms.

Years ago the goal of stormwater management was to collect and convey runoff offsite as soon as possible. Storm sewer systems were built underground to convey water away from developed areas and directly to local streams. In 1972 the Environmental Protection Agency (EPA) passed the Clean Water Act. The Clean Water Act did not directly address stormwater management, but regulated pollutant discharge to surface waters and set requirements to create specific standards for individual pollutants. Pennsylvania adopted Act 167, the Pennsylvania Stormwater Management Act of 1978, which made an attempt to control flooding by limiting the peak flow rates of new development to the pre-development peak flow rates.

Many developments were previously designed with detention basins to control the stormwater runoff leaving the site to meet runoff volume requirements. Detention basins are designed to collect water from storm sewers and swales and reduce the peak flow rate from the site. Detention basins manage stormwater on a site by site basis but do not take into account the overall development of the watershed.

Traver and Chadderton (1982) studied the effects that detention basins have on the watershed downstream from their outfall. They found that basins were only fully effective for the actual site for which they were built. The detention basins reduce the peak flow but change the time to peak, total runoff volume, and extend the duration of peak flows. They found that this would still cause significant increases in peak flows downstream when combined with flows from other developments within the watershed. For this reason they recommended a whole watershed stormwater management assessment to effectively control peak rates.

Emerson (2004) modeled the Valley Creek Watershed with and without the existing detention basins during small storm events (<2 year storm) and found that there was either no benefit or even a negative effect from the detention basins. Most of this negative effect is from combining the increased runoff and extended periods of increased flows from sites throughout the watershed. This illustrates the need for a new stormwater approach that looks at the entire storm hydrograph; peak rates, volumes and timing, and all aspects of they hydrologic cycle in an attempt to develop land with a minimum impact on natural stormwater flows.

Stormwater regulations are evolving to include volume control in addition to peak rate control. Since each watershed has different stormwater issues and needs,

Pennsylvania has looked to local government agencies to develop watershed specific stormwater regulations through Act 167 Stormwater Management Plans. Act 167 requires that the 353 watersheds delineated in Pennsylvania create Watershed Management Plans to address current and future stormwater issues. This means that counties and municipal governments have to work together to create a comprehensive plan rather than stormwater being regulated on a municipal level.

Many local regulations require that pre-development peak flow rates be maintained or reduced for the 2 through 100 year storms. In southeastern Pennsylvania, the 2-year storm event encompasses at least 95% of the annual runoff volume (Final Draft PA BMP Manual, April 2006). More flooding events occur as a result of these small storms after areas have been developed due to the overall increase in runoff volume. This effect is causing a change in emphasis of stormwater management from peak control to volume control. Stormwater management measures can never fully eliminate the natural flooding from extreme events but can prevent more frequent storms from causing serious damage.

To address stormwater management issues adequately, a comprehensive stormwater management policy must provide standards for peak rate control, total runoff volume, groundwater recharge, channel protection and water quality. In 2001, Pennsylvania DEP held a number of forums to develop a new stormwater management policy. As a result of these public meetings the following objectives were identified (Final Draft PA BMP Manual, April 2006):

- To address critical water quality issues;
- To sustain stream base flow and groundwater in general through stormwater management systems which infiltrate and provide for groundwater recharge;
- To minimize site-specific and watershed-wide flooding problems; and
- To prevent serious stream bank erosion and overall stream impact with related aquatic biota damage.

These objectives will be achieved through implementation of the EPA's National Pollutant Discharge Elimination System (NPDES) Phase II stormwater permitting program. This includes construction permits for land development as well as permits for Municipal Separate Storm Sewer Systems (MS4s).

All projects that will ultimately disturb one acre or more are required to obtain a NPDES Construction Permit (Post Construction Stormwater Management Plan) from PADEP. To obtain a permit it must be demonstrated that the project will: protect all impacted streams according to their use as designated by Chapter 93, Water Quality Standards, of the Pennsylvania Code; maintain the existing water quality of those streams; provide an erosion and sediment control plan outlining protection measures during construction; and identify and design all BMPs that will be utilized, including plans for their operation and maintenance.

Under the NPDES Phase II MS4 program, additional municipalities are required to obtain a permit from PADEP for their stormwater discharges. The permit requires that the municipalities implement a stormwater management program with "minimum control measures" in the following areas:

- Public Education
- Public participation and involvement
- Proper management of illicit discharges
- Proper management of construction phase stormwater
- Proper management of post-construction phase stormwater, and
- Implementation of adequate pollution prevention and housekeeping measures.

More information about Pennsylvania's Comprehensive Stormwater Policy can be obtained at the Pennsylvania Department of Environmental Protection's website: http://www.dep.state.pa.us/dep/deputate/watermgt/wc/Subjects/StormwaterManagement/GeneralInformation/default.htm. (PA BMP Manual, April 2006)

In addition to the new stormwater regulations, Pennsylvania is in the final stages of creating a BMP manual to guide engineers, developers and municipalities in properly selecting and implementing BMPs for projects. The manual describes many of the BMPs, and provides guidelines for selection and design based on site parameters and the ultimate goal of the BMP. Most of the BMPs involve some aspect of infiltration and/or evapotranspiration as the focus of stormwater management is switching from peak rate reduction to volume reduction in an effort to maintain pre-development conditions more adequately. Often, stormwater is collected either in a surface pond and allowed to infiltrate/evapotranspirate or it is captured in underground storage and slowly released into the soil.

An innovative approach to convey stormwater to an underground storage facility is to use some type of porous pavement to allow direct flow to the BMP. There are a

variety of porous media including porous asphalt, porous concrete, porous pavers, and reinforced turf. With this technique a surface that would otherwise be impervious becomes available for infiltration. Porous asphalt and porous concrete are laid on top of crushed stone with at least 40% void space which provides storage for stormwater runoff and allows it to slowly percolate into the soil. The stone layer is underlain by a layer of geotextile fabric which prevents any soil from migrating up into the void space of the stone and thereby, reducing the available storage capacity.

In 2002, Villanova University voluntarily retrofitted an existing paved area with a porous concrete infiltration BMP. Cahill Associates of West Chester, PA completed the hydrologic design for this site in 2001. Cahill conducted percolation tests in mid-September with a finalized design being completed shortly thereafter (Ladd, 2004). The site was instrumented for research and demonstration opportunities. Funding for the project was provided by the Pennsylvania DEP 319 Non Point Source Grant Program. The site is currently part of the United States EPA Non Point Source National Monitoring Program which provides water quality and quantity data from BMPs across the country (Kwiatkowski, 2004).

1.3 Site Design and Construction Overview

Villanova University is located in Southeastern Pennsylvania, approximately 20 miles west of Philadelphia. The porous concrete site was constructed on Villanova's main campus and serves as a pedestrian walkway between two dormitories as seen in Figure 1.1. The site was retrofitted from a standard concrete walkway. The low vehicular traffic makes the site an ideal application for porous concrete with less wear and tear on the surface and little risk of gasoline or oil spills.

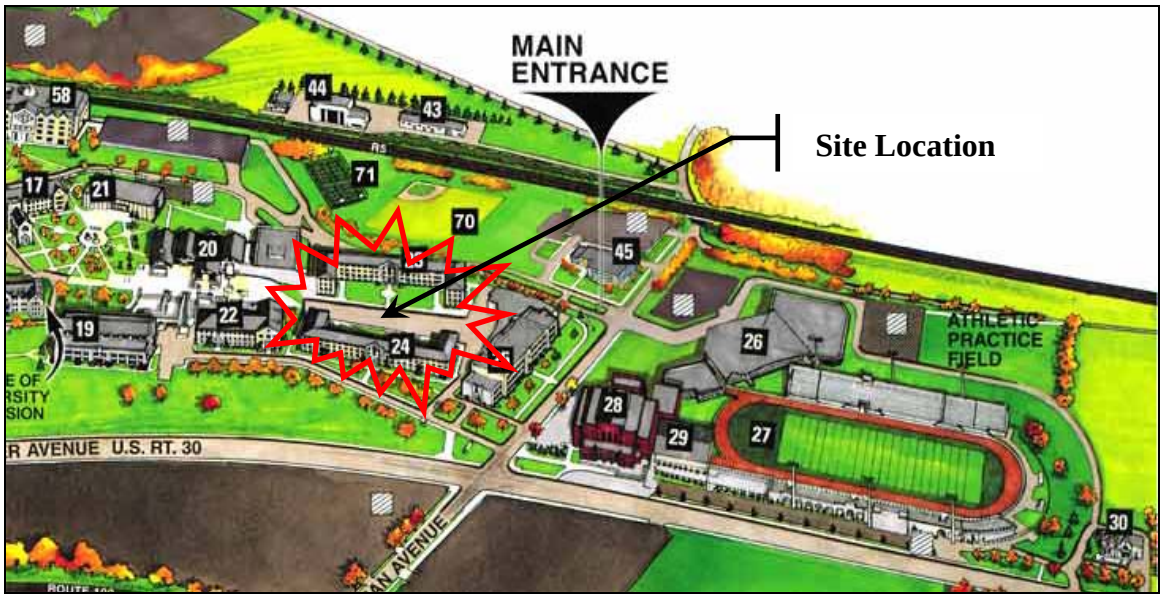

Figure 1.1 Porous Concrete Infiltration Basin BMP Location Map at Villanova University

The drainage area to the site is approximately 1.3 acres (57,700 SF) which drains to the Mill Creek Watershed. The site is approximately 62% impervious which includes some standard concrete and asphalt areas as well as portions of the dormitory rooftops whose downspouts are directly connected to the rock storage beds. There are also grass areas that runoff to the porous concrete surface during heavy rain.

The site was designed to capture and infiltrate the runoff produced by 2" of rainfall. The goal was to reduce the effects of development on the watershed by returning the hydraulics of the site to the predevelopment conditions. Overflow from the site enters the existing storm sewer system and flows downstream in the watershed.

The original design called for the entire walkway to be constructed of porous concrete. Shortly after construction, in August 2002, the surface failed and turned to gravel. The initial data collected from the site as well as field observations during this time suggested that it was not necessary to have the entire walkway surface porous concrete (Kwiatkowski, 2004).

Reconstruction took place in the spring of 2003. This time the porous concrete was used as a border around standard concrete which was crowned to drain to the porous surface. The new site layout can be seen below in Figure 1.2.

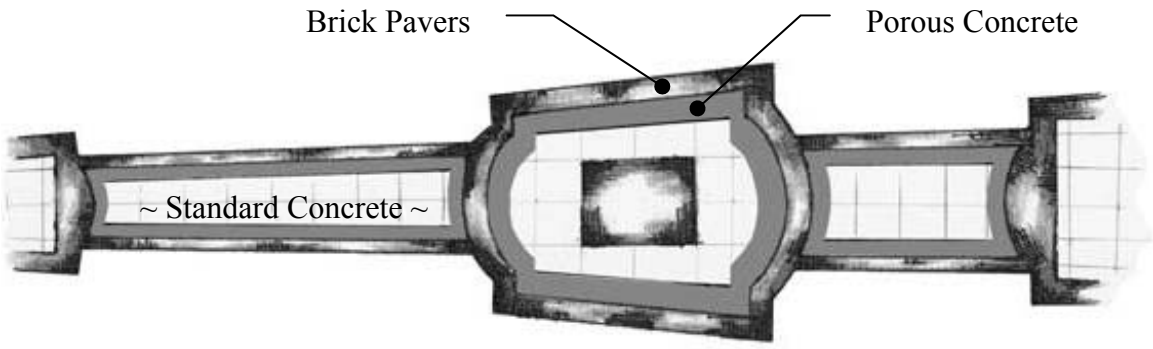

Figure 1.2 Illustration of New Surface Design (Cahill 2003)

Figure 1.3 shows the original concrete walkway before the retrofit and the new walkway after the redesign. *Lessons Learned*, an article in Stormwater Magazine (Traver et al., 2004) discusses the design and construction of the site.

Figure 1.3 Pre (left) and Post (right) Construction Photograph of the Porous Concrete Site

While the new surface performed better than the original porous concrete, some damage was noticed about a year after construction. Approximately 40% of the new surface had begun to fail. It was noticed that these sections had been pored from the end

of the batches of concrete when the material was more difficult to work. These sections were replaced in October 2004. *Lessons Learned II*, an article in Stormwater Magazine (Traver et al., 2005) describes the repairs that were made.

The surface has been maintained by using a vacuum street sweeper to remove fines and debris from the pores. Recent testing of the surface in the spring of 2006 indicated that while some areas appear to be clogged, sweeping the surface can help to restore the infiltration capacity of the porous concrete.

Under the walkway surface is a series of rock storage beds. Due to the slope of the site, three tiered infiltration beds were designed, separated by earthen berms, as illustrated in Figure 1.4.

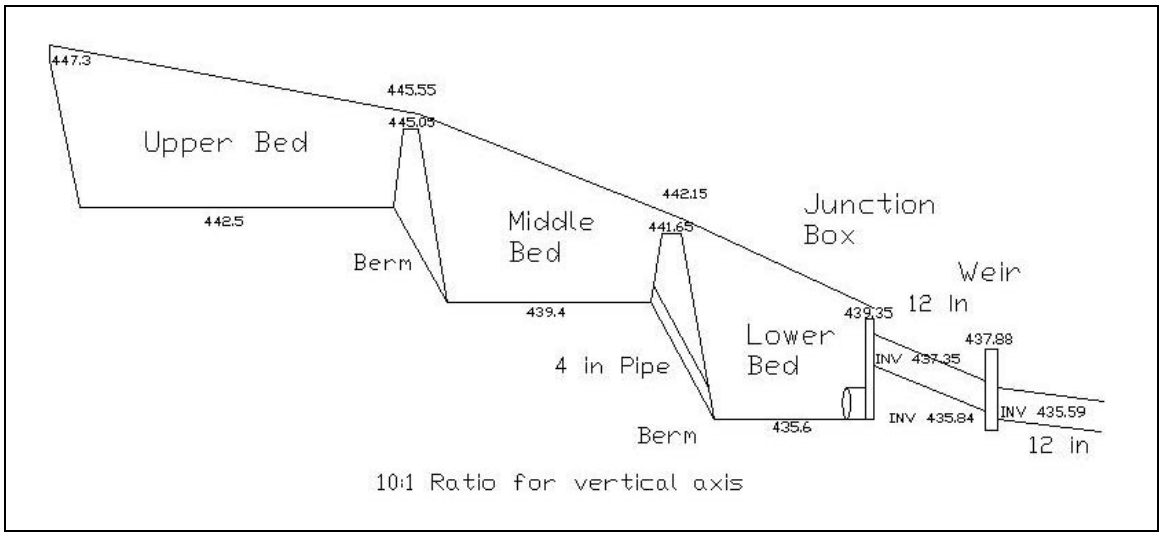

Figure 1.4 Profile of Infiltration Beds and Overflow Pipes

The drainage area to each bed was delineated accordingly, as seen in Figure 1.5 to estimate the area contributing runoff to each bed.

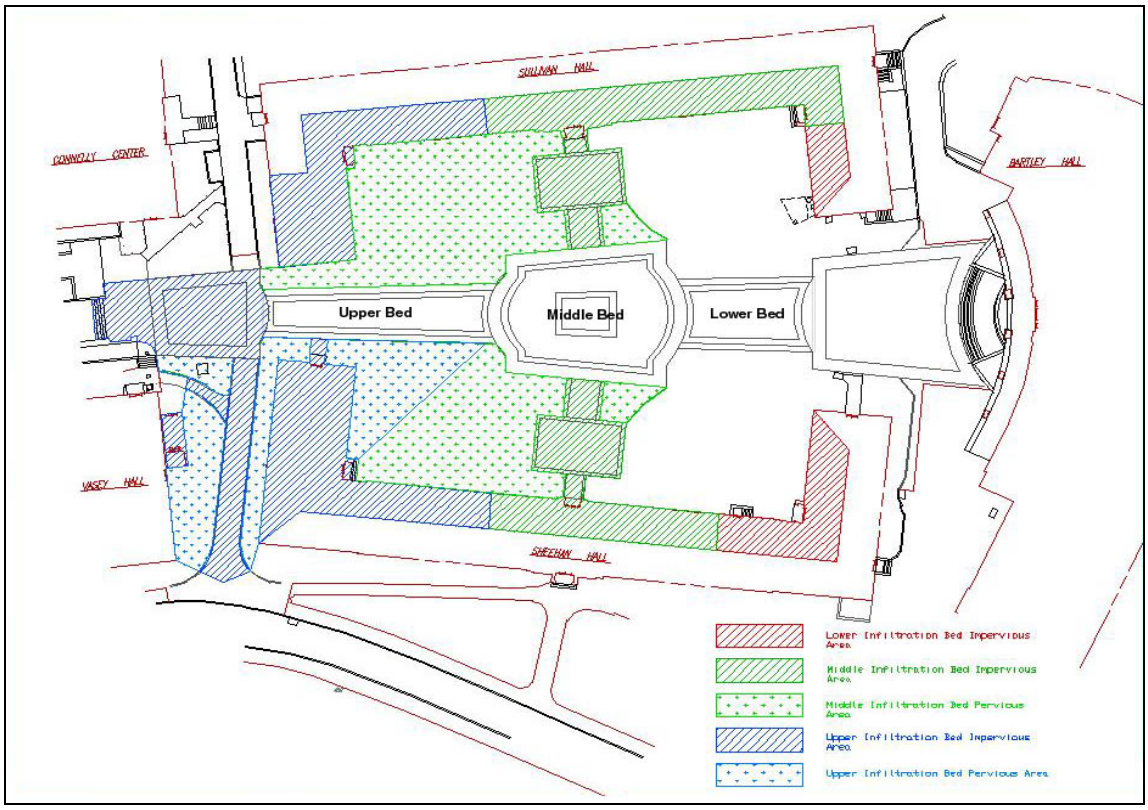

Figure 1.5. Drainage Area Schematic of the Site

The porous concrete BMP uses porous concrete to allow runoff from the site to enter the infiltration beds under the walkway. Porous concrete is similar to a standard concrete mix but without the fine material to allow for larger, interconnected pore spaces which results in a pervious surface. The infiltration capability is illustrated in Figure 1.6.

Figure 1.6 Illustration of the Ability of Porous Concrete to Convey Water

Runoff also enters the beds through a slot drain at the top of the drainage area, roof leaders which are directly connected to the beds, and an inlet which captures runoff from an asphalt driveway. The inlet was originally set above the grade of the pavement so a speed bump was installed to allow water to pond and then be diverted into the inlet. The result can be seen in Figure 1.7.

Figure 1.7 Speed Bump After Installation (left) and During a Storm (right)

The three infiltration beds are 3-4 feet deep and filled with 3-4 inch clean-washed course stone aggregate with approximately 40% void space which provides storage during storm events. The beds are wrapped in a geotextile fabric to prevent soil from migrating up into the voids. Six inch perforated HDPE pipes run along the bottom of the beds to help distribute runoff. A choker course of 2-4 inch stone was placed above the aggregate as a base for the standard and porous concrete. Figure 1.8 shows a typical cross-section of the beds and Figure 1.9 shows the beds during construction.

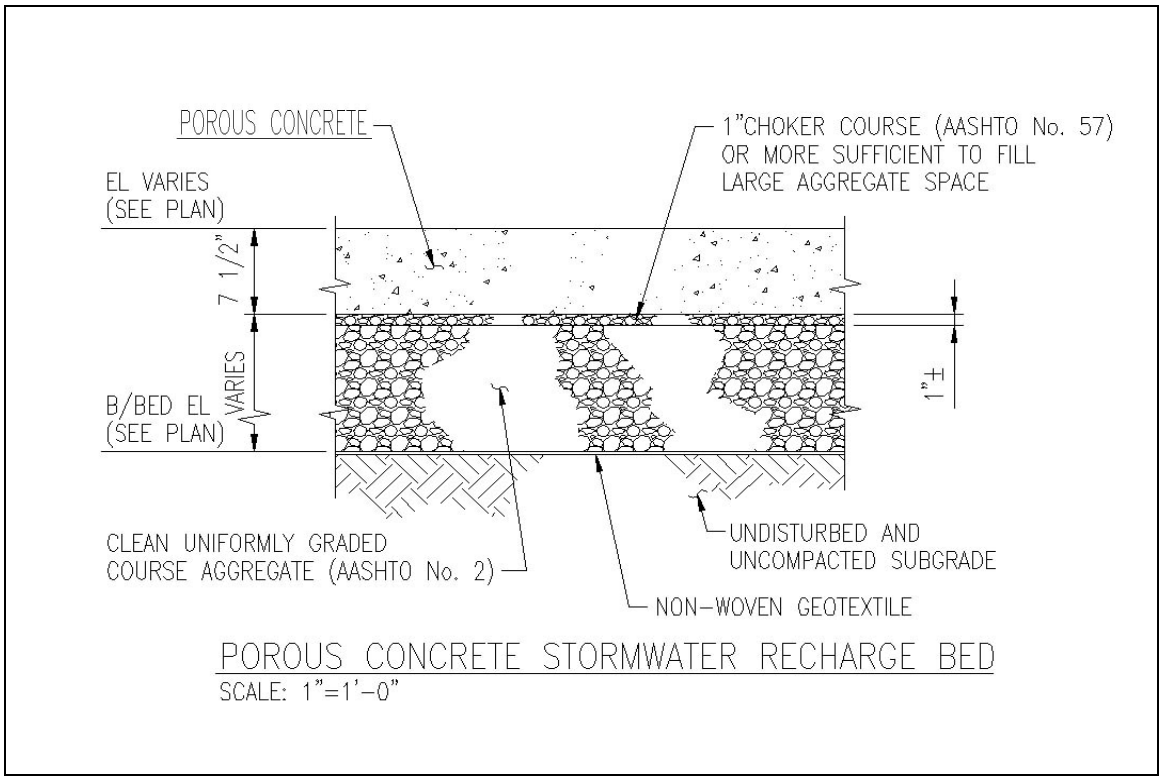

Figure 1.8 Cross Section of an Infiltration Bed (Cahill, 2003)

Figure 1.9 Middle Infiltration Bed Under Construction

The middle and lower beds were constructed with overflow pipes to prevent water from coming back up through the porous concrete. The middle bed overflows to the lower bed and the lower bed has an overflow pipe located in the junction box shown in Figure 1.10.

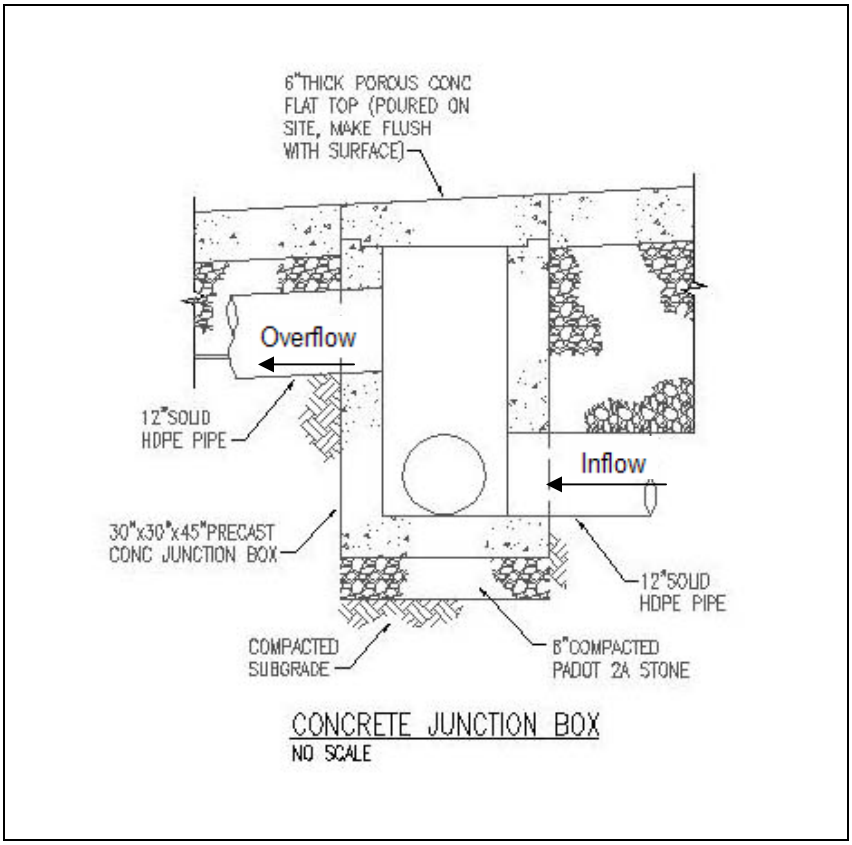

Figure 1.10 Sketch of Junction Box (Cahill, 2003)

Once the water in the lower bed reaches a depth greater than 18 inches, overflow is directed to the storm sewer through the original outlet. A weir was constructed in the inlet as seen in Figure 1.11, which is used in conjunction with a pressure transducer, which measures the height of the water behind the weir, to calculate the outflow from the site.

Figure 1.11 Weir Outlet Control Structure

This section gave overview of the design and construction of the site. Previous Masters Thesis by Kwiatkowski (2004) and Ladd (2004) provide a more detailed description of the layout and construction process of the porous concrete site. Information on this and other sites at Villanova University can be found on the Villanova Urban Stormwater Partnership's website (www.villanova.edu/vusp).

1.4 Research Objective

The primary objective of this research was to model the infiltration from the large rock beds that store runoff from the porous concrete site by developing a modified Green and Ampt equation to adjust for the temperature of the ponded water and the moisture content of the soil using recorded field data. This study considered the different storm parameters and soil conditions that affect the model's performance. The model was verified using storms with varying ponded depths, temperatures and initial moisture contents, as well as by comparing the developed model results with the results of the Green and Ampt model using typical values. Sensitivity analyses were performed to

determine the influence of temperature and moisture content on the infiltration rate. Statistical analyses were used to quantify the reliability of the results. Recommendations for designing similar underground stormwater storage and infiltration facilities were made based on the conclusions of this study. Suggestions for further research have been offered.

Chapter 2: Literature Review

2.1 Introduction

The Pennsylvania Stormwater Management Act of 1978, Act 167, made an attempt to control flooding by limiting the peak flow rates of new development to the pre-development peak flow rates. Detention basins have been widely used in developed areas to meet the peak rate requirements (Traver and Chadderton, 1983), but they have three main weaknesses. First, they are not designed to reduce runoff volumes, which along with extended peak runoff rates, can cause downstream erosion. Second, they are designed for 2 to 100 year storms which constitute only a small portion of the yearly rainfall and third, their design is based on a site-by-site basis which does not guarantee performance on a watershed scale (Emerson et al., 2005). The study by Traver and Chadderton (1983) illustrated the effect that detention basins have on the hydrograph of a watershed for a rainfall event. It was found that the peak flows could still be increased downstream even if the detention basin controlled flows at the point where they were designed. This was due to the prolonged peak flow rates, changes in the time of concentration (Tc) of the developed subareas and increased runoff volumes. They recommended that stormwater management be designed to recreate the pre-development hydrograph characteristics, including volume and Tc, and not just the peak flow rate. Suggestions to accomplish this included studying the efficiency of recharge detention facilities. One such facility is an infiltration basin such as the porous concrete site. The following sections will describe some of the current design procedures for infiltration basins as well as the factors that influence the infiltration rate.

2.2 Infiltration Basin Design

Infiltration basins are used to store stormwater temporarily, which then infiltrates into the soil through the bottom of the basin. The problem in infiltration design is to make sure that the infiltration rate can be maintained which will impact the adequacy of the storage volume. (Guo and Hughes, 2001) "Unlike detention basins, there do not exist widely accepted design standards and procedures for infiltration practices." (Akan, 2002)

Maryland Department of Natural Resources (1984) suggested that the required capture volume be calculated based on a hydrograph truncation method. In this method the necessary volume is the area under the design runoff hydrograph from the post-development conditions from time equal to zero until the time during the recession limb that the flow equals the pre-development flow.

Akan (2002) developed a procedure based on the Green and Ampt equation because of its use of physical parameters and ease of use. The procedure uses equations to calculate the maximum water depth and algebraic equations to determine the storage time which can be compared to local requirements. In this method the first step is to consider the filling process when the first amount of runoff enters the basin. Any lateral infiltration is neglected as the vertical infiltration usually controls the process. The Green and Ampt equation is used to model the infiltration rate as well as the increasing depth of the wetting front below the basin. The infiltration rate is set equal to the rate of runoff entering the basin when inflow rate is less than the infiltration capacity. The second step looks at the emptying process to determine the draining time of the basin which is also calculated by the Green and Ampt equation.

Guo and Hughes (2001) developed a method to design infiltration basins based on overflow risk. The volume is determined based on the soil water storage capacity as well as on cost and overflow risk. The Green and Ampt diffusion theory is used to model the seepage of the water through the soil under the basin. The initial and saturated soil moisture contents are used to determine the drain time from the basin as a function of the distance from the basin bottom to the ground water table. The basin volume is estimated as the drainage area multiplied by the depth of the design rainfall over the watershed. In this study the effects of ground water mounding were taken into consideration. For this reason a conservative approach was taken and the storage volume was set equal to the soil water storage capacity to determine the minimum area for the bottom of the basin and the maximum water depth in the basin. The overflow risk between storm events is also used as a design consideration. Overflow risk depends on two probabilities; "(1) that the next event will come between the time the basin was initially filled and the drain time and (2) the rainfall depth of the next event will exceed the available storage volume in the basin". (Guo, 2002)

The Pennsylvania Best Management Practices Manual (Draft, April 2006) also presents design guidelines for subsurface infiltration basins. A basin infiltration area with a ratio of 5:1 to the total impervious area and 8:1 to the total drainage area is recommended as well as a 72-hour draining period. The manual also advises that a maximum depth of water in the bed of two feet be used to avoid any compaction of the bottom of the bed. The soil's infiltration rate is also considered in the design recommendations, with a factor of safety of two suggested for infiltration rates of less

than 1.0 inch per hour. Other site selection and construction requirements are also given as part of the overall design process.

2.3 Modeling Infiltration[1]

Groundwater recharge is composed of two main functions, infiltration and percolation. Infiltration is defined as "the physical process of water entry into the soil" and involves the displacement of air into the soil matrix by water (Al-Muttair and Al-Turbak, 1991). Soil water movement or percolation is the process of water flow from one point within the soil to another. Infiltration and percolation must both be taken into consideration when modeling water flow into the soil because the rate of infiltration is controlled by the rate of percolation (Hsu et al., 2002).

The process of infiltration of water into soil and movement of that water through the soil profile have been studied and characterized using many different equations, both empirically and physically based. Richard's equation, which was derived from the Darcy equation, was one of the first equations to describe both infiltration and percolation in unsaturated soil (Hsu et al., 2002). One of the most famous and widely used infiltration models to determine infiltration capacities of subsurface soils is the Green and Ampt equation.

Due to its simplicity and satisfactory performance, the Green and Ampt method has been the topic of many studies. It has been applied to a variety of infiltration situations, including steady and unsteady rainfall and various soil conditions. (Freyburg et al., 1980) While the original Richard's equation is a more sophisticated model, the Green and Ampt equation provides a physically based model that is relatively simple to apply (Akan, 2002). "Moreover, the model is well documented, and it has been verified

[1] Portions of this section are taken from Braga (2004) Masters thesis

in the past in various studies (Akan, 2002)." Because the intent of this paper is to develop recommendations for the design of infiltration basins that can be easily applied in engineering practice, the Green and Ampt model will be discussed further and used in the analysis of the infiltration rate. Factors influencing the infiltration rate will also be examined.

2.3.1 Green and Ampt Model

The Green-Ampt formula is a physically approximate and mathematically exact solution to surface infiltration (Hsu et al., 2002). The original formula,

$$f_p = K_s \frac{(S - L)}{L} \qquad \text{Equation 2.1}$$

where f_p = infiltration rate [L/T], K_s = saturated hydraulic conductivity [L/T], S = capillary suction at the wetting front [L] and L = distance from the ground surface to the wetting front [L]; assumes that the soil surface is covered by ponded water of negligible depth and that the water is infiltrated into a homogeneous soil with uniform water content (Green and Ampt, 1911).

During the infiltration process, it is assumed that water enters the soil uniformly to create a discrete "wetting front" a distance L from the surface separating the saturated soil above from the unsaturated soil below. This value can be determined by the following equation:

$$L = \frac{F}{IMD} = \frac{F}{(\theta_s - \theta_i)} \qquad \text{Equation 2.2}$$

in which F = cumulative infiltrated water [l] and IMD = initial moisture deficit or the saturated soil moisture content less the initial soil moisture content (Viessman and Lewis, 2003). Figure 2.1 illustrates the Green-Ampt variables using a sample soil profile.

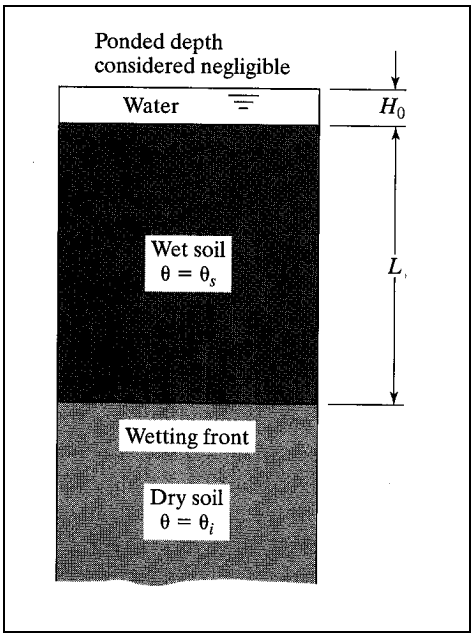

Figure 2.1 Definition Sketch for Green and Ampt Model (Viessman and Lewis, 2003)

Additionally, by combining Equations 2.1 and 2.2:

$$f_p = \frac{dF}{dt} = K_s(1 + \frac{S(\theta_s - \theta_i)}{F}) \qquad \text{Equation 2.3}$$

All variables in Equation 2.3 are measurable soil properties, which is why Green-Ampt formula is characterized as "physically approximative." Additionally, Equation 2.3 can be integrated with control bounds of F = 0 at t = 0 to obtain Equation 2.4.

$$F - S(\theta_s - \theta_i)\ln(\frac{F + S(\theta_s - \theta_i)}{S(\theta_s - \theta_i)}) = K_s t \qquad \text{Equation 2.4}$$

This form of the Green-Ampt equation is more suitable for use in watershed modeling processes than Equations 2.1 or 2.3 because it relates the cumulative infiltration, F to the time at which infiltration began. This equation assumes a ponded surface so that the actual infiltration rate is equal to the infiltration capacity at all times; therefore, the equation does not deal with the potential for rainfall intensity to be less than the infiltration rate (Viessman and Lewis, 2003).

2.3.2 Infiltration Rate with Varying Ponded Depth

Many studies have applied of the Green and Ampt equation to various situations but none have examined the model for its suitability in cases where the surface water depth changes considerably with time. The storage-suction factor in the Green and Ampt equation assumes a constant ponded depth of water which does not accurately represent the conditions in a recharge basin where the depth is decreasing (Freyberg et al., 1980)

In a study done by Al-Muttair and Al-Turbak (1991) the Green and Ampt model was used to characterize the infiltration process in an artificial recharge basin with a decreasing ponded depth, as illustrated in Figure 2.2.

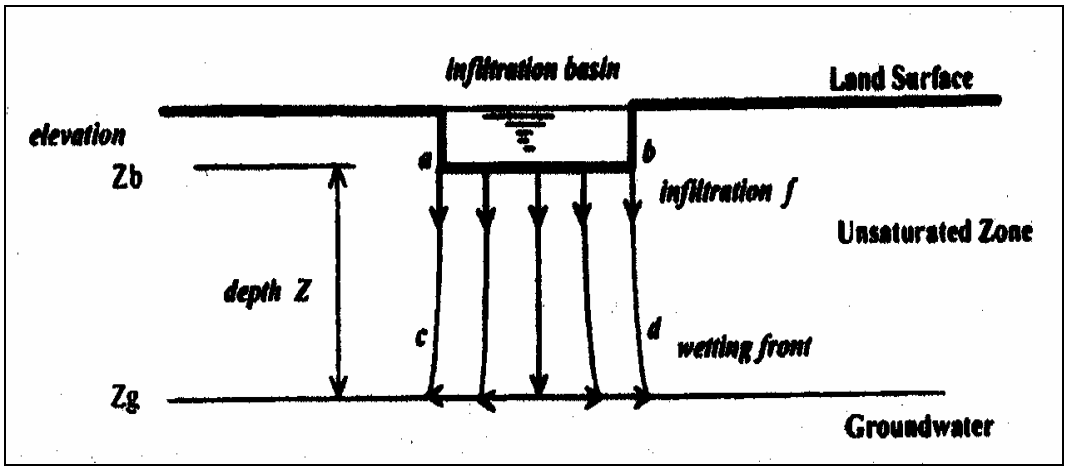

Figure 2.2. I-D Infiltration Basin Sketch for Green and Ampt Model (Guo and Hughes, 200)

Freyberg et al. (1980) investigated the performance of the Green and Ampt equation for modeling infiltration rates where the depth of ponded water varies with time. "Rapidly varying surface water depths can result in vertical infiltration rates that vary with time in a manner substantially different from the power law decay commonly observed for constant surface water depths (Freyberg et al., 1980)." Previous definitions of the effective suction head parameter in the Green and Ampt equation state that it is

dependent on soil moisture properties and the initial moisture content and independent of time and surface water depth. The study by Freyberg et al. found that the best value of effective suction head may actually vary with time, surface water depth, initial moisture content, and soil type.

2.3.3 Initial Moisture Content's Influence on Infiltration Rate

Having a good estimate of the infiltration rate of a soil is important when evaluating the rainfall-runoff process over a period of time because the volume of infiltration from one event influences the initial water content of the soil for ensuing events. Most watershed models use a single value to represent the relationship between infiltration capacity and soil water storage when modeling runoff from continuous rainfall events. The examination of this relationship under ponded conditions and uniform water content found that the relationship was not unique. This non-unique relationship can be derived from the Philip equation, the results of which depend on the initial moisture content of the soil. (Bloomfield, 1981)

The Green and Ampt equation includes a pressure head which Green and Ampt described as 'a constant of the soil depending on capillary forces acting on the moving boundary of the water' (Aggelides and Youngs, 1978). Many efforts have been made to relate this pressure head to soil water relationships. Aggelides and Youngs (1978) presented experimental data from infiltration studies on a sand column with varying initial moisture contents after both wetting and draining. The calculated Green and Ampt parameters were compared with various theoretical estimates using the data from the experimental column. The results of the study did show a dependence of the pressure head on the initial water content but found that a constant value, the 'water entry

pressure' taken to be half of the soil water pressure at air entry, gave a better estimation of the actual infiltration rate than the other theoretical estimates that were evaluated.

The 'infiltration theory' developed by Philip (1957) uses a single given parameter for the moisture content at the top of the soil which is used to determine the permeability coefficient, K. The infiltration model developed from that theory also uses a steady-state permeability coefficient. Field experiments, however, show that the steady state moisture content and the corresponding value of K that results during infiltration is a function of the initial moisture content. Experiments conducted on sand samples showed that the steady-state permeability coefficient decreased at first with an increase in the initial moisture content and then increased, indicating the existence of a critical moisture content (Gusev, 1978).

An experiment run by Hino et al. (1988) on a cylindrical lysimeter with artificial rainfall investigated the relationships among the initial soil suction, total rainfall, rainfall intensity, runoff loss, runoff ratio and the time between rainfall and runoff occurrence. They showed conclusively that "the loss of infiltrated rainfall is uniquely correlated with the initial soil-moisture content and is independent of the total amount of rainfall as well as of the rainfall intensity, if it does not exceed the infiltration rate of the soil".

The hydraulic conductivity of soil is dependent on the moisture content which means that the greater the soil moisture content, the faster the movement of the water through the soil. As the initial moisture content of the soil decreases, the velocity of the wetting front decreases due to the increased volume of water that can be held in the voids in the soil. (Hino et al., 1988)

2.3.4 Water Temperature Effects on Infiltration Rate

It has been widely recognized that the physical and chemical properties of soil are affected by the temperature. The change in the viscosity of water with temperature makes the hydraulic properties of soil particularly temperature dependent. Often, though, infiltration measurements are taken without consideration of the temperature because the effects are considered too small compared to other parameters. (Jaynes, 1990)

A study by Constantz and Murphy (1991) modified the Green and Ampt equation to adjust for the temperature sensitivity of the infiltration rate of ponded water. They used the relationship between the temperature and the viscosity of water to adjust the value of the unsaturated hydraulic conductivity as follows:

$$k_T = K_{sat}(\eta_r/\eta_{20}) \qquad \text{Equation 2.5 (Constantz and Murphy, 1991)}$$

Where: η_r = viscosity of water at the average temperature

η_{20} = viscosity of water at 20˚C

The temperature dependence of the infiltration rate was tested by measuring the rates at 5, 25 and 60 °C. The modification to the Green and Ampt equation was tested by measuring the infiltration rate at 5 °C and applying equation 2.5 to predict the infiltration at 25 and 60 °C.

It was concluded that the infiltration was "strongly dependent" on the temperature of the water. The infiltration rate for the sample soils varied as much as 300 to 400% for temperatures between 5 and 60 °C. The results of predicting infiltration using the simple viscosity adjustment were completely successful at predicting the final infiltration rate at both 25 and 60 °C. The initial infiltration rate was predicted correctly at 25 °C though it was not as successful at 60 °C where the infiltration rate was over predicted. This over-

prediction was attributed to an increase in saturation of the transmission zone with increasing temperatures.

Like the experiment by Constantz and Murphy (1991), most investigations of the relationship between temperature and infiltration have been conducted in laboratory experiments. A five year field study by the U.S. Water Conservation lab showed that the infiltration rate varied by about 30% from the average value and that the variations followed changes in temperature at the soil surface (Jaynes, 1990). In this study the infiltration rate was measured by maintaining the ponded depth in the basin and measuring the inflow of water. A conceptual model was created to explain the fluctuations in infiltration rate with temperature based on changes in the water's viscosity. A numerical model was used to show that the conceptual model was successful at explaining the changes in infiltration rate.

2.3.5 Infiltration Recovery

Dependence of the infiltration rate on the initial moisture content of the soil suggests an effect on the infiltration capacity depending on the time between rainfall events. After a rainfall event the moisture content will decrease as water in the soil is redistributed. Depending on the duration of dry weather the moisture content will be less or more than the critical moisture content, which will affect the infiltration capacity, accordingly (Gusev, 1978).

While there are simple algebraic equations that relate the infiltration rate to time their uses are limited in watershed modeling because they don't take into consideration the water draining from the soil between events which results in an increase in the predicted infiltration rate. The Philip equation to determine the relationship between the

infiltration and the soil water storage can be used to model infiltration under continuous rainfall conditions. This allows the model to include the recovery of the infiltration rate during the periods between rainfall (Bloomfield, 1981).

Chapter 3: Site Analysis

3.1 Introduction

This research focused on the infiltration rate from an underground rock storage bed. Data from the porous concrete site was used to create a predictive model of the infiltration process based on the moisture content of the soil, as well as other soil characteristics, depth of water stored in the bed, and water temperature. This chapter describes the methods used for data collection.

3.2 Site Instrumentation

The porous concrete site has been instrumented to collect data to monitor the site responses to rainfall events. Equipment used at the site to collect water quantity data includes a rain gage, pressure transducers and water content reflectometers. This section gives a brief overview of the equipment and the various data collected at the site. For a more detailed description refer to the previous study by Kwiatkowski (2004).

3.2.1 Rain Gage

To obtain rainfall information, a rain gage was installed on the roof of Bartley Hall. The rain gage used is a Campbell Scientific (CS) TE525WS Tipping Bucket Rain Gage (Campbell, 2003c), which has an eight-inch collector diameter. Each tip of the gage reflects 0.01 inches of rainfall and tips are recorded in 5 minute increments A CS CR200 Datalogger (Campbell, 2003a) is used to collect and store data from the Tipping Bucket Rain Gage and a CS NL100 Network Link Interface (Campbell, 2003b) allows the data to be downloaded remotely over the Villanova computer network.

3.2.2 Pressure Transducers

Three pressure transducers are used to collect data throughout the site. The first pressure transducer, Instrumentation Northwest (INW) PS-9805, is located in the junction box in the lower infiltration bed to collect information about the depth and temperature of the water stored in the lower bed (Instrumentation Northwest, 2002a). A second pressure transducer, INW PT2X, records the depth and temperature of the water in the upper infiltration bed (Instrumentation Northwest, 2004). The final pressure transducer, INW PS-9800, is located in the inlet which connects the overflow pipe from the lower bed to the existing storm sewer (Instrumentation Northwest, 2002b). It was installed in conjunction with a V-notch weir to measure the flow from the site. The pressure transducers in the lower bed and the inlet are connected to a CS CR23X Micrologger (Campbell, 2000) which is used to power the instruments and collect and store data. A CS NL100 Network Link Interface (Campbell, 2003b) allows the data to be downloaded remotely over the Villanova computer network. Data from the pressure transducer located in the upper bed is collected by connecting a laptop computer to the data port at the site. All data is recorded in 15 minute increments.

3.2.3 Water Content Reflectometers

Twelve Campbell Scientific CS616 Water Content Reflectometers (moisture meters) (Campbell, 2006) were installed at the site to measure the volumetric water content of the surrounding soil in different locations and at various depths throughout the site. They were installed in four groups of three, two groups underneath the lower infiltration bed and two groups underneath grass areas at depths of 0.3 m (1 ft), 0.6 m (2 ft), and 1.2 m (4 ft) relative to the undisturbed soil at the bottom of the lower infiltration

bed. A CS CR23X Micrologger (Campbell, 2000) is used to power the instruments, and to collect and store data. A CS NL100 Network Link Interface (Campbell, 2003b) allows the data to be downloaded remotely over the Villanova computer network. Currently, three of the four moisture meter groups are functioning; one of the groups below the infiltration bed and both of the groups below the grass areas. All data is recorded in 5 minute increments.

3.3 Soil Analysis[2]

During the construction of the site, several soils tests were performed to describe some of the basic soil properties more accurately. Testing included a sieve analysis, Atterberg limits, hydrometer testing, a flexible wall hydraulic conductivity test and percolation tests. This section gives a brief overview of the testing and results utilized in the current research. For complete descriptions and results of all soils testing, refer to the previous study by Kwiatkowski (2004).

3.3.1 Soil Classification

Using a soil sample from the lower infiltration bed, the soil was classified using the Unified Soil Classification System (USCS). This was done by performing a grain-size analysis as well as Atterberg limits in accordance with American Society for Testing and Materials (ASTM) standards. The results of the grain-size analysis utilizing sieve data, soil wash, and hydrometer data are shown in Figure 3.1. The soil's liquid limit (LL) and plastic limit (PL) were determined, using the Atterberg limits, as 42.9%, and 33.0%, respectively which resulted in a plasticity index (PI) of 9.9%. These results led to a USCS classification of sandy silt (ML) with low plasticity.

[2] Portions of this section are taken from Kwiatkowski (2004) Masters Thesis.

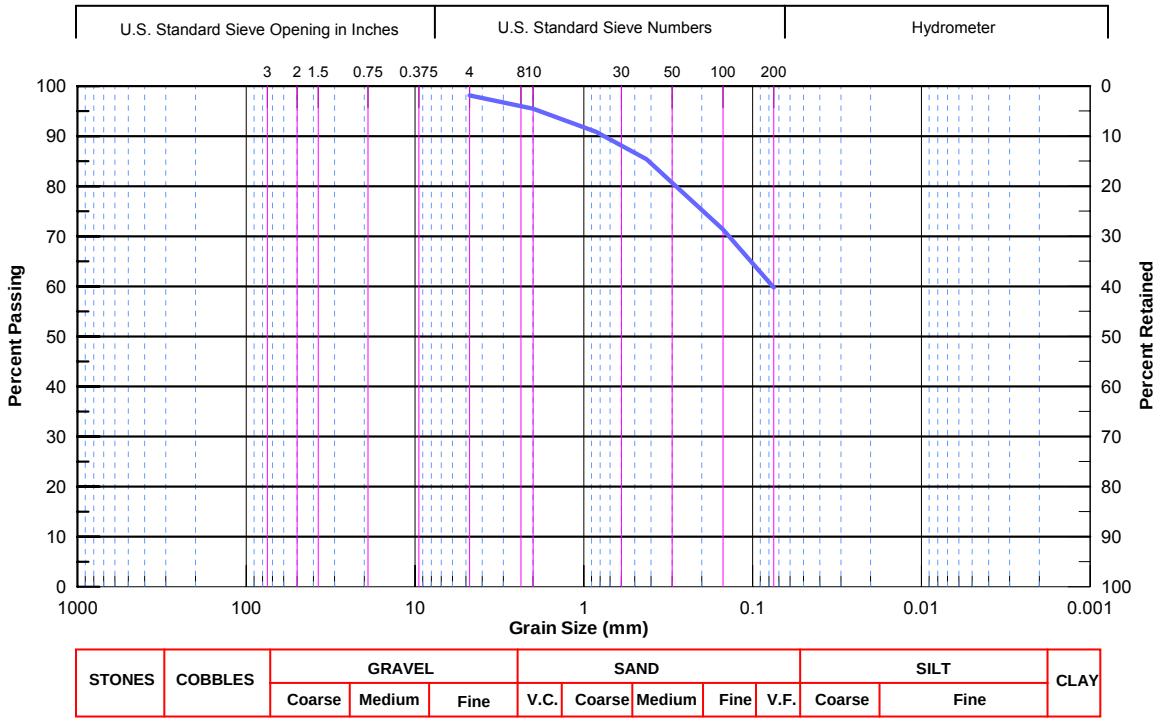

Figure 3.1 Grain Size Analysis

3.3.2 Flexible Wall Hydraulic Conductivity

A flexible wall hydraulic conductivity test was performed to determine the hydraulic conductivity of the site's underlying soil. The testing was performed on an undisturbed sample, taken at the approximate depth of the bed bottom from the surrounding grass area, using a hollow tube. Four tests were run with an average saturated hydraulic conductivity (K_{sat}) of 1.67 x 10^{-4} cm/sec (0.24 in/hr).

3.3.3 Soil Suction Test

The soil suction of the site's underlying soil was determined using a filter paper test as outlined by ASTM D 5298-94. As it was extremely difficult to obtain undisturbed samples at the site, samples were molded to replicate field conditions. Samples were

prepared at 5, 10, 13, 16, 20 and 25% of target gravimetric moisture contents by adding specific amounts of water to each sample.

The soil suction curve was created by measuring the matrix suction for each of the samples. Matrix suction is defined as "the negative pressure (expressed as a positive value), relative to ambient atmospheric pressure on the soil water, to which a solution identical in composition with the soil water must be subjected in order to be in equilibrium through a porous permeable wall with the soil water." The results of the filter paper test are presented in Table 3.1.

Parameter	Target Soil Moisture Content (%)					
	5	10	13	16	20	25
Matrix Suction (log kPa)	4.45	5.06	3.41	3.08	2.19	1.15

Table 3.1 Soil Suction Results

The resulting soil suction curve is shown in Figure 3.2. "Soil suction is a measure of the free energy of the pore-water in a soil. Soil suction in practical terms is a measure of the affinity of soil to retain water and can provide information on soil parameters that are influenced by the soil water; for example, volume change, deformation, and strength characteristics of the soil" (ASTM D 5298-94).

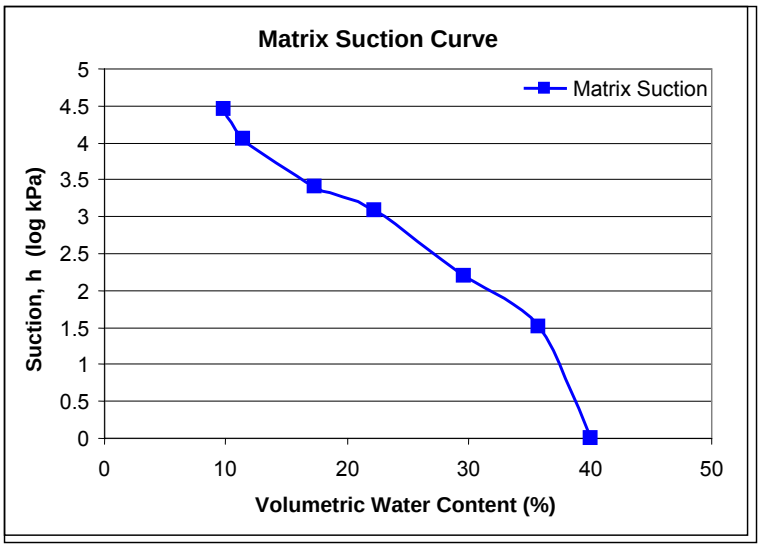

Figure 3.2 Matrix Suction Curve

Chapter 4: Model Development and Analysis

4.1 Introduction

This chapter describes the development and verification of a rock bed infiltration BMP model developed from the Green and Ampt relationship and based on the soil moisture and porosity. It also gives an overview of a parameter sensitivity analysis. Specifically, the purpose of this research is to incorporate temperature and moisture content to develop a more accurate infiltration model. This research modeled the infiltration of the ponded water after the rainfall had ended.

The Green and Ampt equation for infiltration was used as the basis for this model. If water has ponded on the surface it can be assumed that the upper layer of the soil is saturated which follows the assumptions of the Green and Ampt model. The hydraulic conductivity and capillary suction were adjusted for the initial moisture content of the soil using parameters obtained from fitting a curve to the data from a filter paper analysis using the van Genuchten method. The hydraulic conductivity was further adjusted for the temperature of the stored water by correcting for the viscosity of the water. To verify that this process does indeed produce a better model, field data collected from the Porous Concrete Infiltration BMP at Villanova University was utilized. Thirty-two storm events were used to verify this model.

Sensitivity analyses were performed to determine the significance of the various input parameters. The effects of the initial moisture content and water temperature on the infiltration process were observed.

4.2 Model Input Parameters

This model used the basic Green and Ampt infiltration equation as described in Chapter 2. For the purpose of this research the following version of the Green and Ampt equation was used to develop the model.

$$f_i = K_{sat}\left(\frac{\Psi + h_i + z_i}{z_i}\right) \qquad \text{Equation 4.1}$$

f_i = infiltration rate (in/hr)

K_{sat} = Saturated Hydraulic Conductivity (in/hr)

Ψ = capillary suction (in)

h_i = ponded depth (in)

z_i = wetting front depth (in)

The necessary input parameters are the hydraulic conductivity, the initial depth of water ponded in the bed, the capillary suction and the initial depth of the wetting front.

4.2.1 van Genuchten Curve Fitting

In the Green and Ampt model, the initial moisture content affects the capillary suction (Ψ) and the hydraulic conductivity (K). These quantities are often estimated as constants for a soil, but adjusting these values to account for the initial moisture condition should result in a more accurate infiltration model.

Initial soil testing performed for the porous concrete site included a filter paper test, described earlier, from which the soil water characteristic curve (SWCC) was developed. One method commonly used to describe the SWCC mathematically is the van Genuchten method. The van Genuchten equation was developed to estimate the relative hydraulic conductivity using the predictive models developed by Burdine and Mualem (van Genuchten, 1980). Knowing the saturated hydraulic conductivity and the

SWCC an equation was created to determine the hydraulic conductivity for a range of moisture contents. Van Genuchten used the parameters α, n and m to fit the relative hydraulic conductivity equation to the individual SWCC.

Using Equation 4.2, α and n were varied to provide the best fit to the test data.

$$\theta(\Psi) = \theta_r + \frac{\theta_s - \theta_r}{\left(1 + (\alpha\Psi)^n\right)^m}$$ Equation 4.2 (van Genuchten, 1980)

Where: $0 < m < 1$ and $m = 1 - 1/n$

$\theta(\Psi)$ = moisture content relative to capillary suction

θ_r = residual moisture content

θ_s = saturated moisture content

α, n, m = curve fitting parameters

Working backward, each value of capillary suction found in the filter paper test was used as a known value in Equation 4.2 to calculate estimated moisture contents. The sum of the square error (SSE) between the recorded moisture content and the estimated value was calculated and then α and n were optimized by the Excel Solver tool in order to minimize the sum of the square errors (SSE). Figure 4.1 shows the curve fit to the filter paper test data and Table 4.1 gives the curve parameters.

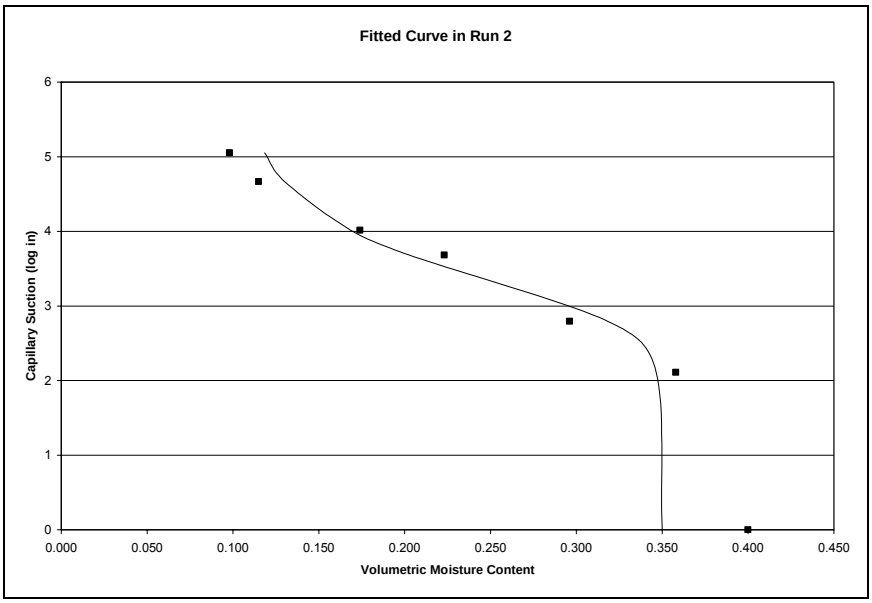

Figure 4.1 Fitted Curve with Optimized α and n Values

θr	0.1000
θs	0.3500
α	0.0010
n	1.5536
m	0.3563
SSE	0.00421

Table 4.1 Fitted Curve Parameters

This process was also run while allowing Solver to calculate optimized values of θ_s and θ_r, in addition to α and n. Figure 4.2 shows the resultant curve fit to the filter paper test data and Table 4.2 gives the curve parameters for this run.

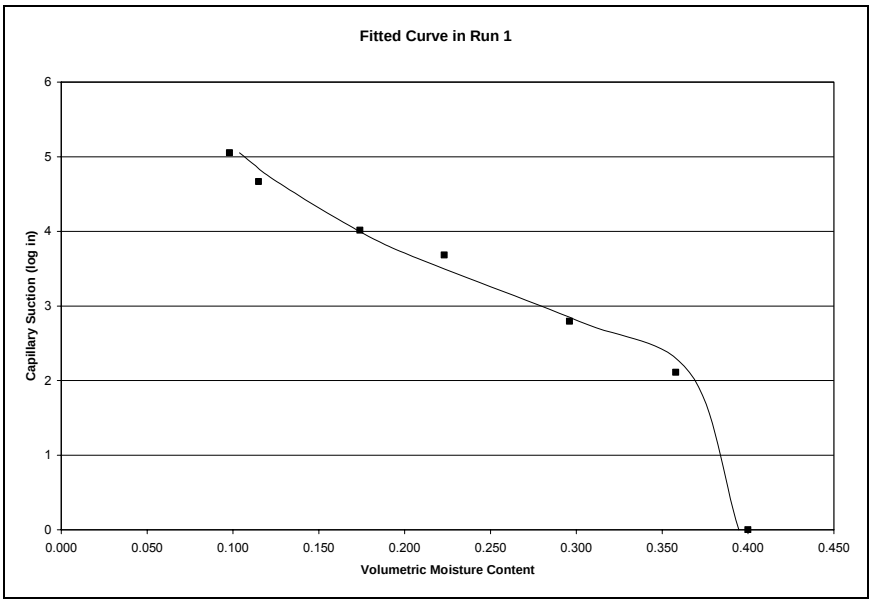

Figure 4.2 Alternate Fitted Curve with Optimized α, n, θr and θs

θr	0.0000
θs	0.3946
α	0.0046
n	1.2129
m	0.1756
SSE	0.00068

Table 4.2 Alternate Fitted Curve Parameters

While this resulted in a better fit overall, the given parameters in the first run more accurately describe the field conditions of the soil because θ_r cannot be zero and 0.35 is a more realistic value for θ_s. Thus, α, n, θ_s and θ_r values from the first run were used in further computations.

This mathematical model of the SWCC enables the initial water content of the soil to be entered into the model to obtain the capillary suction value, using the optimized α and n parameters, by rearranging Equation 4.2 as follows:

$$\Psi(\theta) = \frac{\left(\left(\frac{\theta_s - \theta_r}{\theta(\Psi) - \theta_r}\right)^{1/m}\right)^{1/n}}{\alpha}$$ Equation 4.3 (Celia et al., 1993)

The α and n values, along with the initial moisture content, were then used to calculate an adjustment factor to relate the hydraulic conductivity to the moisture content of the soil.

$$k_r(\theta_e) = \theta_e^{1/2}\left(1 - \left(1 - \theta_e^{1/m}\right)^m\right)^2$$ Equation 4.4 (van Genuchten, 1980)

Where: $\theta_e = \frac{\theta - \theta_r}{\theta_s - \theta_r}$ Dimensionless Moisture Content

4.2.2 Hydraulic Conductivity

The soil's saturated hydraulic conductivity is typically used as an input in the Green and Ampt model. This study demonstrates the benefits of using a hydraulic conductivity that is specific to the individual storm conditions. The research focused on adjusting the hydraulic conductivity to account for the initial moisture content of the soil and the average water temperature during infiltration. The van Genuchten curve fitting parameters were used to calculate the correction factor to adjust the hydraulic conductivity relative to the initial water content using Equation 4.4.

The adjustment for temperature was made by calculating a conductivity that accounts for the viscosity of the water at the average temperature relative to the viscosity at 20˚C at which the saturated value was calculated in the laboratory using equation 2.5. Figure 4.3 shows the adjustment to the hydraulic conductivity based on temperature.

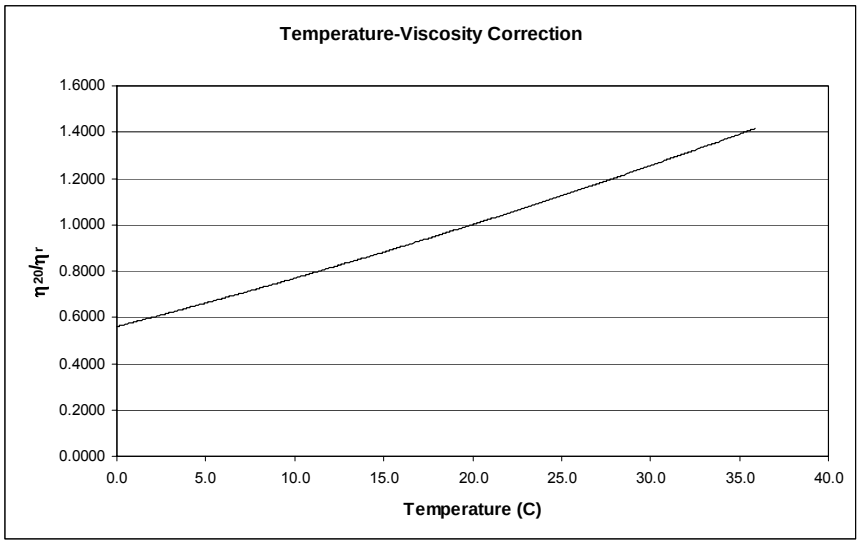

Figure 4.3 Viscosity Correction for Water Temperature

Aggelides (1978) has recommended that the saturated hydraulic conductivity (K_{sat}) be estimated as one half the value found in the laboratory to account for air entrapment. That suggests that the actual hydraulic conductivity of the soil in the field is less than what can be achieved in the laboratory. Using that estimation and combining the adjustment factors from Equations 4.4 and 2.5 the adjusted hydraulic conductivity becomes:

$$K_{adj} = k_r(\theta e) K_s \left(\eta 20 / \eta r \right) \qquad \text{Equation 4.5}$$

Where: $K_s = (0.5)K_{sat}$

For simplicity, the average temperature of the ponded water was used as the input for the model. To determine whether this was a reasonable representation of the temperature, a comparison of the average value with the recorded data was performed. The MSE of the average value to the recorded was calculated to determine the fit of the average line. The slope and y-intercept of the best fit line were also calculated. The slope gives a picture of how close the graph of the recorded data is to being horizontal.

The y-intercept of the best fit line was compared to the average value and the error between the values was calculated. This shows how different the best fit line was from the average value. The results of this analysis, given in Table 4.3, indicate that the average temperature is an adequate representation of the temperature throughout the duration of the storm.

Storm Date	Average Temp. (°C)	Minimum Temp. (°C)	Maximum Temp. (°C)	ΔT	MSE	slope	y-intercept	Error
10/14/03	19.43	17.96	20.10	2.14	0.15	-0.0008	19.45	-0.03
10/26/03	16.10	15.56	16.44	0.88	0.06	0.0388	15.67	0.42
11/4/03	16.89	16.00	17.18	1.18	0.09	-0.0305	17.31	-0.42
11/19/03	14.02	13.07	14.57	1.51	0.15	0.0120	13.55	0.47
11/28/03	11.70	10.08	12.57	2.49	0.61	-0.0426	12.91	-1.21
1/4/04	8.06	7.60	8.65	1.05	0.11	-0.0614	8.62	-0.57
3/30/04	10.37	8.51	11.22	2.71	0.62	0.1200	9.10	1.27
4/12/04	10.86	8.97	12.77	3.80	0.76	0.0352	9.45	1.41
4/23/04	15.98	14.08	16.60	2.53	0.36	0.0430	15.20	0.79
5/2/04	16.16	13.94	17.33	3.39	1.40	-0.0873	17.76	-1.59
6/22/04	25.34	24.56	26.21	1.65	0.16	0.0668	24.73	0.61
7/12/04	25.89	24.41	26.26	1.84	0.19	0.0263	25.32	0.57
7/18/04	25.27	24.29	25.63	1.34	0.15	-0.0192	25.55	-0.28
7/23/04	26.42	25.65	26.90	1.25	0.09	0.0015	26.40	0.02
7/27/04	25.17	24.56	25.50	0.93	0.07	0.0514	24.74	0.42
8/1/04	25.89	24.52	26.92	2.40	0.30	0.0328	24.98	0.91
9/18/04	22.05	20.12	23.07	2.96	0.58	-0.0263	22.86	-0.82
9/27/04	21.51	20.76	21.77	1.00	0.06	0.0219	21.19	0.32
10/14/04	17.68	16.62	18.07	1.45	0.11	0.0409	17.16	0.52
10/30/04	15.34	15.05	15.58	0.53	0.04	0.0257	15.03	0.32
11/4/04	13.32	10.60	14.61	4.01	0.52	-0.0070	13.67	-0.34
11/12/04	10.51	9.26	11.28	2.02	0.31	-0.0160	11.31	-0.79
12/9/04	8.70	7.23	9.37	2.15	0.36	-0.0235	9.67	-0.97
12/23/04	5.44	3.35	8.31	4.96	1.78	-0.0921	7.71	-2.27
1/5/05	6.56	6.19	7.21	1.03	0.10	-0.0395	7.08	-0.52
2/14/05	5.40	5.26	5.60	0.34	0.01	-0.0086	5.56	-0.15
5/20/05	16.53	15.93	17.06	1.13	0.14	-0.0556	16.99	-0.46
6/3/05	18.85	18.33	19.08	0.75	0.04	0.0221	18.53	0.31
7/15/05	25.86	25.28	26.17	0.89	0.05	0.0437	25.49	0.37
7/17/05	26.00	25.52	26.19	0.67	0.03	0.0580	25.73	0.27
10/7/05	20.77	19.79	21.25	1.47	0.14	-0.0083	20.96	-0.20
10/21/05	16.29	15.01	16.95	1.93	0.19	-0.0206	16.72	-0.43
Minimum	**5.40**	**3.35**	**5.60**	**0.34**	**0.01**	**-0.0921**	**5.56**	**-2.27**
Maximum	**26.42**	**25.65**	**26.92**	**4.96**	**1.78**	**0.1200**	**26.40**	**1.41**
Average	**17.01**	**15.88**	**17.70**	**1.82**	**0.30**	**0.0031**	**17.07**	**-0.06**

Table 4.3 Results of the Average Temperature Analysis

4.2.3 Initial Depth of Ponded Water

The initial depth of water in the bed used in the model is the maximum ponded depth after the rainfall has ended. The maximum ponded depth for storms where the depth exceeded the 18" (45.72 cm) overflow was set, in the first time step, so that the depth was less than 18" (45.72 cm). This was done so that the recorded decrease in bed depth was only due to infiltration and not to flow through the overflow pipe.

4.2.4 Capillary Suction

The capillary suction, or soil suction defined earlier, is often taken to be a constant for the soil, but as the SWCC illustrates, this parameter can vary greatly depending on the water content of the soil. Like the hydraulic conductivity, this parameter is also calculated for each storm using the van Genuchten curve fitting parameters as described earlier using Equation 4.3.

4.2.5 Initial Depth of the Wetting Front

The initial depth of the wetting front was estimated using the data from the water content reflectometers. The fifteen minute data was analyzed visually to determine when each meter first showed an increase in water content due to the rainfall infiltrating from the storage bed. Figure 4.4 shows graphically how each moisture meter responds to a rainfall event.

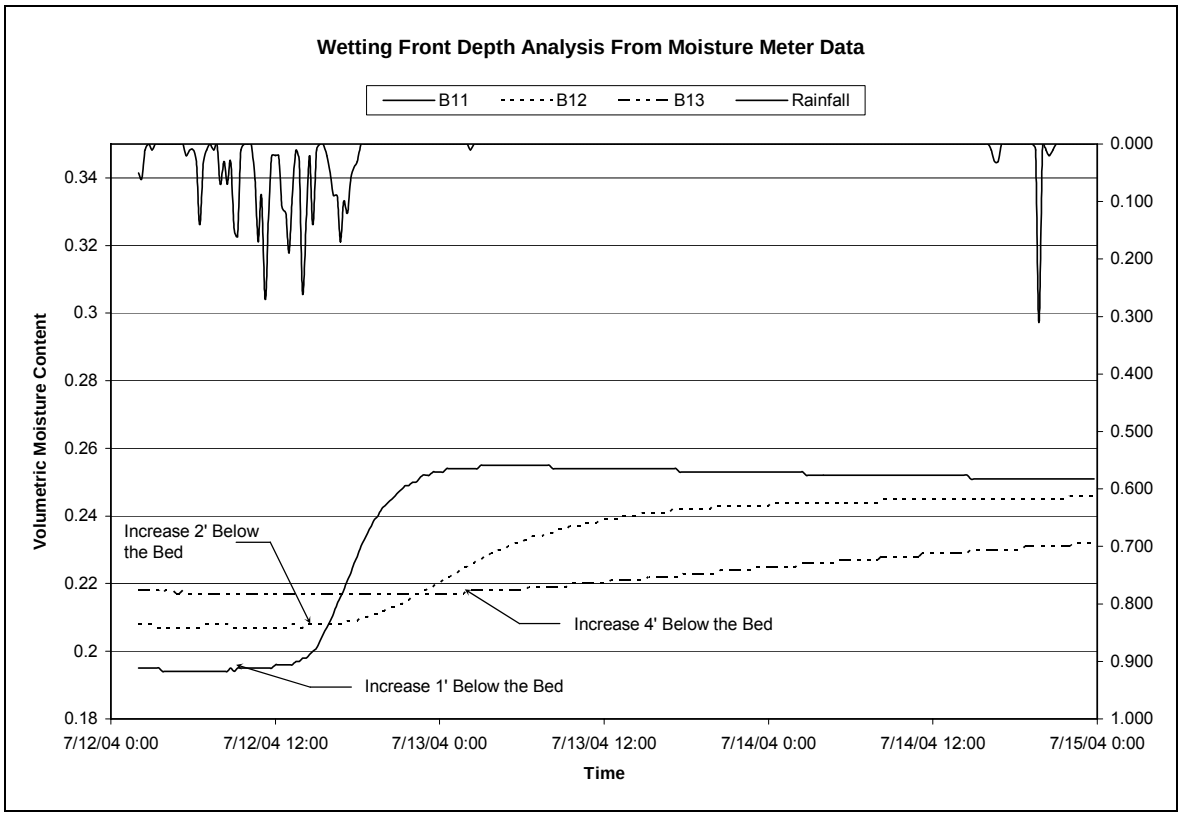

Figure 4.4 Water Content Reflectometer Response Determination

From those response times at 1.0 ft (0.3 m), 2.0 ft (0.6 m) and 4.0 ft (1.2 m) below the bed, the wetting front depth at the time of the initial bed depth was estimated by interpolating between points. In instances where the maximum bed depth occurred before the moisture meter at 1.0 ft (0.3 m) responded or after the moisture meter at 4.0 ft (1.2 m) responded, the data had to be extrapolated at the same rate as before or after that point. Because this is an estimated parameter, a sensitivity analysis was performed to determine the significance of the term for the model. The analysis will be described later in this chapter.

4.3 Model Calculations

This study used the theory of the Green and Ampt equation to model the infiltration from the subsurface rock storage bed. The objective was to adjust the input

parameters to account for initial conditions to increase the accuracy of the standard Green and Ampt model. This was performed using an Excel spreadsheet which calculated the infiltration rate and ponded depth in each time step (Bill Heasom, personal communication, March 2006). A sample of the spreadsheet can be seen in Appendix A.

4.3.1 Quantity of Infiltrated Water

To calculate the cumulative quantity of water that has infiltrated at each time step the infiltration rate from the previous time step is multiplied by the time increment and added to the quantity of water infiltrated from the previous time step as follows:

$$F_i = (f_{i-1})(\Delta t) + F_{i-1} \qquad \text{Equation 4.6}$$

F_i = cumulative infiltration at t = i

f_{i-1} = infiltration during previous time increment

Δt = time increment

F_{i-1} = cumulative infiltration at previous t = i-1

The initial value for the first time step was taken as the initial depth of the wetting front multiplied by the initial available soil capacity ($\Delta\theta$).

The available soil capacity was calculated for each storm using two different methods. Method 1 subtracted the recorded initial moisture content from the saturated moisture content, θ_s, of 0.35. Method 2 calculated the change in moisture content over the duration of the storm and subtracted that value from θ_s.

4.3.2 Ponded Depth of Water

The ponded depth at each time step is then calculated using Equation 4.7.

$$h_i = h_{i-1} - \frac{(F_i - F_{i-1})}{n_{rock}} \qquad \text{Equation 4.7}$$

h_i = ponded depth at t = 1

h_{i-1} = ponded depth at t = i-1

n_{rock} = porosity of the rock in the storage bed

In equation 4.7, the quantity of water infiltrated during the previous time increment is divided by the porosity of the rock bed and then subtracted from the ponded depth at the previous time step. The value of the ponded depth is always decreasing since it is the draining period that is being studied. The porosity of the rock bed is a constant value for the site, which in this case is 0.40. The initial value at the first time step is the initial ponded depth, an input parameter which was described earlier. A summary of the characteristics of the ponding during each storm event is presented in Appendix D.

4.3.3 Depth of the Wetting Front

The depth of the wetting front at each time step was calculated as follows:

$$z_i = z_{i-1} + (F_i - F_{i-1})/\Delta\theta \qquad \text{Equation 4.8}$$

z_i = wetting front depth at time t = i

z_{i-1} = wetting front depth at time t = i-1

This adds the amount of infiltrated water during the previous time increment, divided by the initial available soil capacity, to the depth of the wetting front from the previous time increment. This distributes the water that infiltrates through the soil based on the Green and Ampt assumption that the soil above the wetting front is completely saturated. The initial value used in the first time step was taken from water content reflectometer data as described in Section 4.2.5. A summary of the responses for each moisture meter can be seen in Appendix C.

4.3.4 Infiltration Rate

The final value calculated in the model for each time increment is the infiltration rate. This is simply the Green and Ampt infiltration equation calculated for each time increment.

$$f_i = K_{adj}\left(\frac{\Psi + h_i + z_i}{z_i}\right) \qquad \text{Equation 4.9}$$

These calculations were performed in fifteen minute increments from the time of the maximum ponded depth to the minimum depth before another peak or when the bed was empty. The modeled ponded depth over the duration was then compared to the actual ponded depth data to obtain the goodness of fit of the model.

4.4 Data Filtering

The level of water stored in the lower bed has been measured by a pressure transducer and recorded in five minute increments since September 2003. This research utilized the data from September 2003 through December 2005. Using a twelve hour dry period as the minimum separation between individual storm events, various storm parameters were calculated for each isolated event. Once the list of all storms was compiled, different qualifications were applied to develop a list of storms that could be adequately modeled.

The first step was to remove any storms from the list where the water never ponded in the storage bed. Since this research has identified the infiltration rate as the slope of the recession limb of the bed depth after the rain has ceased, there needs to have been some measurable water depth in the bed, generally 1.0 inch (2.54 cm) or more.

The next step was to analyze the data from the water content reflectometers for the remaining storms. Because the initial depth of the wetting front was estimated from

the moisture meter response time, there needed to be an increase in the moisture content seen in at least the first two moisture meters to estimate a rate of movement of the wetting front. For that reason it was also necessary to choose storms where the response time increased with depth below the bed for each moisture meter. If not, then it was likely that the response seen during that time period was from the previous storm event.

The final step was to eliminate any storms where the water content at 1.0 ft (0.3 m) below the bed was recorded at a level higher than the saturated value of 0.35 used in the model. In instances where the water content was seen at a higher level there may have been other factors influencing the readings. These cases seem to be limited to the colder winter months.

After those reductions to the storm list for the period between September 2003 and December 2005, a total of 32 storms remained to be used to verify the model. The storm data for the storm events that were modeled can be seen in Appendix B.

4.5 Model Verification

To determine if using temperature and initial moisture content specific data results in a better model of the infiltration rate, the model was verified in a number of ways. Storm events from all seasons were modeled to ensure that a range of temperatures was used for verification. The storms had varying maximum ponded depths as well as different initial moisture conditions to make sure that the model would work for all storm events and not just events with specific initial conditions. Table 4.4 illustrates the range of parameters used to verify the model.

Storm Date	MSE	Average Temp. (°C)	Ponded Depth (in)	Ponded Depth (m)	θ_i
October 14, 2003	9.592	19.43	8.21	0.21	0.184
October 26, 2003	0.152	16.10	19.71	0.50	0.198
November 4, 2003	0.018	16.89	1.97	0.05	0.227
November 19, 2003	0.818	14.02	11.98	0.30	0.206
November 28, 2003	0.168	11.70	4.53	0.11	0.222
January 4, 2004	0.181	8.06	1.08	0.03	0.201
March 30, 2004	4.177	10.37	3.33	0.08	0.212
April 12, 2004	4.302	10.86	13.28	0.34	0.218
April 23, 2004	1.941	15.98	2.89	0.07	0.215
May 2, 2004	0.073	16.16	3.23	0.08	0.225
June 22, 2004	1.472	25.34	2.10	0.05	0.204
July 12, 2004	3.691	25.89	21.37	0.54	0.195
July 18, 2004	0.322	25.27	3.22	0.08	0.235
July 23, 2004	0.850	26.42	3.07	0.08	0.218
July 27, 2004	0.196	25.17	21.04	0.53	0.225
August 1, 2004	0.333	25.89	21.71	0.55	0.251
September 18, 2004	0.085	22.05	17.10	0.43	0.169
September 27, 2004	8.662	21.51	23.02	0.58	0.191
October 14, 2004	9.237	17.68	5.21	0.13	0.177
October 30, 2004	0.764	15.34	1.73	0.04	0.191
November 4, 2004	0.370	13.32	9.39	0.24	0.206
November 12, 2004	3.791	10.51	9.65	0.25	0.217
December 9, 2004	8.465	8.70	7.20	0.18	0.231
December 23, 2004	4.073	5.44	4.52	0.11	0.19
January 5, 2005	1.837	6.56	2.76	0.07	0.185
February 14, 2005	2.875	5.40	8.95	0.23	0.176
May 20, 2005	0.859	16.53	1.87	0.05	0.179
June 3, 2005	1.671	18.85	5.69	0.14	0.181
July 15, 2005	0.340	25.86	3.46	0.09	0.207
July 17, 2005	0.137	26.00	1.61	0.04	0.231
October 7, 2005	1.012	20.77	22.55	0.57	0.167
October 21, 2005	0.102	16.29	5.73	0.15	0.196
Minimum		**5.40**	**1.08**	**0.03**	**0.17**
Maximum		**26.42**	**23.02**	**0.58**	**0.25**
Average		**17.01**	**8.54**	**0.22**	**0.20**

Table 4.4 Initial Parameters for Modeled Storms

It was also necessary to establish whether the storm specific initial conditions produced an adequate infiltration model. This was done by calculating the mean square error between the model's ponded depth and the actual ponded depth.

$$MSE = SSE/n \qquad \text{Equation 4.10}$$

$$SSE = \Sigma (y_i - y_{ai})^2$$

y_i = modeled ponded depth at t = i

y_{ai} = actual ponded depth at t = i

Smaller values of MSE indicate better model predictions of the infiltration from the rock storage bed.

The most important conclusion was to determine whether the developed model, with adjustments for temperature and initial moisture content, would result in a more accurate model than the Green and Ampt model using standard values. To determine this, the model was run for each storm event using typical values that an engineer designing a similar system might use. The saturated hydraulic conductivity was assumed to be the value of 0.24 in/hr as calculated in the laboratory. The capillary suction was estimated at 6.57 in, a standard value for this soil type as used in a previous infiltration study of the site performed by Braga (2005). The estimated initial wetting front depths were the same values used in the developed models. The initial moisture deficit, θ_s-θ_i, was taken as 0.10, a conservative value for design purposes in lieu of soil testing (Bedient and Huber, 2002).

The MSE between the standard model and the recorded field data was calculated. The MSE of the developed model and the standard model were then compared to see if the developed model provided a better fit to the actual data. The percent change of the fit

from the standard model was then compared to get a better understanding of the benefits of the developed model.

$$\% \text{ Change of fit} = (MSE_s - MSE_d)/MSE_s \qquad \text{Equation 4.11}$$

MSE_s = MSE of the standard model to the recorded data

MSE_d = MSE of the developed model to the recorded data

The larger the positive calculated percent change of fit, the greater the improvement of the developed model over the standard model.

4.6 Sensitivity Analysis

A major concern when using storm specific initial conditions is the reliability of the data. It is important to know how any error in the data will affect the results of the model. Often times, field testing can be cost prohibitive. It is important to know which parameters should be measured accurately and which can reasonably be estimated without adversely affecting the model results. The following section describes the sensitivity analyses that were performed on the developed model.

4.6.1 Hydraulic Conductivity and Wetting Front Depth

In this study, the saturated hydraulic conductivity was known based on soils testing performed at the site. It is important to know what effect different values of the saturated hydraulic conductivity will have on the model to determine the value of this parameter and its accurate measurement. This information is also valuable since there may be variability or error from the test.

Another parameter that may contain error is the initial depth of the wetting front. For purposes of this research, this parameter was estimated from the water content reflectometer data, as discussed earlier. In actual design practices, for a hypothetical

storm, this data would clearly not be available. If one is modeling the entire storm event this value would initially be zero under dry conditions. Under wet conditions it would be necessary to have modeled the recovery rate of the soil between storm events. There is no generally accepted method of performing such an analysis.

Even the values used in this study from recorded field data may not be entirely accurate as the initial depth was an interpolated or even extrapolated value. Also, an increase in the value recorded by the water content reflectometer may not actually be an indication of a distinct wetting front at that location and time since the values did not increase to a saturated level immediately as the assumption of the Green and Ampt theory suggests.

As with the hydraulic conductivity, it is important to understand how much any variability in this parameter will affect the outcome of the model. It is the hypothesis of the author that the change in the wetting front depth between time steps, not the value of the initial condition, influences the model.

A sensitivity analysis was conducted to determine the significance of these parameters. Five storm events were chosen at random to perform the analysis. For each event the saturated hydraulic conductivity and initial wetting front depth were varied individually. The percent change in the parameter value was then compared with the percent change in the mean square error of the model's fit to the recorded data.

4.6.2 Initial Moisture Content and Temperature

The parameters this research is focused on are the initial moisture content and the temperature of the water stored in the rock bed. Because these are storm specific, the benefit of including these terms in the model is not necessarily to model the individual

storm better, but to determine critical conditions or seasonal conditions to design subsurface infiltration basins more effectively. It is also of value to see the effect that varying these parameters has on the results of the model. It is also necessary to determine if both parameters have a significant effect on the results or if one has a greater effect than the other.

A "test storm" was created to study the importance of these parameters. The goal was not to see how the results compared to recorded data, but to see how the factors affected the model, overall. Each parameter was varied from the initial "test storm" parameters. Graphs of the ponded depth vs. time were compared to the initial model run. The percent change from the original run was also computed to determine the relationship between the parameter and the outcome of the model.

Chapter 5: Results and Discussion

5.1 Introduction

The model was verified by using the 32 selected storm events. Sensitivity analyses were performed to analyze the influence of the model input parameters. The Mean Square Error (MSE) was calculated to quantify the results of the model, with lower values signifying a better fit to the recorded data. As stated in Chapter 4, the MSE is calculated using Equation 4.10:

$$MSE = SSE/n \qquad \text{Equation 4.10}$$

$$SSE = \Sigma (y_i - y_{ai})^2$$

y_i = modeled ponded depth at t = i

y_{ai} = actual ponded depth at t = i

This value was used as the basis for the verification and sensitivity analyses performed on the model. This chapter presents the results of the model verification and sensitivity analyses and discusses the relative importance of the data on the model predictions.

5.2 Initial Moisture Content Determination

The value of the initial moisture content used in the model calculations was obtained from the water content reflectometer data. The value was taken as the moisture content 1.0 ft (0.3 m) below the bottom of the bed at the time when the rainfall began. There were times, however, when the moisture content was recorded at a level higher than the porosity of the soil. One hypothesis was that the data from the water content reflectometers gives a more accurate representation of the increase in water content of the soil during the storm than it does of the actual value of the water content.

To check this hypothesis, the model was run for each storm event using both the initial moisture content as recorded by the moisture meter (Method 1) and also using an adjusted value (Method 2). The adjusted value was calculated by subtracting the total increase in moisture content recorded by the water content reflectometer from the saturated moisture content of 0.35 used in this study. A comparison of the results of the two methods is shown below in Table 5.1. The percent improvement column represents the increase in accuracy of the better method over the other.

Storm	Ponded Depth (in)	Method 1	Method 2	% Improvement
01/04/04	1.079	0.344	**0.181**	47.45%
07/17/05	1.605	0.326	**0.137**	58.08%
10/30/04	1.698	0.839	**0.764**	8.98%
05/20/05	1.874	1.003	**0.859**	14.37%
11/04/03	1.952	1.042	**0.018**	98.25%
06/22/04	2.095	1.472	1.472	0.00%
01/05/05	2.723	2.756	**1.837**	33.35%
04/23/04	2.890	2.616	**1.941**	25.80%
07/23/04	3.071	2.729	**0.850**	68.85%
07/18/04	3.170	2.704	**0.322**	88.09%
05/02/04	3.193	2.656	**0.073**	97.25%
03/30/04	3.279	6.063	**4.177**	31.12%
07/15/05	3.413	3.317	**0.340**	89.74%
11/28/03	4.494	5.532	**0.168**	96.97%
12/23/04	4.539	5.651	**4.073**	27.93%
06/03/05	4.886	4.660	**1.671**	64.15%
10/14/04	5.206	12.838	**9.237**	28.05%
10/21/05	5.718	3.374	**0.102**	96.99%
12/09/04	7.200	10.922	**8.465**	22.50%
10/14/03	8.177	17.942	**9.592**	46.54%
02/14/05	8.950	24.430	**2.875**	88.23%
11/04/04	9.390	19.970	**0.370**	98.15%
11/12/04	9.573	12.486	**3.791**	69.64%
11/19/03	11.947	21.925	**0.818**	96.27%
04/12/04	13.280	**4.302**	34.863	87.66%
09/18/04	17.050	25.070	**0.085**	99.66%
09/27/04	17.923	**8.662**	24.948	65.28%
08/01/04	17.927	**0.333**	59.920	99.45%
07/12/04	17.940	**3.691**	18.875	80.45%
10/26/03	17.957	**0.152**	9.383	98.38%
07/27/04	17.977	**0.196**	8.886	97.79%
10/07/05	17.987	**1.012**	31.698	96.81%

Table 5.1 Model Results (MSE)

The data in Table 5.1 is sorted by initial ponded depth which reveals that using Method 1 produces a better model for storms where the initial ponded depth was approximately 18 in (0.46 m), while using Method 2 was better for smaller ponded depths, generally less than 12 in. (0.3 m). To determine why one method worked better

than the other for different initial depths, the initial and maximum moisture content were analyzed to look for differences between the larger and smaller storm events. Table 5.2 presents the results of the analysis which revealed that while there seemed to be no difference in the initial moisture contents, the storms which were modeled more accurately with Method 1 reached higher maximum moisture contents than those that were modeled more accurately with Method 2.

Moisture Content				
	Method 2		Method 1	
	Initial	Maximum	Initial	Maximum
Minimum	0.167	0.240	0.169	0.215
Maximum	0.251	0.271	0.235	0.246
Average	0.206	0.253	0.203	0.234

Table 5.2 Moisture Content Analysis

Six of the seven events for which Method 1 produced a better model were events that exceeded the 18 in. (0.46 m) overflow pipe. If the one smaller storm, 4/12/04, is removed from the above analysis, the lowest maximum moisture content of Method 1 is greater than the highest maximum moisture content of Method 2.

The original hypothesis when using an adjusted moisture content was that the moisture meter was not recording the actual moisture content level, but rather the change in moisture content during the storm. This analysis, however, led to the hypothesis that the difference in preferred method is due to air entrapment. For the smaller ponded depths the moisture content plateaus at lower levels because there is not enough head to force air out of the soil. For events with larger ponded depths the head forces more air out of the soil allowing the moisture content of the soil to reach higher levels but below saturation. Method 2 worked better for the smaller events because it shifted the moisture

content up to simulate saturation, which for these events occurs between 0.215 and 0.246. Method 1 worked better for larger events because the head forces the moisture content to reach levels closer to the actual saturation of the soil (0.35). Research has also indicated that the level of saturation that is achieved is related to the temperature of the water (Constantz and Murphy, 1991) which could also explain why the maximum moisture content was not the same for every storm event.

5.3 Model Verification Results

To determine whether the developed model is effective at estimating the infiltration of the stored runoff it was verified using storms with various storm parameters and comparing the results to a standard Green and Ampt model. The results of the model verification are discussed in the following sections.

5.3.1 Standard versus Developed Model

The most important verification was to determine if the model developed in this study resulted in a better infiltration model than the standard Green and Ampt equation. The results of the developed model were compared to the results of the model run with typical values of capillary suction (Ψ) and saturated hydraulic conductivity (K_{sat}). Table 5.3 compares the MSE of the developed model with that of the standard model where the target prediction of the models is the recorded ponded depth.

Storm	Developed Model MSE	Standard Model MSE	% Improvement
10/14/03	9.592	15.063	36.32%
10/26/03	0.152	13.645	98.89%
11/04/03	0.018	1.106	98.35%
11/19/03	0.818	22.042	96.29%
11/28/03	0.168	5.346	96.86%
01/04/04	0.181	0.350	48.37%
03/30/04	4.177	5.668	26.31%
04/12/04	4.302	21.301	79.80%
04/23/04	1.941	2.409	19.41%
05/02/04	0.073	2.716	97.31%
06/22/04	1.472	1.422	-3.51%
07/12/04	3.691	10.807	65.85%
07/18/04	0.322	2.510	87.17%
07/23/04	0.850	2.348	63.80%
07/27/04	0.196	6.600	97.03%
08/01/04	0.333	15.568	97.86%
09/18/04	0.085	18.092	99.53%
09/27/04	8.662	14.243	39.18%
10/14/04	9.237	10.908	15.31%
10/30/04	0.764	0.795	3.93%
11/04/04	0.370	18.309	97.98%
11/12/04	3.791	17.276	78.06%
12/09/04	8.465	12.097	30.03%
12/23/04	4.073	5.103	20.19%
01/05/05	1.837	2.903	36.73%
02/14/05	2.875	24.694	88.36%
05/20/05	0.859	0.848	-1.25%
06/03/05	1.671	4.017	58.41%
07/15/05	0.340	2.484	86.30%
07/17/05	0.137	0.468	70.79%
10/07/05	1.012	4.438	77.19%
10/21/05	0.102	5.152	98.03%
	Minimum		**3.93%**
	Maximum		**99.53%**
	Average		**66.99%**

Table 5.3 Comparison of the Developed and Standard Models

For 30 of the storm events that were used to verify the proposed model, the adjusted parameters produced an infiltration model which more closely fit the recorded ponded depth than the standard model did. On average, the developed model produced a

66.99% better fit to the recorded data with a minimum increase of 3.93% and a maximum of 99.53%. Only two of the events had better results with the standard method although the MSE of the developed and standard models were essentially the same. Figure 5.1 illustrates the amount of improvement achieved by using the developed model.

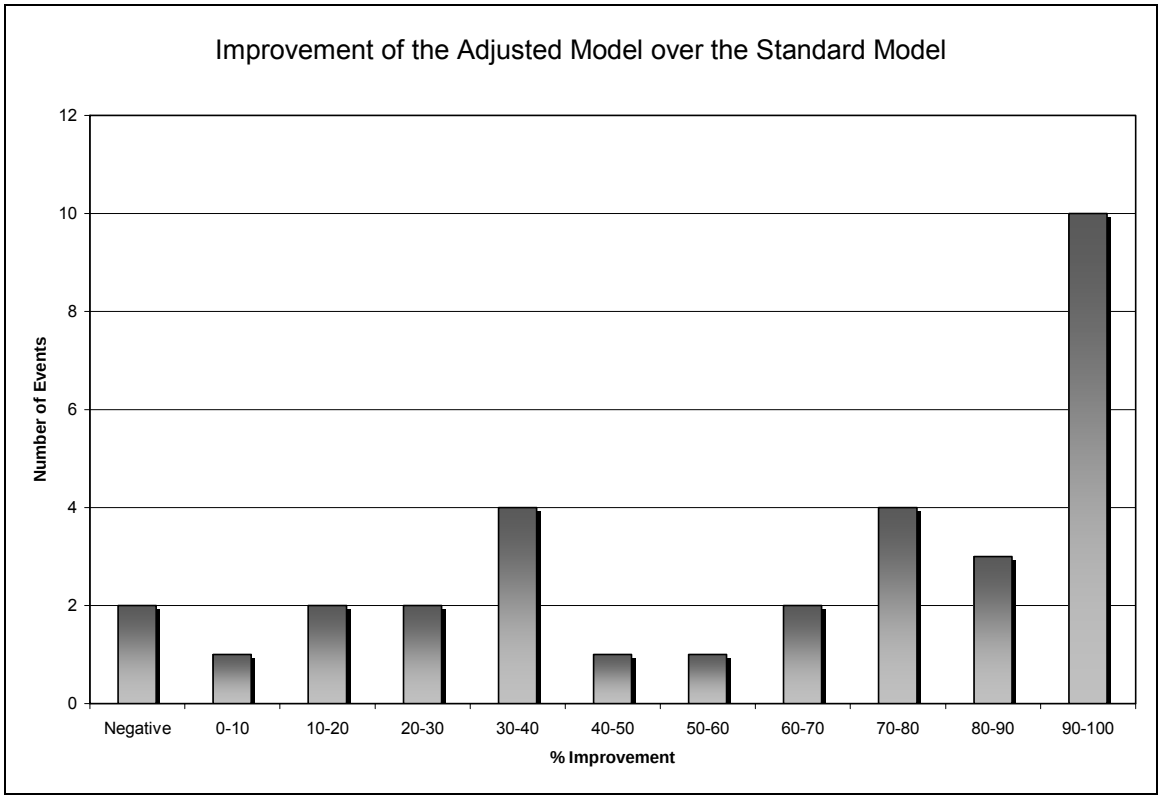

Figure 5.1 Improvement of the Developed model over the Standard Model

A summary of the results from the standard model and the developed model, methods 1 and 2, is presented in Appendix E. Graphical comparisons of the results of the different models for each storm are found in Appendix F.

5.3.2 Reproducibility

To determine whether the developed model would work for all storm conditions, it was run on storms with various initial parameters. The results of each of the 32

modeled storms run were graphed versus the temperature of the water, the recorded value of the initial moisture content, and initial ponded depth as seen in Figures 5.2 to 5.4.

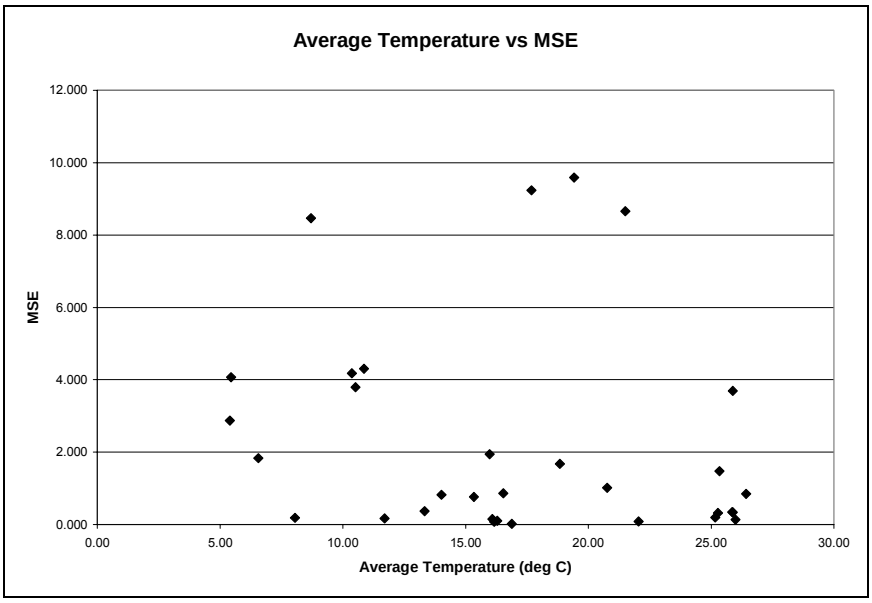

Figure 5.2 Average Water Temperature vs. MSE of the Developed Model

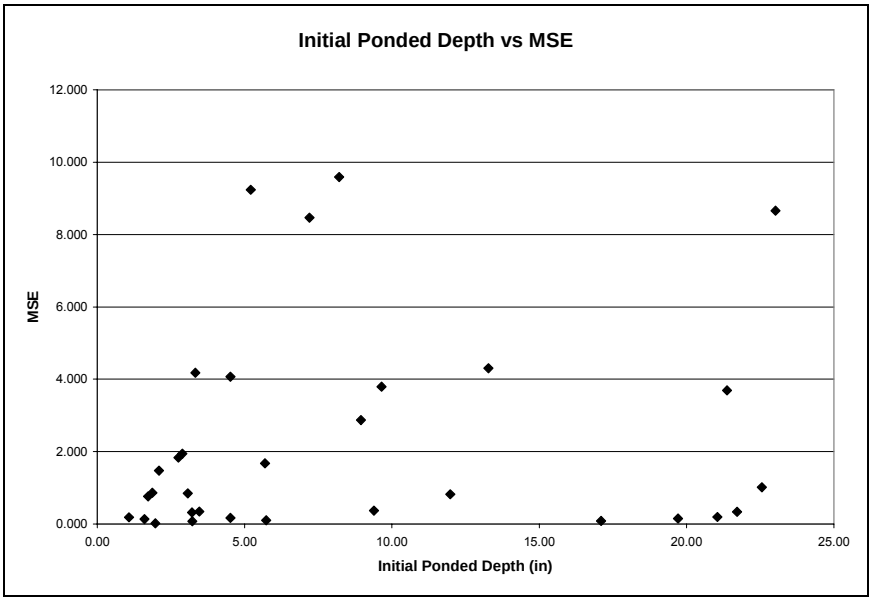

Figure 5.3 Initial Ponded Depth vs. MSE of the Developed Model

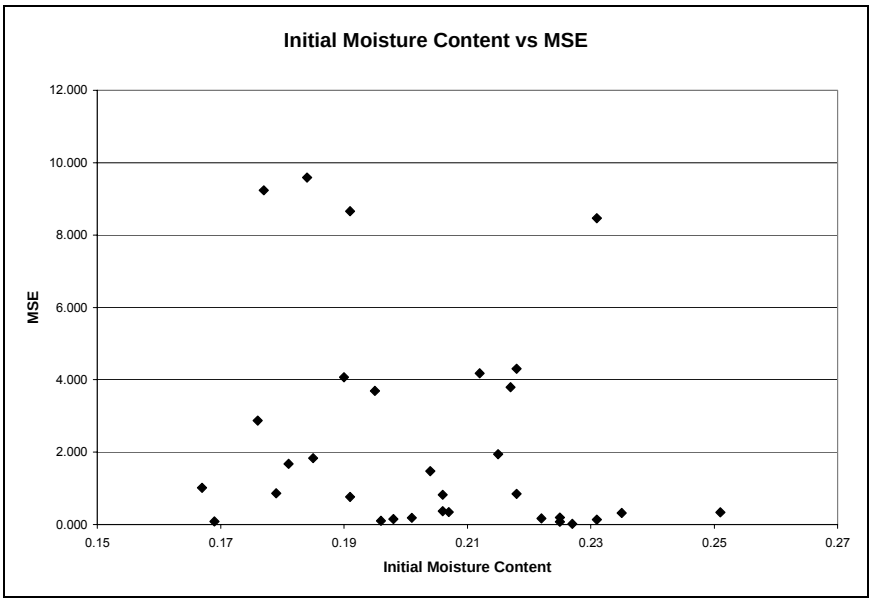

Figure 5.4 Initial Moisture Content vs. MSE of the Developed Model

These figures demonstrate that no clear pattern exists between any of the parameters and the MSE. This illustrates that there is no relationship between the parameters and the model results. To check this, different trendlines were fit to the data, but as the R^2 values show in Table 5.4, no strong relationship exists between the tested input parameters and the model results. This suggests that the developed model can be effectively applied to a variety of storms having a wide range of initial conditions.

	Average Temperature	**Ponded Depth (in)**	**θ_i**
Linear	0.0386	0.0156	0.0504
Logarithmic	0.0360	0.0556	0.0489
Polynomial (2nd Order)	0.0400	0.0809	0.0519
Power	0.0792	0.0459	0.0918
Exponential	0.0627	0.0105	0.0961

Table 5.4 R^2 Values of Trendlines Fit to Graphs in Figures 5.2 though 5.4

5.4 Sensitivity Analysis Results

Sensitivity analyses were performed to determine the effects of various input parameters. By varying input parameter values and measuring the change in the proposed model results, it was determined which parameters have a greater effect on the developed model. This section presents these results.

5.4.1 Wetting Front Depth

The initial wetting front depth, h_w, was estimated from the water content reflectometer data as described in Chapter 4. Because this data would not normally be available to a designer, it was important to investigate the effect that this parameter has on the model results. A sensitivity analysis was performed on five storms by varying the initial wetting front depth from 1 to 100 inches as well as having Excel solve for the optimized value of the initial depth. The five storms were selected randomly from the original 32 storm events. The MSE of each run and the percent change from the original run are presented in Table 5.5. Graphical results comparing each run are found in Appendix G.

		Original	h_w = 1	h_w = 25	h_w = 50	h_w = 100	optimized h_0
11/04/03	MSE	0.018	0.517	0.024	0.033	0.137	0.018
	Δ%		-2732.27%	-32.36%	-78.61%	-651.53%	1.18%
07/12/04	MSE	18.875	1.926	10.712	26.679	52.412	0.770
	Δ%		89.80%	43.25%	-41.35%	-177.68%	95.92%
10/14/04	MSE	9.237	13.316	6.487	2.903	0.162	0.000
	Δ%		-44.16%	29.78%	68.57%	98.24%	100.00%
01/11/05	MSE	0.233	0.110	0.232	0.288	0.361	0.093
	Δ%		52.88%	0.69%	-23.49%	-54.98%	60.23%
06/03/05	MSE	1.671	6.291	1.737	0.270	0.534	0.001
	Δ%		-276.55%	-3.96%	83.83%	68.03%	99.92%

Table 5.5 MSE Results of the Wetting Front Depth Sensitivity Analysis

Table 5.6 presents the wetting front depths of the original run with the estimated value of the wetting front depth as well as the optimized values calculated using the Excel Solver function in the final run. Solver determined the optimal value by holding all other parameters constant and varying the initial wetting front depth to minimize the MSE of the model.

	Original	Optimized
11/04/03	35.34	33.58
07/12/04	37.79	2.23
10/14/04	10.34	130.81
01/11/05	25.62	0.65
06/03/05	25.76	67.67

Table 5.6 Wetting Front Depths for Original and Optimized Runs

The wetting front depth sensitivity analysis showed no real pattern but it did show the impact of the value of the wetting front depth on the model. Changing the wetting front depth greatly affected the accuracy of the model but the measured value only produced the best model in one of the five storm events. This illustrates the need for further research to determine the most accurate way to estimate this parameter.

5.4.2 Saturated Hydraulic Conductivity

The site specific saturated hydraulic conductivity is not always available and is often estimated based on the hydrologic soil group. A sensitivity analysis was performed to determine the need for accuracy in this parameter. The same five storms from the analysis of the initial wetting front depth were used. The saturated hydraulic conductivity was increased and decreased by 10% and 20% and the MSE from each run was compared to the original run. The values of saturated hydraulic conductivity used in the analysis are presented in Table 5.7. Graphical results comparing runs are found in Appendix H.

	(in/hr)	(cm/hr)
K_{sat} +20%	0.2840	0.7214
K_{sat} +10%	0.2604	0.6613
Original	0.2367	0.6012
K_{sat} -10%	0.2130	0.5411
K_{sat} -20%	0.1894	0.4810

Table 5.7 Saturated Hydraulic Conductivity Sensitivity Analysis

The results of the analysis are summarized in Table 5.8.

	Original	K_{sat} +20%	K_{sat} +10%	K_{sat} -10%	K_{sat} -20%
11/04/03	0.018	0.029	0.018	0.031	0.057
		-58.80%	1.59%	-69.39%	-213.78%
07/12/04	18.875	11.485	14.880	23.543	28.974
		39.15%	21.17%	-24.73%	-53.51%
10/14/04	9.237	10.056	9.680	8.711	8.072
		-8.86%	-4.79%	5.70%	12.62%
01/11/05	0.233	0.170	0.200	0.270	0.310
		26.93%	14.15%	-15.65%	-32.95%
06/03/05	1.671	2.302	2.001	1.310	0.924
		-37.77%	-19.78%	21.62%	44.67%

Table 5.8 MSE Results of the Saturated Hydraulic Conductivity Sensitivity Analysis

The values of the adjusted hydraulic conductivity that resulted from the changes to the saturated hydraulic conductivity are given in Table 5.9.

K_{adj} Values					
	Original	K_{sat} +20%	K_{sat} +10%	K_{sat} -10%	K_{sat} -20%
11/04/03	0.0076	0.0091	0.0084	0.0068	0.0061
07/12/04	0.0061	0.0074	0.0068	0.0055	0.0049
10/14/04	0.0051	0.0061	0.0056	0.0046	0.0041
01/11/05	0.0057	0.0069	0.0063	0.0052	0.0046
06/03/05	0.0055	0.0066	0.0060	0.0049	0.0044

Table 5.9 Effects of Ksat on Kadj

As with the wetting front depth examination, no real pattern emerged from this analysis. Also similar, the measured value did not always produce the best model. The analysis did, however, show the large variability of the results of the model that this

parameter caused, which highlights the need for an accurate value of saturated hydraulic conductivity. More research is needed to determine the most appropriate method of obtaining this value.

5.4.3 Temperature

One of the main parameters studied in this paper is the temperature of the ponded water. The verification of the model illustrated that adjusting for the temperature of the water produces a more accurate model. A sensitivity analysis showed the effects that the temperature of the water has on the infiltration of the water from the bed.

The temperature analysis was run on a simulated storm with a fifteen inch ponded depth and initial condition as listed in Table 5.10.

T	(°C)	20.0
θ_i		0.20
ho	(in)	15.00
z	(in)	26.00
ψ	(in)	5077.15
K_{adj}	(in/hr)	0.0021
$\Delta\theta$	(in^3/in^3)	0.150

Table 5.10 Initial Parameters of the Test Storm

Figure 5.5 shows the depth of water versus time graph that resulted from the model run with the initial conditions.

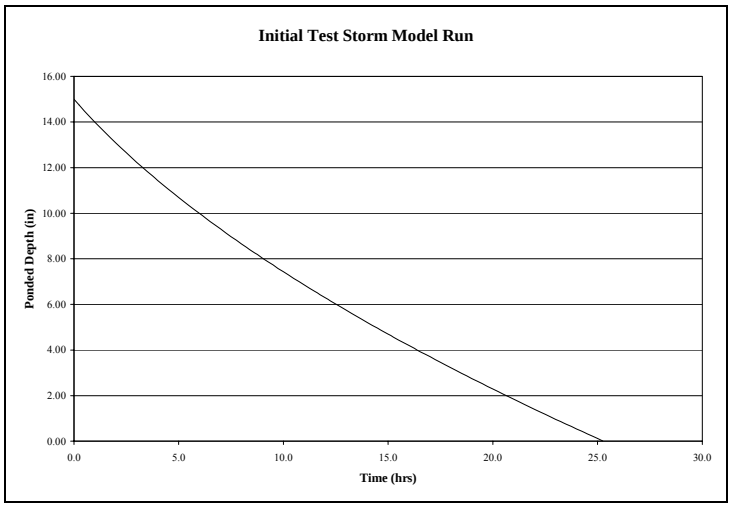

Figure 5.5 Ponded Depth vs Time of the Initial Run of the Test Storm

The sensitivity analysis was performed by varying the temperature between 5 and 35 degrees Celsius and the MSE of each run was compared to the initial run with a temperature of 20 degrees Celsius. Runs 1-4 performed on the simulated storm varied the temperature input as follows:

Initial Run – Temperature at 20°C
Run 1 – Temperature at 5°C
Run 2 – Temperature at 15°C
Run 3 – Temperature at 25°C
Run 4 – Temperature at 35°C

Depending on the temperature input, the bed emptied within 22 to 38.25 hours compared to the initial run at 20 degrees Celsius which emptied in 25.25 hours as seen in Figure 5.6:

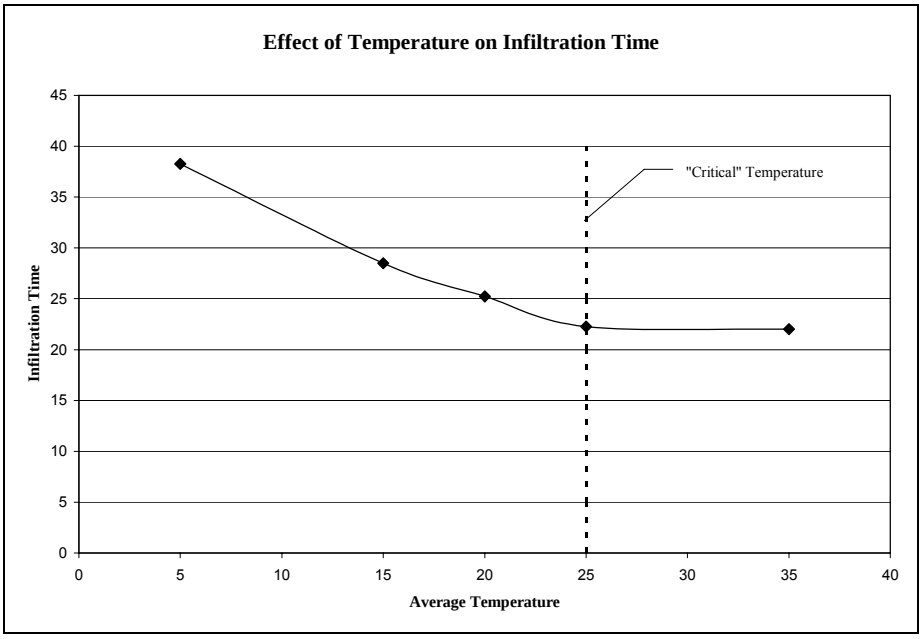

Figure 5.6 Total Infiltration Time vs. Average Temperature of Ponded Water

Figure 5.7 shows the variation in the model when run for different temperatures.

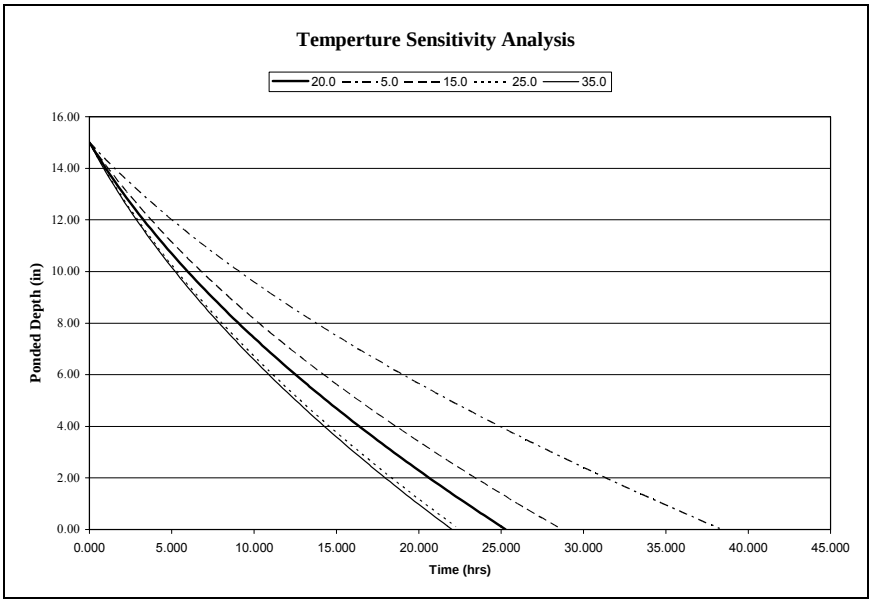

Figure 5.7 Ponded Depth vs. Time for Various Temperatures

		Initial	Run 1	Run 2	Run 3	Run 4
T	(°C)	20.0	5.0	15.0	25.0	35.0
θ_i		0.20	0.20	0.20	0.20	0.20
h_0	(in)	15.00	15.00	15.00	15.00	15.00
z	(in)	26.00	26.00	26.00	26.00	26.00
Y	(in)	5077.15	5077.15	5077.15	5077.15	5077.15
K_{adj}	(in/hr)	0.0021	0.0014	0.0019	0.0024	0.0024
$\Delta\theta$	(in^3/in^3)	0.150	0.150	0.150	0.150	0.150
Infiltration Time	(hr)	25.250	38.250	28.500	22.250	22.000

Table 5.11 Input Parameters and Results of Temperature Sensitivity Analysis

	Run 1	Run 2	Run 3	Run 4
T	-75.00%	-25.00%	25.00%	75.00%
K_{adj}	-34.09%	-11.87%	12.45%	14.76%
Infiltration Time	51.49%	12.87%	-11.88%	-12.87%

Table 5.12 Percent Change of Parameter Results

This analysis was performed to illustrate the effects of temperature on the infiltration process and its importance in accurate modeling. Table 5.12 shows the percent change from the initial run value of the parameters that were affected by the temperature. For both affected parameters, the effect of the temperature change was less than the percent change in the temperature but it did show up to a 51.49% change in the time to drain the basin from the original time at 20°C. Between 5 and 25° C there was a 12 hour difference in the time it took the bed to empty. Increasing the temperature another 10° to 35° C only decreased the infiltration time by 15 minutes. From this it can be concluded that modeling an infiltration basin with a range of temperatures from 5 to 25° C will provide a better understanding and estimate of the BMP's overall performance and efficiency.

5.4.4 Initial Moisture Content

The initial moisture content of the soil affects multiple parameters and calculations performed in the adjusted Green and Ampt model. A sensitivity analysis was performed to study how a change in that value affects the results of the model, based on the same test storm used for the temperature analysis. The data and graph of the initial run of this storm are shown in Table 5.10 and Figure 5.5.

The residual and saturated moisture contents (θ_r and θ_s) used in the van Genuchten curve fitting were 0.10 and 0.35, respectively. The sensitivity analysis was performed by running the same simulated storm used in the temperature analysis using various initial moisture contents between θ_r and θ_s as follows:

Initial Run – Initial Moisture Content at 0.20
Run 5 – Initial Moisture Content at 0.11
Run 6 – Initial Moisture Content at 0.17
Run 7 – Initial Moisture Content at 0.23
Run 8 – Initial Moisture Content at 0.28
Run 9 – Initial Moisture Content at 0.34

Figure 5.8 shows how the initial moisture content varies the calculated infiltration time of the event.

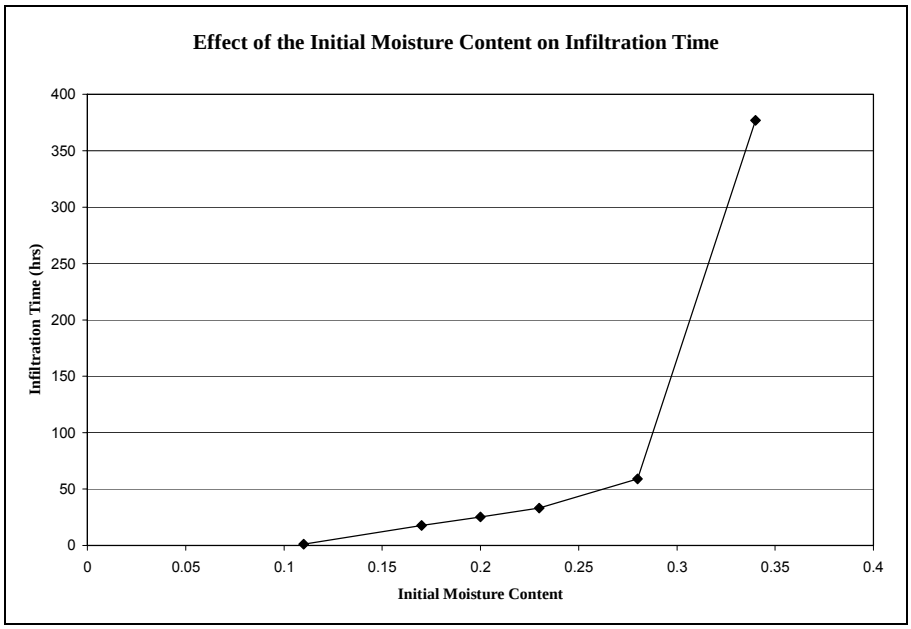

Figure 5.8 Total Infiltration Time vs. Initial Moisture Content

The results can be seen graphically in Figure 5.9:

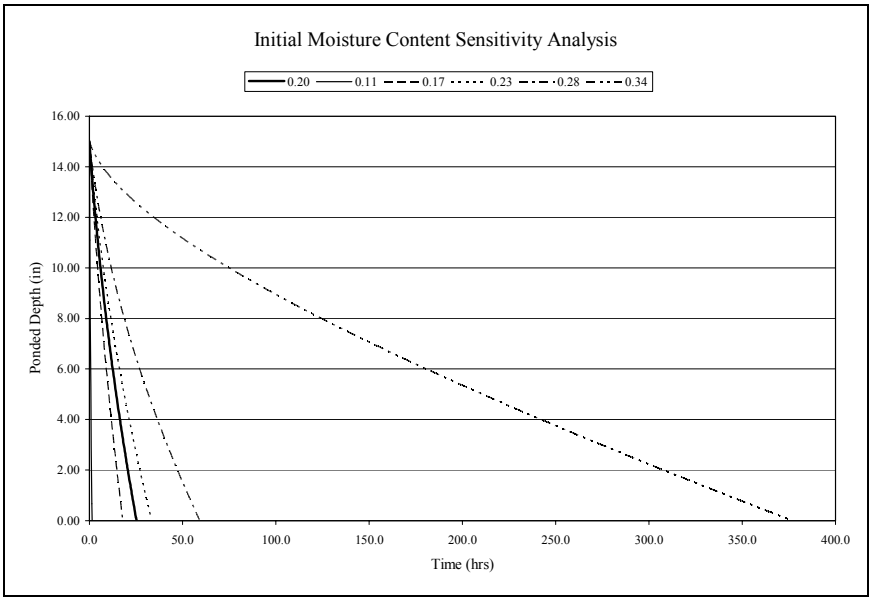

Figure 5.9 Ponded Depth vs. Time for Various Initial Moisture Contents

		Run 5	Run 6	Run 7	Run 8	Run 9
T	(°C)	20	20	20	20	20
θ_i		0.11	0.17	0.23	0.28	0.34
h_0	(in)	15.00	15.00	15.00	15.00	15.00
z	(in)	26.00	26.00	26.00	26.00	26.00
Y	(in)	342021.51	9992.44	2974.63	1333.53	262.77
K_{adj}	(in/hr)	0.0005	0.0014	0.0030	0.0049	0.0080
$\Delta\theta$	(in^3/in^3)	0.240	0.180	0.120	0.070	0.010
Infiltration Time	(hr)	1.250	17.750	33.250	59.000	377.000

Table 5.13 Input Parameters and Results of Initial Moisture Content Sensitivity Analysis

Table 5.14 illustrates the effects of different initial moisture contents on the other parameters in the model as well as the results. The percent change of each value compared to the original value from Run 5 is presented.

	Run 5	Run 6	Run 7	Run 8	Run 9
θ_i	-45.00%	-15.00%	15.00%	40.00%	70.00%
Y	1315367.35%	38332.47%	11340.87%	5028.97%	910.65%
K_{adj}	-77.57%	-33.39%	41.82%	131.91%	276.81%
$\Delta\theta$	60.00%	20.00%	-20.00%	-53.33%	-93.33%
Time	-95.05%	-29.70%	31.68%	133.66%	1393.07%

Table 5.14 Percent Change in Parameter Results from Initial Run

In all cases, the increase or decrease of the parameter was larger than the percent change of the initial moisture content. This illustrates the significance of the value of the initial moisture content on the results of an infiltration model. Specific conditions could be run to demonstrate a certain scenario or the model can be run for a range of initial moisture conditions to create an overall view of the BMP's performance.

Chapter 6: Summary and Conclusion

The results of the verification of the model are shown in Table 5.1. It was demonstrated that the developed model created in this study produced a more accurate model than a standard Green and Ampt model approximately 94% of the time. The increase in accuracy was illustrated in Figure 5.1. Ten of the thirty two storms had results that were improved more than 90% from the standard model. Two methods of determining the initial moisture content model input were utilized to obtain the best overall results. Method 1 used the recorded value of the initial moisture content while Method 2 used a value of initial moisture content that was adjusted based on the saturation level. It was hypothesized that the larger ponded depths resulted in higher maximum moisture contents because the head allowed for more air to be pushed out of the voids of the soil while in smaller events, the moisture content leveled off at lower values due to lack of head and increased levels of air remaining in the soil.

Table 4.4 listed the initial ponded depths, average temperatures and initial moisture contents of the modeled storm events. This verification was done to illustrate that the model was verified using storms with a variety of initial conditions. It was important to ensure that the model produced improved results for all conditions and not only in specific cases. A trendline analysis was performed on the graphs of the initial parameters versus the MSE of the modified model to demonstrate that no relationship existed between any of the parameters and the model results.

The wetting front depth and saturated hydraulic conductivity were estimated parameters in the model. The wetting front depth was calculated based on the response times of the water content reflectometers at various depths below the bed. The saturated

hydraulic conductivity was taken from soils testing performed at the site. Sensitivity analyses were performed on these parameters to determine the effects that they have on the model. The results of these analyses are shown in Tables 5.5 and 5.8. While both factors did affect the model results, the initial wetting front depth had a greater effect.

The parameters used to modify the Green and Ampt model were the average temperature of the ponded water and the initial water content of the soil. Sensitivity analyses were performed for these parameters by varying the values used in a test storm. The goal was to show the influence that these factors have on the time it took for the underground rock storage bed to empty. The results of these analyses can be seen in Figures 5.7 and 5.9. The 700% increase in the temperature of the water, from 5 to 35°C, varied the infiltration time of fifteen inches of ponded depth from 22 hours to 38.25 hours which represents a 172% increase in infiltration time depending on the temperature of the ponded water. The higher the temperature of the ponded water the faster the bed emptied up to 25°C. Temperatures higher than 25°C had essentially no change on the results of the model.

The sensitivity analysis for the initial moisture content, which was varied by approximately 310%, from 0.11 to 0.34, showed that the infiltration time varied from 1.25 hours to 377 hours. This represents a 30,160% change in infiltration time depending on the initial moisture content used in the model. Lower initial moisture contents resulted in faster infiltration while levels near saturation can severely increase the time it takes the bed to empty.

This analysis showed that both parameters greatly affected the results of the infiltration model while the initial moisture content clearly has a much larger effect on

the infiltration rate. The results illustrate the importance of taking these factors into consideration when modeling the infiltration from a large underground rock storage bed.

The results of this research can be used by designers to obtain a more accurate image of the infiltration from an underground rock storage bed. First, the modification and sensitivity analysis of the saturated hydraulic conductivity demonstrates the importance of soils testing in the design of infiltration structures. It is vital to have an accurate measurement of the saturated hydraulic conductivity as well as an estimate of the response of that parameter to varying moisture contents.

Secondly, it was demonstrated that using event specific initial moisture content and temperature produced a better infiltration model than using standard or typical values. This information can be used by designers in a variety of ways. Using the proposed method would allow an underground storage bed to be modeled for specific conditions that will be more representative of average site conditions. An infiltration bed in a geographic location that is hot and dry will perform much differently from one in an area that is cold and wet. The modified method can also be used to vary the initial parameters so that designers can see the range of performance of the BMP. This can be especially helpful in urban areas where the size of the BMP may be a consideration.

Average temperature and rainfall can be analyzed to determine what operating conditions are most critical for the particular BMP. For example, it may not be necessary to design for saturated moisture conditions if that is not a normal condition at the site. In general, this proposed model will allow designers to create a better representation of how an underground rock storage bed will actually perform. The best design process would be to utilize continuous modeling to simulate the performance of

the BMP under a variety of temperature and antecedent moisture conditions expected to occur during a typical year.

Chapter 7: Research Recommendations

Recommendations for Future Work

- Because the initial wetting front depth had significant effects on the results of the model, this parameter should be studied further to develop a better estimation. The data of the water content reflectometers should be analyzed to determine how the wetting front depth moves through the soil and if saturation is really reached above that depth.
- It would also be beneficial to determine a relationship between rainfall parameters and wetting front depth. Since this information would not be available to designers, it would be necessary to determine a method of estimating that value based on rainfall.
- In this analysis, two methods of obtaining the initial moisture content were used. One method worked better for storms with larger ponded depths. It was hypothesized that this was due to entrapped air in the soil. This hypothesis should be tested using the data from the water content reflectometers.
- The effect of temperature on the saturation level should be investigated.
- This research focused on the recession limb of the depth of water in the bed due to the lack of information on the inflow to the rock bed. It would be beneficial to install additional instrumentation to measure the inflow of the infiltration bed to look at the efficiency of the BMP and to be able to analyze the entire performance of the site.
- This research focused on individual rainfall events. It would be valuable to be able to model infiltration BMPs with a continuous model. Therefore, more

research needs to be done on the recovery of the infiltration rate between rainfall events. Water content data collected at the Villanova Porous Concrete site could be used to develop a model of the drying process of the soil.

- This research illustrated the importance of having a site specific infiltration rate in modeling BMPs. There are currently a number of methods of measuring this value including percolation tests and double ring infiltrometers. Various methods to measure infiltration could be tested at the Villanova Porous Concrete site to determine which method is more accurate under field conditions.

References

American Society for Testing Materials (2000). "Standard Test Method for Measurement of Soil Potential (Suction) Using Filter Paper (ASTM D 5298-94)," *Annual Book of ASTM Standards*, Section Four, Construction, Volume 4.08.

Aggelides, S. and Youngs, E. G. (1978). "The Dependence of the Parameters in the Green and Ampt Infiltration Equation on the Initial Water Content in Draining and Wetting States." *Water Resources Research*, 14, 857-862.

Akan, A. O. (2002). "Sizing Stormwater Infiltration Structures." *Journal of Hydraulic Engineering*, 128, 534-537.

Al-Muttair, F. F., and Al-Turbak, A. S. (1991). "Modeling of Infiltration from An Artificial Recharge Basin with a Decreasing Ponded Depth." *Journal of King Saud University. Engineering Sciences*, 3, 89-99.

Bedient, P. B. and Huber, W. C. (2002). Hydrology and Floodplain Analysis. Prentice Hall, Inc., 3rd Ed. Upper Saddle River, NJ.

Bloomfield, P. H. I'A., Pilgrim, D. H., and Watson, K. K. (1981). "The Infiltration-Soil Water Storage Relationship at a Point in Watershed Modeling." *Water Resources Research*, 17, 370-376.

Braga, A. (2005). "An Infiltration Analysis of the Villanova Porous Concrete Infiltration Basin BMP." *Masters Thesis*. Villanova University, Villanova, PA.

Campbell Scientific (2000). "CR23X Micrologger Operator's Manual." Campbell Scientific, Logan, UT.

Campbell Scientific (2003). "CR200 Datalogger Operator's Manual." Campbell Scientific, Logan, UT.

Campbell Scientific (2003). "NL100/105 Network Link Interface Instruction Manual." Campbell Scientific, Logan, UT.

Campbell Scientific (2003). "TE525 Tipping Bucket Rain Gage." Campbell Scientific, Logan, UT.

Campbell Scientific (2006). "CS616 Water Content Reflectometer Instruction Manual." Campbell Scientific, Logan, UT.

Celia, M. A. et al. (1993). "Unsaturated Zone Hydrology: Modeling, Monitoring and Remediation, Book 1, Short Course, January 18-21, 1993" Princeton University Water Resources Program, Princeton, NJ.

Constantz, J. and Murphy. F., (1991). "The Temperature Dependence of Ponded Infiltration Under Isothermal Conditions." *Journal of Hydrology*, 122, 119-128.

Emerson, C. H., Welty, C., and Traver, R. G. (2005). "Watershed-Scale Evalutation of a System of Storm Water Detention Basins." *Journal of Hydrologic Engineering*, 10, 237-242.

Freyberg, D. L., Reeder, J. W., Franzini, J. B., and Remson, I. (1980). "Application of the Green-Ampt Model to Infiltration Under Time-Dependent Surface Water Depths." *Water Resources Research*, 16, 517-528.

Green, W. H., and Ampt, G. A. (1911). "Studies of Soil Physics, 1: The Flow of Air and Water Through Soils." *Journal of Agriculture Science*, 4(1), 1-24.

Guo, J. C. Y., and Hughes, W. (2001). "Storage Volume and Overflow Risk for Infiltration Basin Design." *Journal of Irrigation and Drainage Engineering*, 127(3), 170-175.

Guo, J. C. Y. (2002). "Overflow Risk Analysis for Stormwater Quality Control Basins." *Journal of Hydrologic Engineering*, 7(6), 428-434.

Gusev, E. M. (1978). "Dependence of Infiltration Rate on the Initial Soil Moisture Content." *Water Resources*, 5, 656-661.

Hino, M., Odaka, Y., Nadaoka, K., and Sato, A. (1988). "Effect of Initial Soil Moisture Content on the Vertical Infiltration Process – A Guide to the Problem of Runoff-Ratio and Loss." *Journal of Hydrology*, 102, 267-284.

Hsu, S. M., Ni, C., and Hung, P. (2002). "Assessment of Three Infiltration Formulas based on Model Fitting on Richards Equation." *Journal of Hydrologic Engineering*, 7, 373-379.

Instrumentation Northwest (2002). "PS-9805 Submersible Pressure/Temp. Transducer Instruction Manual." Instrumentation Northwest, Kirkland, WA.

Instrumentation Northwest (2002). "Submersible Pressure Transmitter PS9800 Instruction Manual." Instrumentation Northwest, Kirkland, WA.

Instrumentation Northwest (2004). "AquiStar PT2X Smart Sensor Instruction Manual." Instrumentation Northwest, Kirkland WA.

Jaynes, D. B. (1990). "Temperature Variations Effect on Field-Measured Infiltration." *Soil Sci. Soc. of Am. Journal*, 54, 305-312.

Kwiatkowski, M. (2004). "A Water Quantity Study of a Porous Concrete Infiltration Best Management Practice." *Masters Thesis*. Villanova University, Villanova, PA.

Ladd, T. (2004). "A Water Quantity Study of a Porous Concrete Infiltration Best Management Practice." *Masters Thesis.* Villanova University, Villanova, PA.

Maryland Department of Natural Resources. (1984). "Standards and Specifications for Infiltration Practices."

Pennsylvania Department of Environmental Protection (2006). *Pennsylvania Best Management Practices Manual, Draft April 2006*, Pennsylvania Bulletin, 34, 20.

Philip, J. R., (1957). "The Theory of Infiltration: 1. The Infiltration Equation and its Solution." *Soil Sci*., 83, 345-357.

Traver, R. G., and Chadderton, R. A. (1983) "The Downstream Effects of Storm Water Detention Basins" *International Symposium on Urban Hydrology, Hydraulics and Sediment Control*, University of Kentucky, Lexington, KY, 455-460.

Traver, R. and Welker A. (2003). "Quality Assurance – Quality Control Project Plan" Villanova Stormwater Porous Concrete Demonstration Site – A Retrofit.

Traver, R.; Welker, A.; Emerson, C.; Kwiatkowski, M.; Ladd, T.; Kob, L. (2003). "Lessons Learned – Porous Concrete Demonstration Site." *Stormwater*, 5(6).

Traver, R.; Welker, A.; Horst, M.; Braga, A.; Vanacore, M.; Kob, L. (2005). "Lessons Learned II– Porous Concrete Demonstration Site." *Stormwater*, 6(5).

van Genuchten, M. Th. (1980). "A Closed-form Equation for Predicting the Hydraulic Conductivity of Unsaturated Soils." *Soil Sci. Soc. Am. J.*, 44, 892-898.

Viessman Jr., Warren and Lewis, Gary L. (2003). Introduction to Hydrology. Pearson Education, Inc., 5 ed. Upper Saddle River, NJ.

Appendices

Appendix A

Sample Model Worksheet

October 26, 2006

Initial Conditions						
Initial Ponded Depth	Initial Wetting Front Depth	Capillary Suction	Rock Bed Porosity	Adjusted Hydraulic Conductivity	Initial Soil Moisture Deficit	Time Increment
h_0	**h_w**	**Y**	**n**	**K_{adj}**	**$\Delta\theta$**	**Δt**
(in)	(in)	(in)	(in^3/in^3)	(in/hr)	(in^3/in^3)	(hr)
17.96	36.38	5281.29	0.40	0.0019	0.152	0.250

	Cumulative Time (hr)	**Infiltration Rate** (in/hr)	**Cumulative Infiltrated Depth** (in)	**Ponded Depth** (in)	**Wetting Front Depth** (in)	**Recorded Ponded Depth** (in)	**Square Error** $(y_m-y_a)^2$
	0.000	0.27	5.53	17.957	36.38	17.957	0.00
	0.250	0.27	5.60	17.786	36.83	17.800	0.00
	0.500	0.27	5.67	17.617	37.27	17.623	0.00
10/27/03 22:00	0.750	0.26	5.73	17.450	37.71	17.510	0.00
10/27/03 22:15	1.000	0.26	5.80	17.284	38.14	17.363	0.01
10/27/03 22:30	1.250	0.26	5.86	17.121	38.57	17.220	0.01
10/27/03 22:45	1.500	0.26	5.93	16.960	39.00	17.073	0.01
10/27/03 23:00	1.750	0.25	5.99	16.800	39.42	16.897	0.01
10/27/03 23:15	2.000	0.25	6.06	16.642	39.84	16.770	0.02
10/27/03 23:30	2.250	0.25	6.12	16.486	40.25	16.607	0.01
10/27/03 23:45	2.500	0.25	6.18	16.331	40.65	16.467	0.02
10/28/03 0:00	2.750	0.24	6.24	16.178	41.06	16.303	0.02
10/28/03 0:15	3.000	0.24	6.30	16.026	41.46	16.160	0.02
10/28/03 0:30	3.250	0.24	6.36	15.875	41.85	15.983	0.01
10/28/03 0:45	3.500	0.24	6.42	15.727	42.24	15.820	0.01
10/28/03 1:00	3.750	0.23	6.48	15.579	42.63	15.693	0.01
10/28/03 1:15	4.000	0.23	6.54	15.433	43.02	15.550	0.01
10/28/03 1:30	4.250	0.23	6.60	15.288	43.40	15.390	0.01
10/28/03 1:45	4.500	0.23	6.65	15.144	43.78	15.243	0.01
10/28/03 2:00	4.750	0.23	6.71	15.002	44.15	15.083	0.01
10/28/03 2:15	5.000	0.22	6.77	14.861	44.52	14.953	0.01
10/28/03 2:30	5.250	0.22	6.82	14.721	44.89	14.810	0.01
10/28/03 2:45	5.500	0.22	6.88	14.582	45.26	14.667	0.01
10/28/03 3:00	5.750	0.22	6.93	14.444	45.62	14.520	0.01
10/28/03 3:15	6.000	0.22	6.99	14.308	45.98	14.380	0.01
10/28/03 3:30	6.250	0.22	7.04	14.172	46.34	14.247	0.01
10/28/03 3:45	6.500	0.21	7.10	14.038	46.69	14.120	0.01
10/28/03 4:00	6.750	0.21	7.15	13.904	47.04	13.990	0.01
10/28/03 4:15	7.000	0.21	7.20	13.771	47.39	13.847	0.01
10/28/03 4:30	7.250	0.21	7.26	13.640	47.74	13.700	0.00
10/28/03 4:45	7.500	0.21	7.31	13.509	48.08	13.573	0.00
10/28/03 5:00	7.750	0.21	7.36	13.380	48.42	13.410	0.00
10/28/03 5:15	8.000	0.20	7.41	13.251	48.76	13.317	0.00
10/28/03 5:30	8.250	0.20	7.46	13.123	49.10	13.170	0.00
10/28/03 5:45	8.500	0.20	7.51	12.996	49.43	13.043	0.00
10/28/03 6:00	8.750	0.20	7.56	12.870	49.76	12.930	0.00
10/28/03 6:15	9.000	0.20	7.61	12.744	50.09	12.813	0.00
10/28/03 6:30	9.250	0.20	7.66	12.620	50.42	12.707	0.01
10/28/03 6:45	9.500	0.20	7.71	12.496	50.75	12.590	0.01
10/28/03 7:00	9.750	0.20	7.76	12.373	51.07	12.450	0.01

Appendix B

Reduced Storm List

Storm	Rainfall Start	Rainfall End	Rainfall Duration (hr)	Max 1 Hour Precipitation (in)	Total Precipitation (in)	Rainfall Intensity (in/hr)	Antecedant Dry Time (hr)
October 14, 2003	20:10	4:25	8.25	0.62	1.35	0.16	242.6
October 26, 2003	21:05	19:50	22.75	0.86	2.73	0.12	105.5
November 4, 2003	21:00	22:20	49.33	0.16	0.78	0.02	83.9
November 19, 2003	5:05	3:40	22.58	0.68	1.64	0.07	146.8
November 28, 2003	7:50	2:00	18.17	0.32	0.84	0.05	79.7
January 4, 2004	18:20	23:00	28.67	0.12	0.55	0.02	180.2
March 30, 2004	17:40	2:00	8.33	0.2	0.67	0.08	195.3
April 12, 2004	12:15	2:25	62.17	0.23	2.10	0.03	20.5
April 23, 2004	18:10	23:15	5.08	0.44	0.77	0.15	129.2
May 2, 2004	11:35	22:05	34.33	0.28	0.95	0.03	71.3
June 22, 2004	17:35	18:05	0.50	0.59	0.59	1.18	112.9
July 12, 2004	2:00	2:20	24.33	0.7	3.58	0.15	102.3
July 18, 2004	4:55	21:30	16.58	0.15	0.74	0.04	52.8
July 23, 2004	13:50	16:45	2.92	0.73	0.85	0.29	83.3
July 27, 2004	10:40	3:55	17.25	1.13	2.73	0.16	60.8
August 1, 2004	4:20	9:00	4.67	0.97	2.08	0.45	28.8
September 18, 2004	0:55	15:05	14.83	0.51	2.27	0.15	46.1
September 27, 2004	23:05	5:10	30.08	1.38	5.91	0.20	162.7
October 14, 2004	3:35	10:40	7.08	0.29	0.91	0.13	289.4
October 30, 2004	1:55	4:55	3.00	0.47	0.57	0.19	179.0
November 4, 2004	10:45	20:10	9.42	0.44	1.33	0.14	98.8
November 12, 2004	6:30	3:25	20.92	0.13	1.36	0.07	89.5
December 9, 2004	15:25	13:10	44.75	0.04	0.98	0.02	0.0
December 23, 2004	9:30	18:40	9.17	0.01	1.11	0.12	86.8
January 5, 2005	2:10	2:15	48.08	0.1	0.99	0.02	19.8
February 14, 2005	9:35	22:55	13.33	0.22	1.15	0.09	99.6
May 20, 2005	3:30	15:25	11.92	0.14	0.78	0.07	418.0
June 3, 2005	4:30	8:45	28.25	0.26	1.40	0.05	132.3
July 15, 2005	16:15	17:20	1.08	1.01	1.03	0.95	126.6
July 17, 2005	5:55	14:05	32.17	0.24	0.35	0.01	0.0
October 7, 2005	7:05	6:10	47.08	0.89	5.48	0.12	187.0
October 21, 2005	7:40	5:40	46.00	0.25	1.36	0.03	155.3

Appendix C

Initial Moisture Content Analysis

Storm	Water Content at 1 ft (0.3 m)				Water Content at 2 ft (0.6 m)				Water Content at 4 ft (1.2 m)			
	Initial WC at Rainfall Start	*Moisture Meter Response*	*Maximum Water Content*	*Response Time*	*Initial WC at Rainfall Start*	*Moisture Meter Response*	*Maximum Water Content*	*Response Time*	*Initial WC at Rainfall Start*	*Moisture Meter Response*	*Maximum Water Content*	*Response Time*
October 14, 2003	0.184	10/15/03 8:15	0.232	12.083	0.207	10/15/03 16:45	0.220	20.583	0.216	10/16/03 14:15	0.218	42.083
October 26, 2003	0.198	10/27/03 10:15	0.249	13.167	0.214	10/27/03 13:45	0.234	16.667	0.218	10/28/03 5:45	0.221	32.667
November 4, 2003	0.227	11/6/03 2:15	0.233	29.250	0.237	11/6/03 13:30	0.237	40.500	0.235	11/7/03 20:15	0.232	71.250
November 19, 2003	0.206	11/20/03 2:45	0.237	21.667	0.222	11/20/03 9:00	0.237	27.917	0.226	11/20/03 17:45	0.232	36.667
November 28, 2003	0.222	11/29/03 3:15	0.231	19.417	0.231	11/29/03 4:45	0.233	20.917	0.231	11/30/03 2:00	0.230	42.167
January 4, 2004	0.201	1/5/04 6:00	0.219	11.67	0.224	1/5/04 15:30	0.230	21.17	0.446			
March 30, 2004	0.212	3/31/04 8:00	0.246	14.33	0.238	3/31/04 17:15	0.254	23.58	0.255	4/7/04 12:00	0.260	186.33
April 12, 2004	0.218	4/13/04 3:30	0.240	15.25	0.233	4/13/04 8:15	0.242	20.00	0.249			
April 23, 2004	0.215	4/24/04 3:45	0.246	9.58	0.229	4/24/04 14:30	0.247	20.33	0.246	4/27/04 16:30	0.249	94.33
May 2, 2004	0.225	5/3/04 4:30	0.236	16.92	0.238	5/3/04 19:00	0.241	31.42	0.246			
June 22, 2004	0.204	6/23/04 1:00	0.229	7.42	0.219	6/23/04 2:30	0.229	8.92	0.227	6/24/04 7:00	0.229	37.42
July 12, 2004	0.195	7/12/04 9:15	0.255	7.25	0.208	7/12/04 14:15	0.249	12.25	0.218	7/13/04 2:00	0.240	24.00
July 18, 2004	0.235	7/18/04 16:45	0.240	11.83	0.242	7/19/04 0:15	0.242	19.33	0.239			
July 23, 2004	0.218	7/23/04 20:15	0.234	6.42	0.232	7/24/04 1:00	0.238	11.17	0.232			
July 27, 2004	0.225	7/27/04 17:00	0.257	6.33	0.234	7/27/04 22:30	0.257	11.83	0.232	7/28/04 11:15	0.250	24.58
August 1, 2004	0.251	8/1/04 7:30	0.271	3.17	0.254	8/1/04 8:15	0.272	3.92	0.250	8/1/04 15:15	0.267	10.92
September 18, 2004	0.169	9/18/04 10:00	0.243	9.08	0.191	9/18/04 16:30	0.237	15.58	0.205	9/19/04 7:45	0.223	30.83
September 27, 2004	0.191	9/28/04 13:45	0.251	14.67	0.209	9/28/04 20:45	0.250	21.67	0.213	9/28/04 23:15	0.237	24.17
October 14, 2004	0.177	10/14/04 13:15	0.236	9.67	0.201	10/14/04 21:30	0.235	17.92	0.216	10/15/04 10:30	0.226	30.92
October 30, 2004	0.191	10/30/04 12:30	0.215	10.58	0.209	10/30/04 18:45	0.218	16.83	0.216	11/1/04 12:30	0.218	58.58
November 4, 2004	0.206	11/4/04 16:45	0.226	6.00	0.216	11/5/04 2:15	0.227	15.50	0.217	11/5/04 11:30	0.222	24.75
November 12, 2004	0.217	11/12/04 18:15	0.233	11.75	0.224	11/12/04 22:45	0.232	16.25	0.221	11/14/04 2:45	0.224	44.25
December 9, 2004	0.231	12/10/04 7:30	0.234	16.08	0.237	12/11/04 4:45	0.239	37.33	0.231			
December 23, 2004	0.19	12/24/04 2:15	0.238	16.75	0.212	12/24/04 10:15	0.238	24.75	0.221	12/25/04 7:00	0.229	45.50
January 5, 2005	0.185	1/5/05 13:00	0.239	10.833	0.205	1/6/05 5:15	0.271	27.083	0.216	1/7/05 16:15	0.218	62.083
February 14, 2005	0.176	2/15/05 0:00	0.230	14.417	0.196	2/15/05 3:15	0.239	17.667	0.213	2/15/05 20:15	0.229	34.667
May 20, 2005	0.179	5/20/05 17:15	0.237	13.750	0.202	5/20/05 23:00	0.232	19.500	0.219	5/21/05 15:15	0.220	35.750
June 3, 2005	0.181	6/3/05 21:45	0.235	17.250	0.202	6/4/05 2:15	0.227	21.750	0.216	6/4/05 22:45	0.222	42.250
July 15, 2005	0.207	7/15/05 22:45	0.224	6.500	0.222	7/16/05 5:00	0.226	12.750	0.225			
July 17, 2005	0.231	7/17/05 6:15	0.240	0.333	0.229	7/17/05 7:00	0.240	1.083	0.224	7/17/05 16:45	0.233	10.833
October 7, 2005	0.167	10/8/05 7:45	0.251	24.667	0.180	10/8/05 11:00	0.238	27.917	0.191	10/8/05 22:15	0.213	39.167
October 21, 2005	0.196	10/21/05 19:00	0.228	11.333	0.211	10/22/05 9:15	0.223	25.583	0.215	10/22/05 19:15	0.215	35.583

Appendix D

Ponding Characteristics

Storm	Time of Initial Ponding	Time to Ponding	Time Bed Emptied	Maximum Ponded Depth	Average Water Temperature
		(hrs)		(in)	(°C)
October 14, 2003	10/14/03 21:35	1.42	*	8.21	19.229
October 26, 2003	10/27/03 0:50	3.75	*	19.71	16.132
November 4, 2003	11/6/03 17:40	44.67	11/8/03 3:50	1.97	16.990
November 19, 2003	11/19/03 17:20	12.25	11/23/03 10:30	11.98	13.996
November 28, 2003	11/28/03 19:20	11.50	12/1/03 12:25	4.53	11.887
January 4, 2004	1/5/04 11:55	17.58	1/6/04 13:25	1.08	8.016
March 30, 2004	3/31/04 0:00	6.33	*	3.33	9.989
April 12, 2004	4/12/04 18:40	6.42	4/18/04 9:00	13.28	10.342
April 23, 2004	4/23/04 20:00	1.83	4/25/04 12:00	2.89	15.700
May 2, 2004	5/3/04 5:05	17.50	5/5/04 10:25	3.23	17.042
June 22, 2004	6/22/04 17:40	0.08	6/23/04 17:25	2.10	25.372
July 12, 2004	7/12/04 8:25	6.42	*	21.37	25.338
July 18, 2004	7/18/04 12:00	7.08	7/20/04 2:35	3.22	25.034
July 23, 2004	7/23/04 14:20	0.50	7/24/04 21:55	3.07	26.208
July 27, 2004	7/27/04 12:45	2.08	*	21.04	24.813
August 1, 2004	8/1/04 5:35	1.25	8/3/04 19:35	21.71	25.642
September 18, 2004	9/18/04 7:15	6.33	9/21/04 4:25	17.10	22.069
September 27, 2004	9/28/04 9:00	9.92	*	23.02	21.653
October 14, 2004	10/14/04 6:00	2.42	*	5.21	17.042
October 30, 2004	10/30/04 3:05	1.17	10/31/04 7:55	1.73	15.282
November 4, 2004	11/4/04 13:55	3.17	11/8/04 13:00	9.39	13.322
November 12, 2004	11/12/04 12:40	6.17	11/17/04 9:05	9.65	10.341
December 9, 2004	12/9/04 15:30	0.08	12/14/04 6:20	7.20	8.807
December 23, 2004	12/23/04 15:50	6.33	12/25/04 21:35	4.52	5.904
January 5, 2005	1/5/05 10:10	8.00	*	2.76	7.084
February 14, 2005	2/14/05 16:30	6.92	*	8.95	5.492
May 20, 2005	5/20/05 12:05	8.58	5/21/05 8:40	1.87	16.783
June 3, 2005	6/3/05 15:35	11.08	6/5/05 8:25	5.69	18.683
July 15, 2005	7/15/05 16:35	0.33	7/16/05 12:20	3.46	25.708
July 17, 2005	7/17/05 18:05	12.17	7/18/05 5:05	1.61	26.178
October 7, 2005	10/7/05 23:05	16.00	10/10/05 22:45	22.55	21.192
October 21, 2005	10/22/05 13:45	30.08	10/24/05 15:45	5.73	16.436

* Bed was not emptied when next rainfall event began.

Appendix E

Results Summary and Comparison

Storm	Storm Data			Method #1				Method #2				Standard Model			
	h_o	h_w	Temperature	Ψ	K_{adj}	$\Delta\theta$	MSE	Ψ	K_{adj}	$\Delta\theta$	MSE	Ψ	K_{adj}	$\Delta\theta$	MSE
	(in)	(in)	(°C)	(in)	(in/hr)			(in)	(in/hr)			(in)	(in/hr)		
January 4, 2004	1.08	27.79	8.06	400.15	0.0054	0.018	**0.181**	4979.19	0.0016	0.149	0.344	6.57	0.2400	0.100	0.350
July 17, 2005	1.61	54.77	26.00	244.28	0.0092	0.009	**0.137**	2925.94	0.0035	0.119	0.326	6.57	0.2400	0.100	0.468
October 30, 2004	1.70	1.92	15.34	497.68	0.0064	0.024	**0.764**	6094.38	0.0017	0.159	0.839	6.57	0.2400	0.100	0.795
May 20, 2005	1.87	8.87	16.53	1084.13	0.0050	0.058	0.859	7970.89	0.0015	0.171	1.003	6.57	0.2400	0.100	**0.848**
November 4, 2003	1.95	35.34	16.89	185.31	0.0076	0.006	**0.018**	3126.75	0.0027	0.123	1.042	6.57	0.2400	0.100	1.106
June 22, 2004	2.10	1.00	25.34	513.80	0.0081	0.025	1.472	4700.56	0.0025	0.146	1.472	6.57	0.2400	0.100	**1.422**
January 5, 2005	2.72	33.09	6.56	1007.64	0.0039	0.054	**1.837**	6941.50	0.0012	0.165	2.756	6.57	0.2400	0.100	2.903
April 23, 2004	2.89	7.81	15.98	610.69	0.0061	0.031	**1.941**	3842.81	0.0023	0.135	2.616	6.57	0.2400	0.100	2.409
July 23, 2004	3.07	8.84	26.42	366.98	0.0088	0.016	**0.850**	3645.54	0.0030	0.132	2.729	6.57	0.2400	0.100	2.348
July 18, 2004	3.17	18.80	25.27	163.96	0.0093	0.005	**0.322**	2740.52	0.0036	0.115	2.704	6.57	0.2400	0.100	2.510
May 2, 2004	3.19	26.07	16.16	280.84	0.0072	0.011	**0.073**	3233.54	0.0026	0.125	2.656	6.57	0.2400	0.100	2.716
March 30, 2004	3.28	8.76	10.37	659.61	0.0051	0.034	**4.177**	4054.36	0.0019	0.138	6.063	6.57	0.2400	0.100	5.668
July 15, 2005	3.41	4.80	25.86	383.63	0.0087	0.017	**0.340**	4442.90	0.0026	0.143	3.317	6.57	0.2400	0.100	2.484
November 28, 2003	4.49	12.00	11.70	244.28	0.0065	0.009	**0.168**	3402.44	0.0022	0.128	5.532	6.57	0.2400	0.100	5.346
December 23, 2004	4.54	2.63	5.44	897.94	0.0040	0.048	**4.073**	6224.85	0.0012	0.160	5.651	6.57	0.2400	0.100	5.103
June 3, 2005	4.89	25.76	18.85	1007.64	0.0055	0.054	**1.671**	7604.30	0.0016	0.169	4.660	6.57	0.2400	0.100	4.017
October 14, 2004	5.21	10.34	17.68	1103.72	0.0051	0.059	**9.237**	8364.07	0.0015	0.173	12.838	6.57	0.2400	0.100	10.908
October 21, 2005	5.72	54.00	16.29	626.94	0.0061	0.032	**0.102**	5497.12	0.0018	0.154	3.374	6.57	0.2400	0.100	5.152
December 9, 2004	7.20	18.78	8.70	116.84	0.0063	0.003	**8.465**	2925.94	0.0023	0.119	10.922	6.57	0.2400	0.100	12.097
October 14, 2003	8.18	4.94	19.43	897.94	0.0058	0.048	**9.592**	7099.06	0.0017	0.166	17.942	6.57	0.2400	0.100	15.063
February 14, 2005	8.95	19.38	5.40	1007.64	0.0038	0.054	**2.875**	8571.47	0.0010	0.174	24.430	6.57	0.2400	0.100	24.694
November 4, 2004	9.39	4.42	13.32	432.91	0.0062	0.020	**0.370**	4526.60	0.0019	0.144	19.970	6.57	0.2400	0.100	18.309
November 12, 2004	9.57	35.10	10.51	366.98	0.0059	0.016	**3.791**	3709.80	0.0020	0.133	12.486	6.57	0.2400	0.100	17.276
November 19, 2003	11.95	12.48	14.02	610.69	0.0058	0.031	**0.818**	4526.60	0.0020	0.144	21.925	6.57	0.2400	0.100	22.042
April 12, 2004	13.28	124.42	10.86	465.38	0.0057	0.022	34.863	3645.54	0.0021	0.132	**4.302**	6.57	0.2400	0.100	21.301
September 18, 2004	17.05	19.85	22.05	1424.61	0.0050	0.074	**0.085**	10263.09	0.0015	0.181	25.070	6.57	0.2400	0.100	18.092
September 27, 2004	17.92	100.80	21.51	1123.50	0.0056	0.060	24.948	6094.38	0.0020	0.159	**8.662**	6.57	0.2400	0.100	14.243
August 1, 2004	17.93	36.86	25.89	432.91	0.0085	0.020	59.920	2122.10	0.0043	0.099	**0.333**	6.57	0.2400	0.100	15.568
July 12, 2004	17.94	37.79	25.89	1123.50	0.0061	0.060	18.875	5609.72	0.0023	0.155	**3.691**	6.57	0.2400	0.100	10.807
October 26, 2003	17.96	36.38	16.10	952.09	0.0052	0.051	9.383	5281.29	0.0019	0.152	**0.152**	6.57	0.2400	0.100	13.645
July 27, 2004	17.98	30.64	25.17	626.94	0.0076	0.032	8.886	3233.54	0.0032	0.125	**0.196**	6.57	0.2400	0.100	6.600
October 7, 2005	17.99	50.67	20.77	1673.91	0.0044	0.084	31.698	10838.40	0.0014	0.183	**1.012**	6.57	0.2400	0.100	4.438

Appendix F

Individual Model Comparison Results

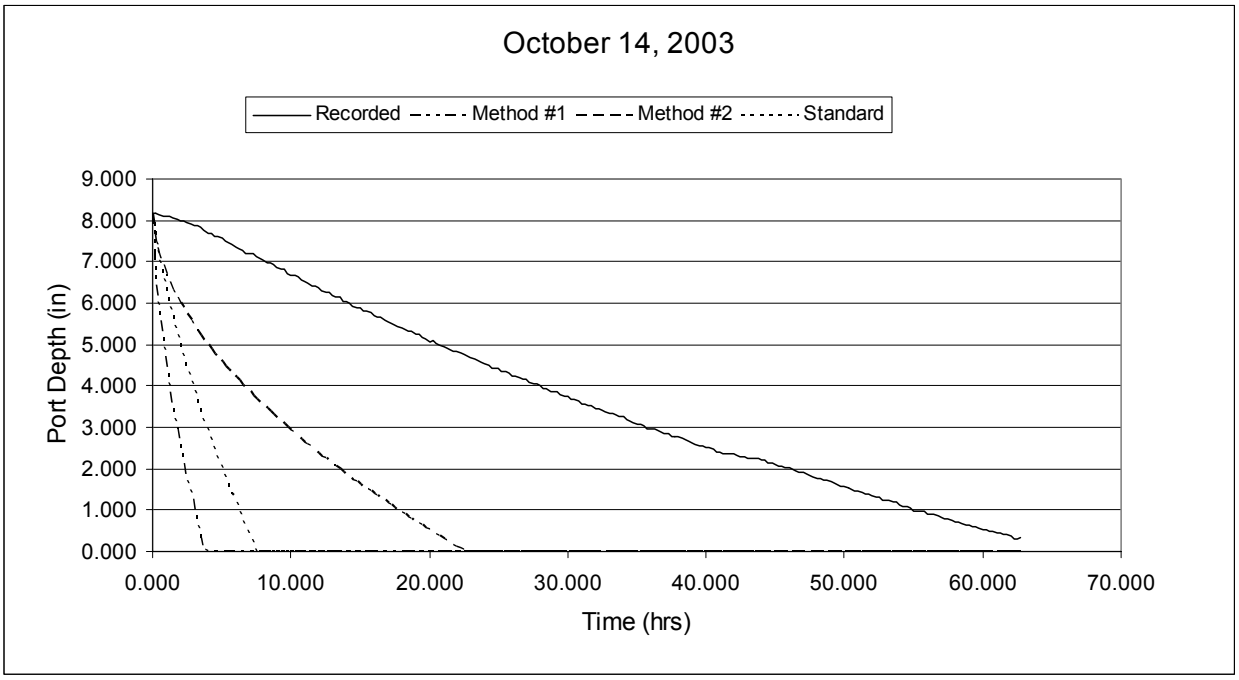
October 14, 2003
Recorded
Method #1
Method #2
Standard
Port Depth (in)
9.000
8.000
7.000
6.000
5.000
4.000
3.000
2.000
1.000
0.000
0.000
10.000
20.000
30.000
40.000
50.000
60.000
70.000
Time (hrs)

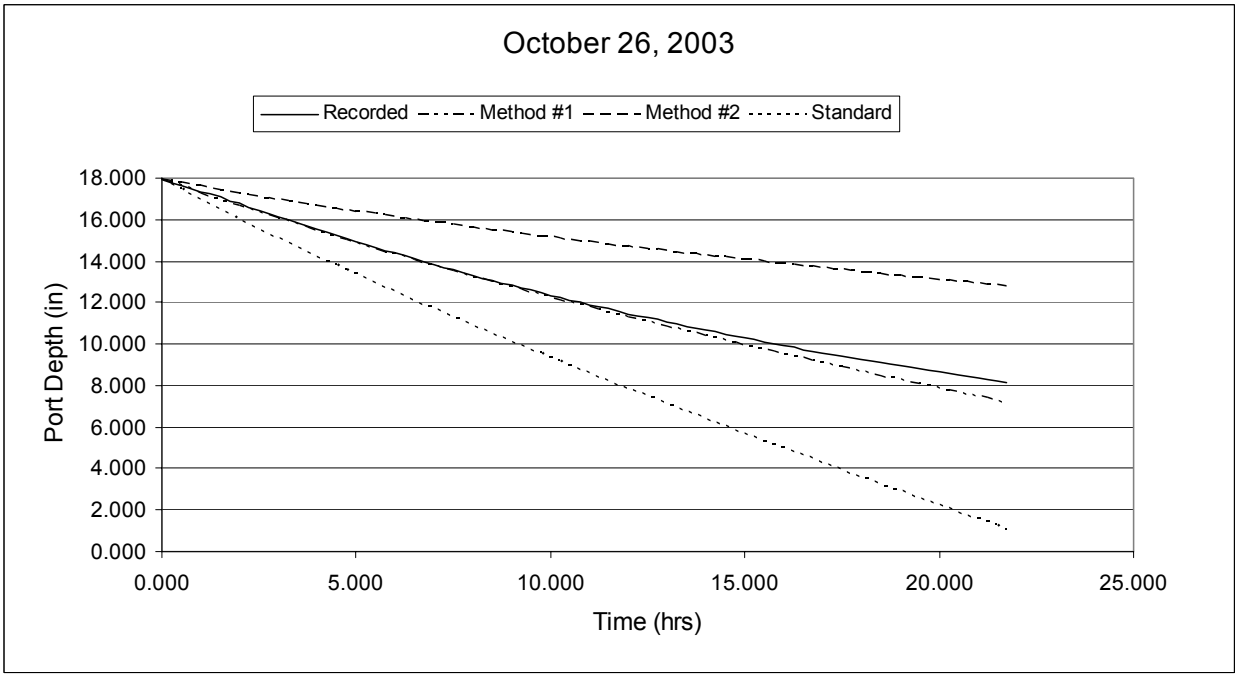
October 26, 2003
Recorded
Method #1
Method #2
Standard
Port Depth (in)
18.000
16.000
14.000
12.000
10.000
8.000
6.000
4.000
2.000
0.000
0.000
5.000
10.000
15.000
20.000
25.000
Time (hrs)

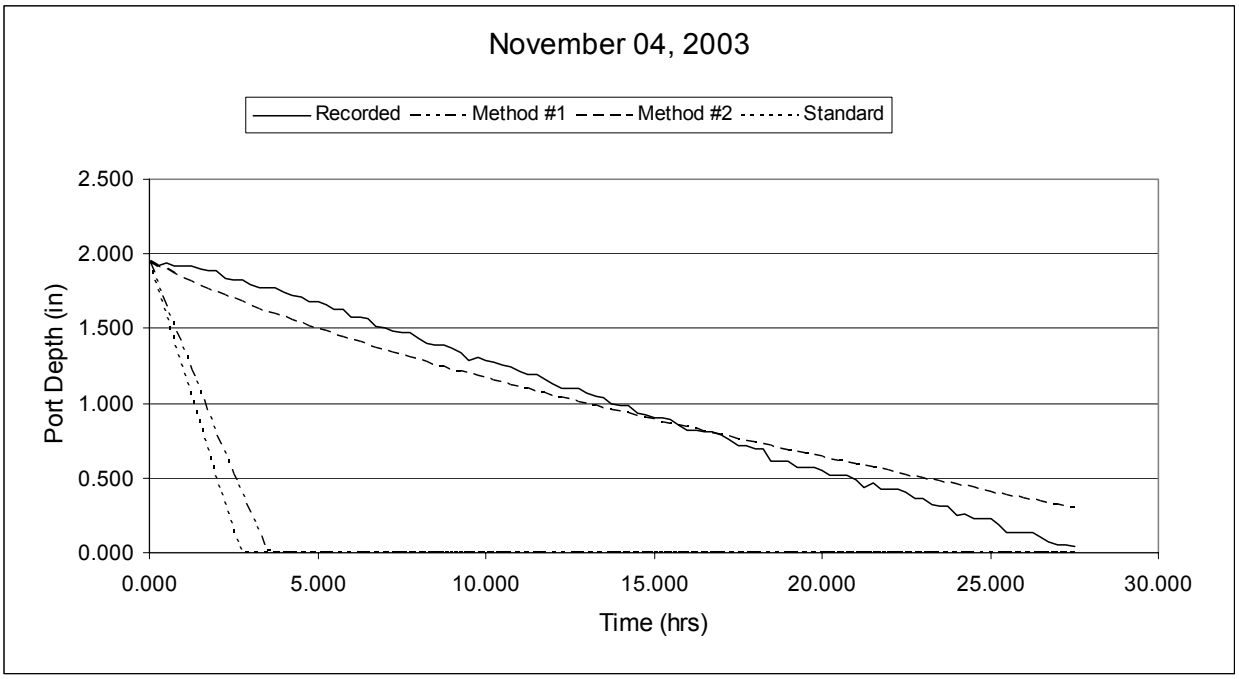
November 04, 2003
Recorded
Method #1
Method #2
Standard
2.500
2.000
1.500
1.000
0.500
0.000
Port Depth (in)
0.000
5.000
10.000
15.000
20.000
25.000
30.000
Time (hrs)

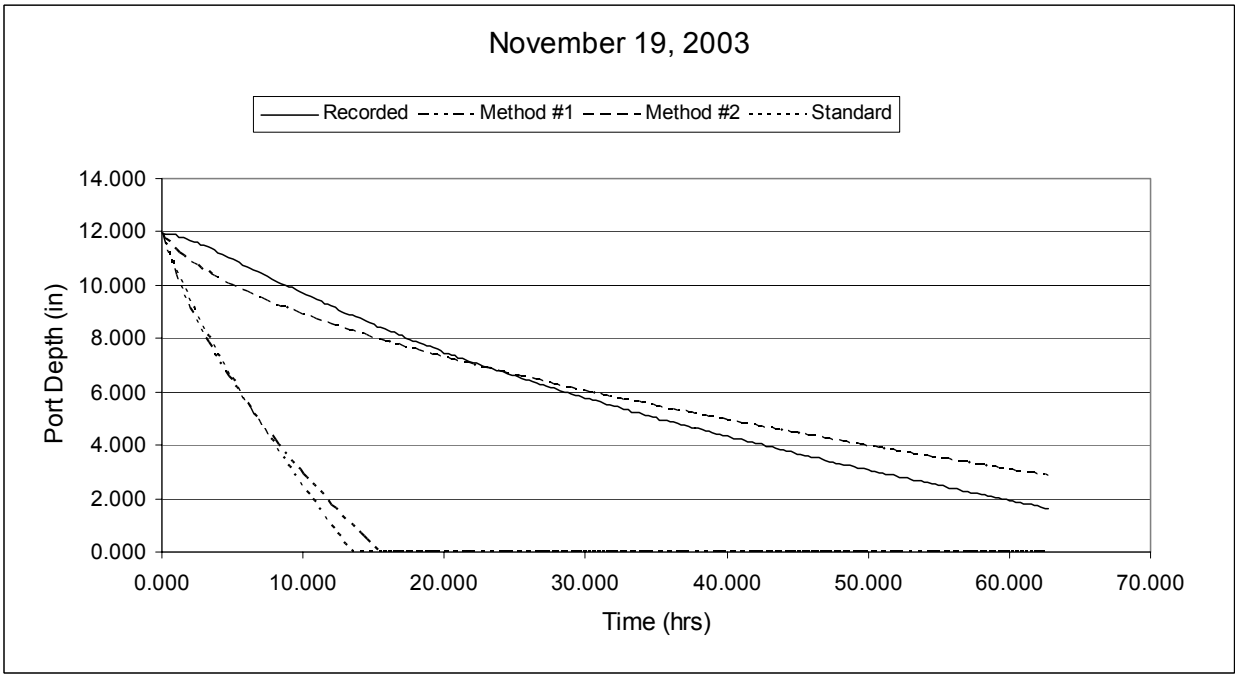
November 19, 2003
Recorded
Method #1
Method #2
Standard
14.000
12.000
10.000
8.000
6.000
4.000
2.000
0.000
Port Depth (in)
0.000
10.000
20.000
30.000
40.000
50.000
60.000
70.000
Time (hrs)

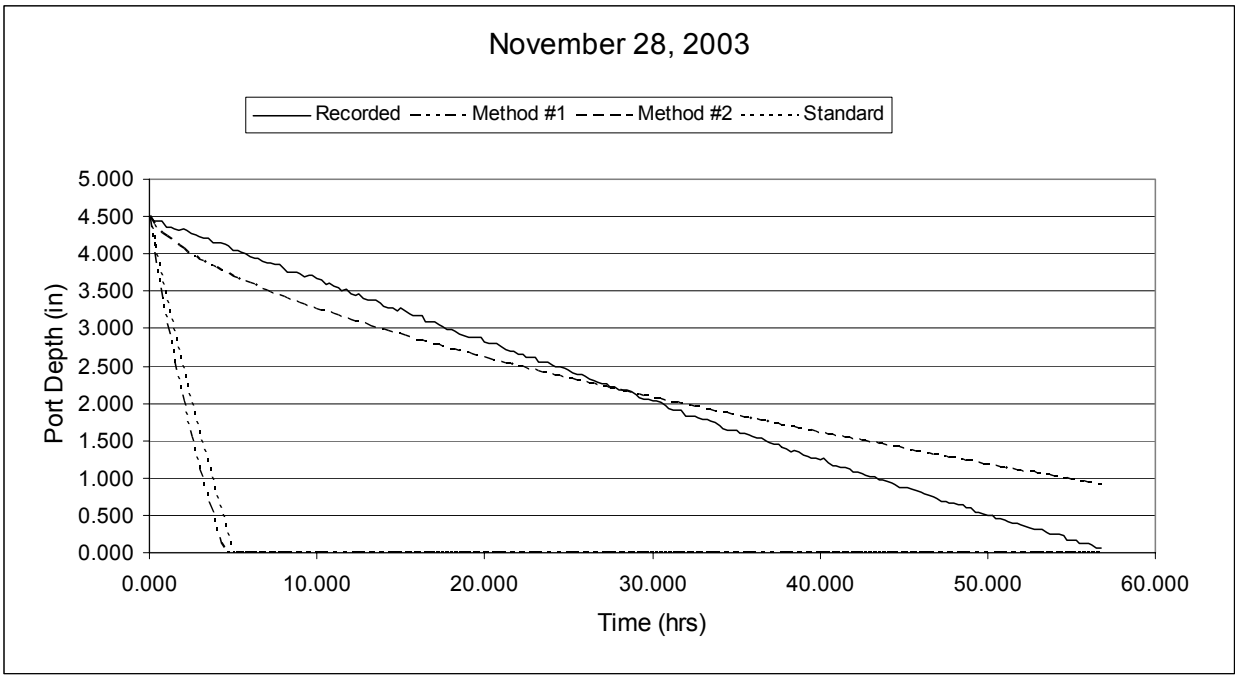
November 28, 2003
Recorded
Method #1
Method #2
Standard
Port Depth (in)
5.000
4.500
4.000
3.500
3.000
2.500
2.000
1.500
1.000
0.500
0.000
0.000
10.000
20.000
30.000
40.000
50.000
60.000
Time (hrs)

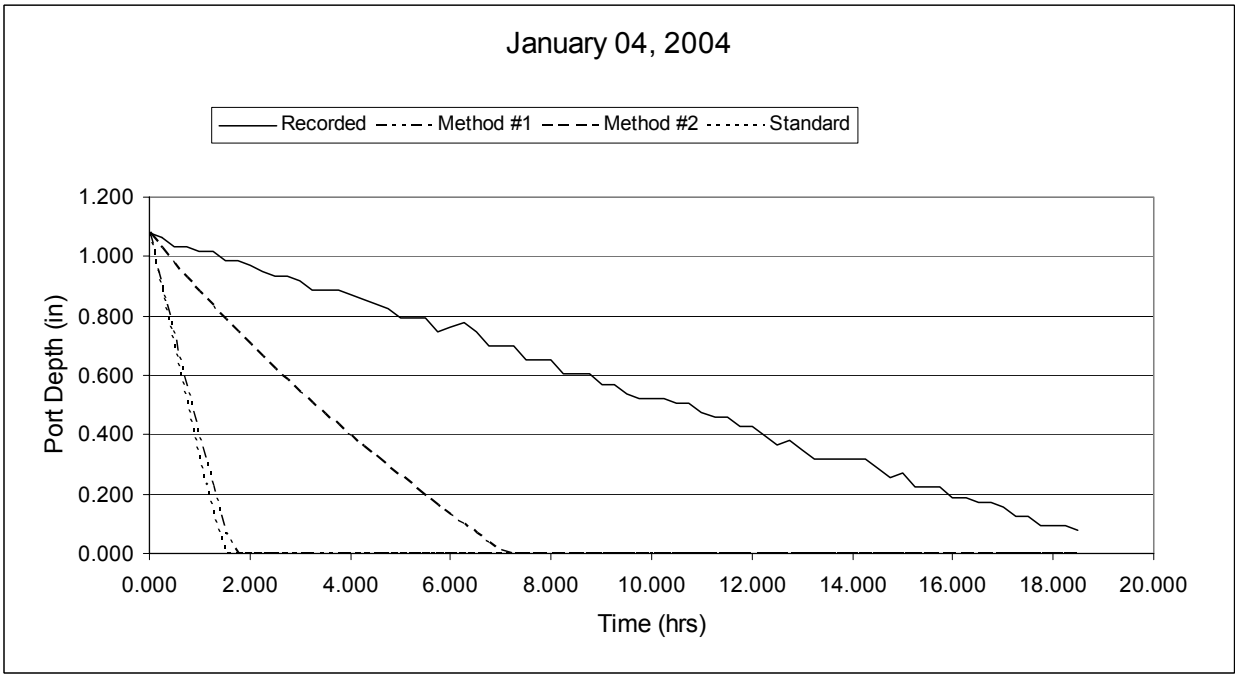
January 04, 2004
Recorded
Method #1
Method #2
Standard
Port Depth (in)
1.200
1.000
0.800
0.600
0.400
0.200
0.000
0.000
2.000
4.000
6.000
8.000
10.000
12.000
14.000
16.000
18.000
20.000
Time (hrs)

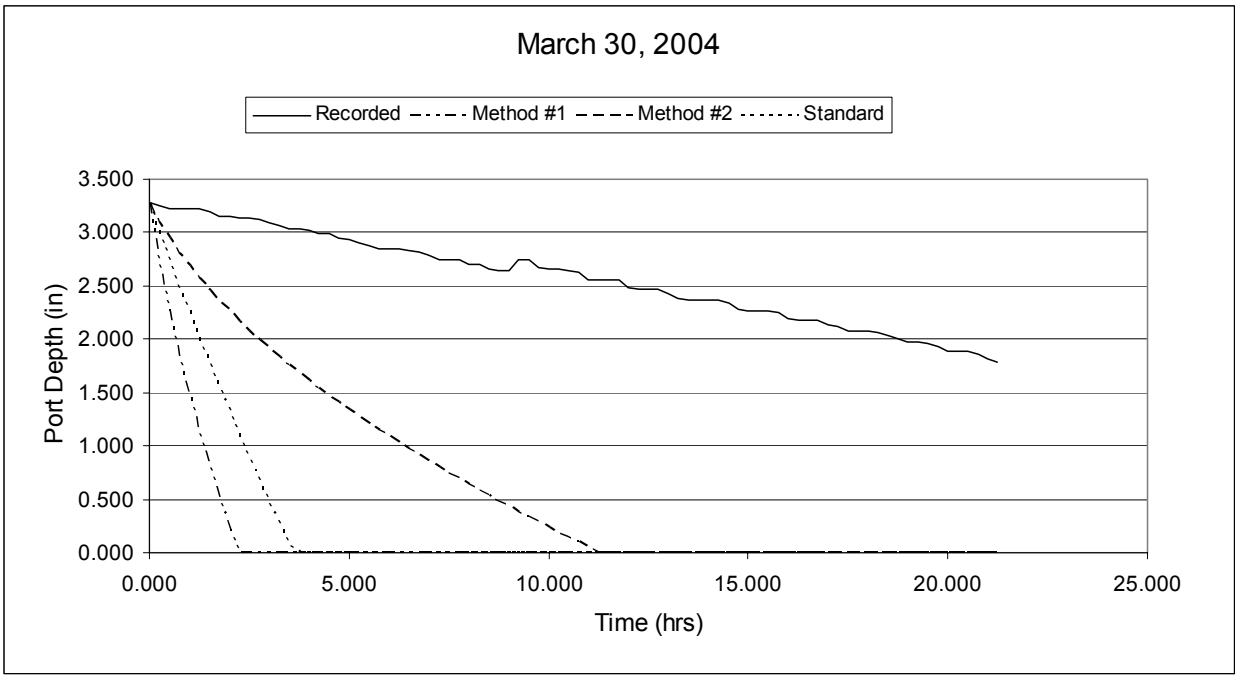
March 30, 2004
Recorded
Method #1
Method #2
Standard
Port Depth (in)
3.500
3.000
2.500
2.000
1.500
1.000
0.500
0.000
0.000
5.000
10.000
15.000
20.000
25.000
Time (hrs)

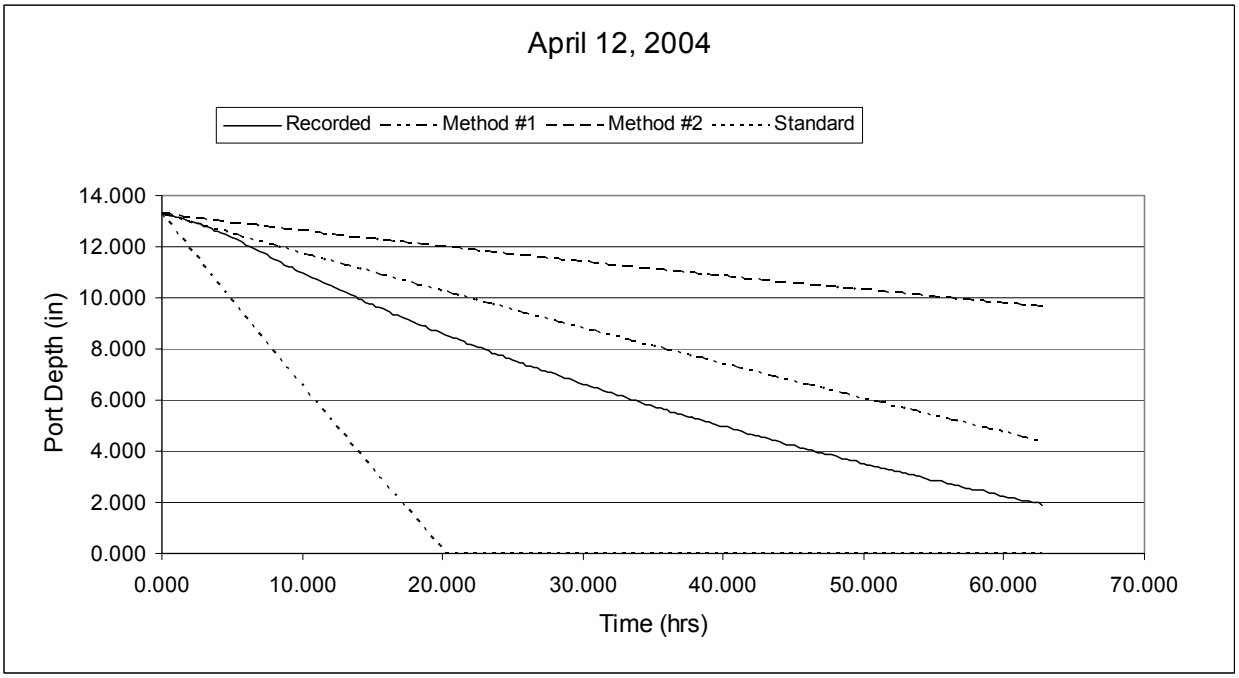
April 12, 2004
Recorded
Method #1
Method #2
Standard
Port Depth (in)
14.000
12.000
10.000
8.000
6.000
4.000
2.000
0.000
0.000
10.000
20.000
30.000
40.000
50.000
60.000
70.000
Time (hrs)

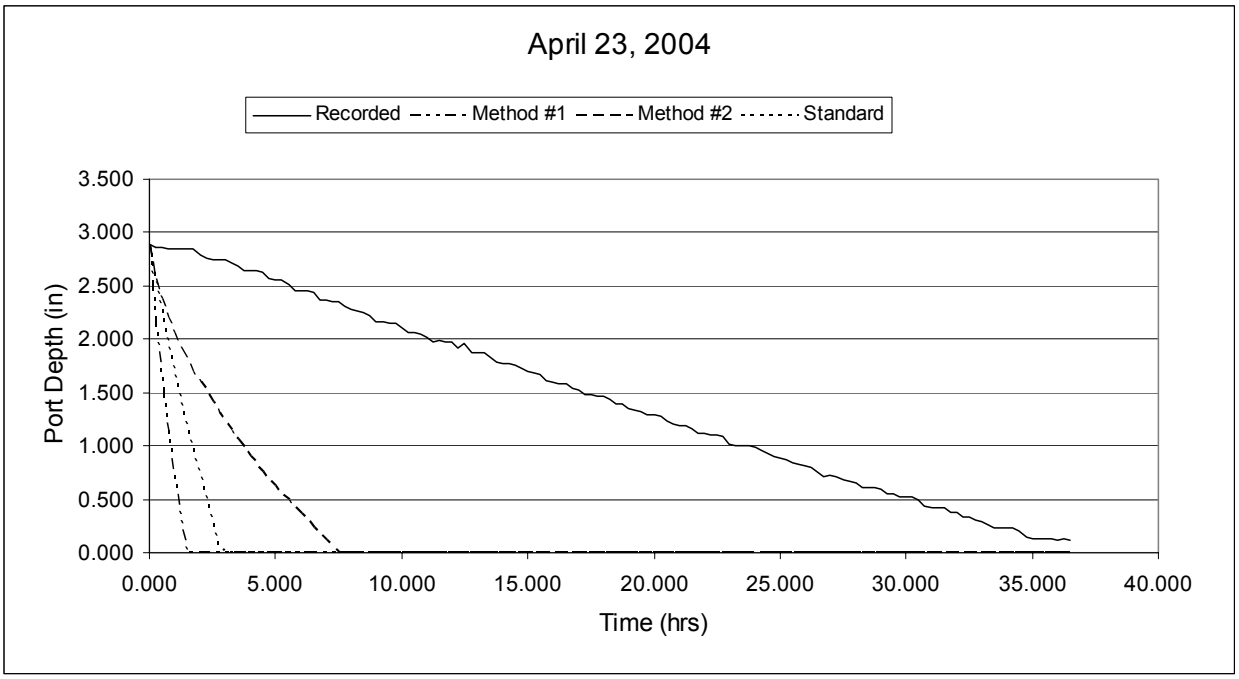
April 23, 2004
Recorded
Method #1
Method #2
Standard
Port Depth (in)
3.500
3.000
2.500
2.000
1.500
1.000
0.500
0.000
0.000
5.000
10.000
15.000
20.000
25.000
30.000
35.000
40.000
Time (hrs)

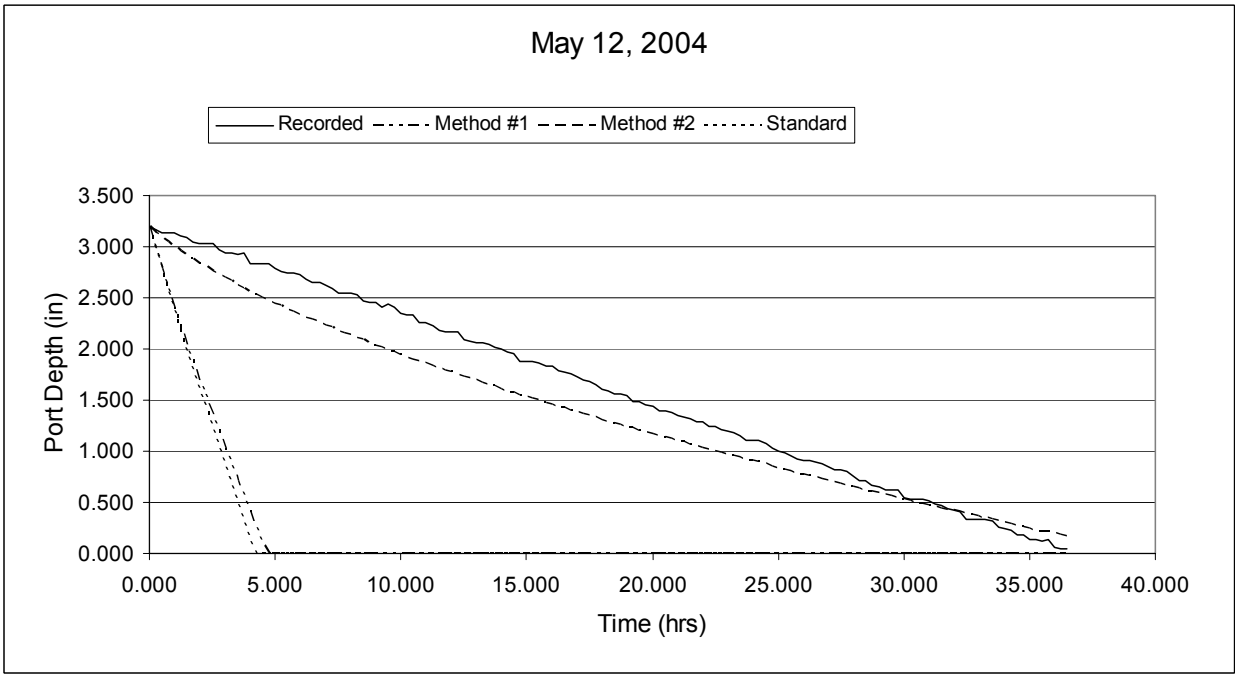
May 12, 2004
Recorded
Method #1
Method #2
Standard
Port Depth (in)
3.500
3.000
2.500
2.000
1.500
1.000
0.500
0.000
0.000
5.000
10.000
15.000
20.000
25.000
30.000
35.000
40.000
Time (hrs)

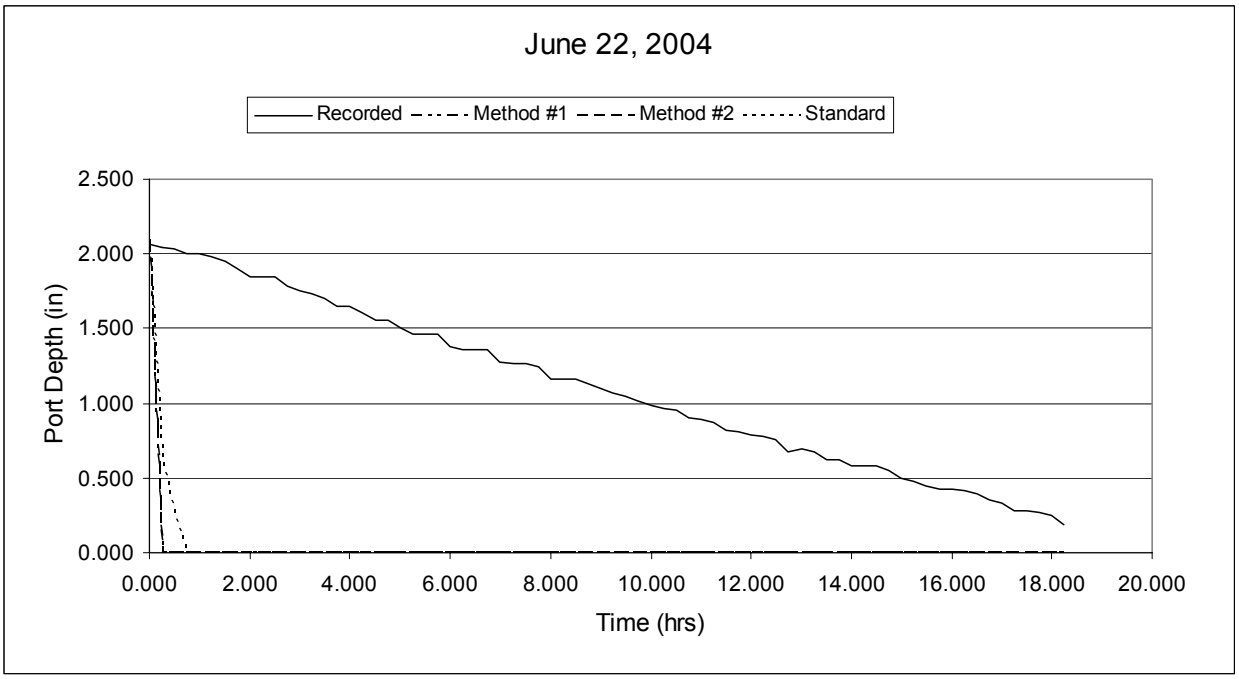
June 22, 2004
Recorded
Method #1
Method #2
Standard
Port Depth (in)
2.500
2.000
1.500
1.000
0.500
0.000
0.000
2.000
4.000
6.000
8.000
10.000
12.000
14.000
16.000
18.000
20.000
Time (hrs)

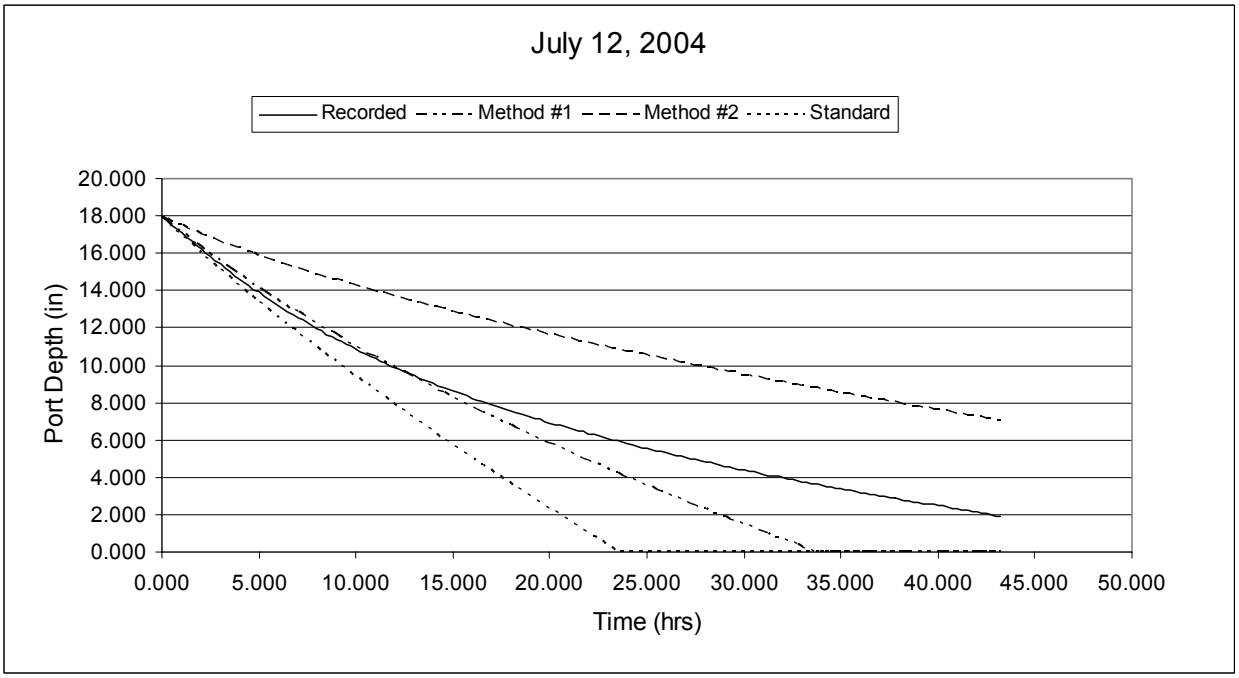
July 12, 2004
Recorded
Method #1
Method #2
Standard
Port Depth (in)
20.000
18.000
16.000
14.000
12.000
10.000
8.000
6.000
4.000
2.000
0.000
0.000
5.000
10.000
15.000
20.000
25.000
30.000
35.000
40.000
45.000
50.000
Time (hrs)

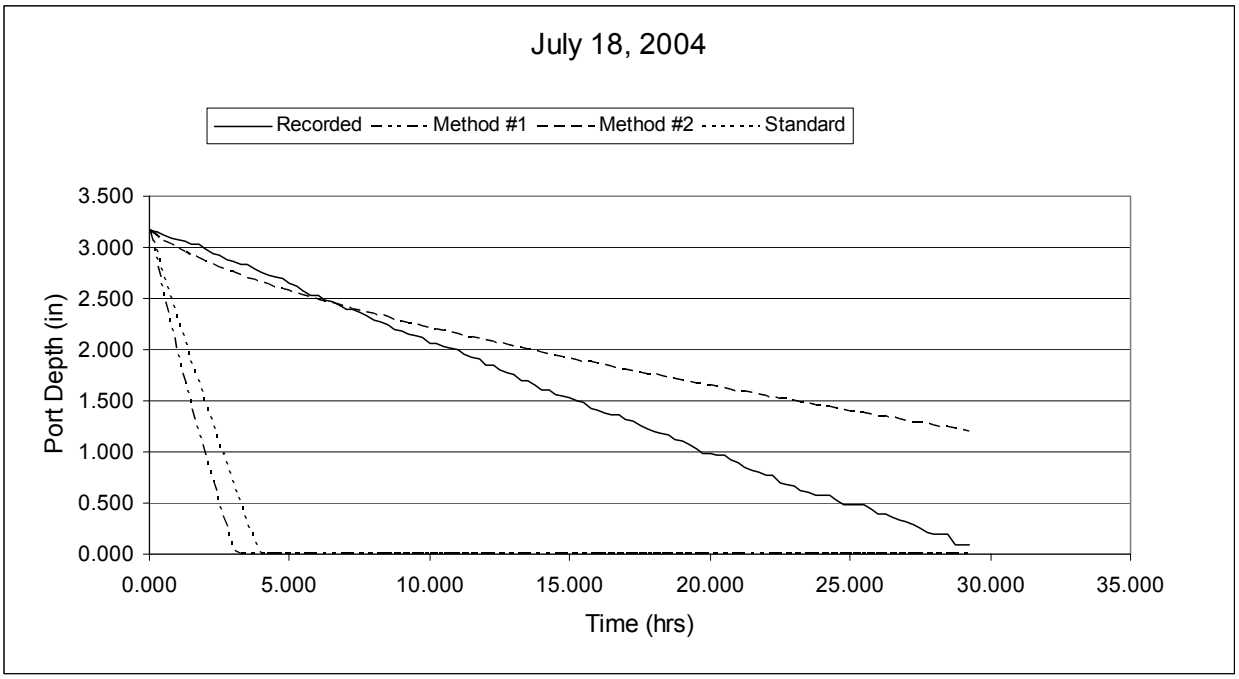
July 18, 2004
Recorded
Method #1
Method #2
Standard
Port Depth (in)
3.500
3.000
2.500
2.000
1.500
1.000
0.500
0.000
0.000
5.000
10.000
15.000
20.000
25.000
30.000
35.000
Time (hrs)

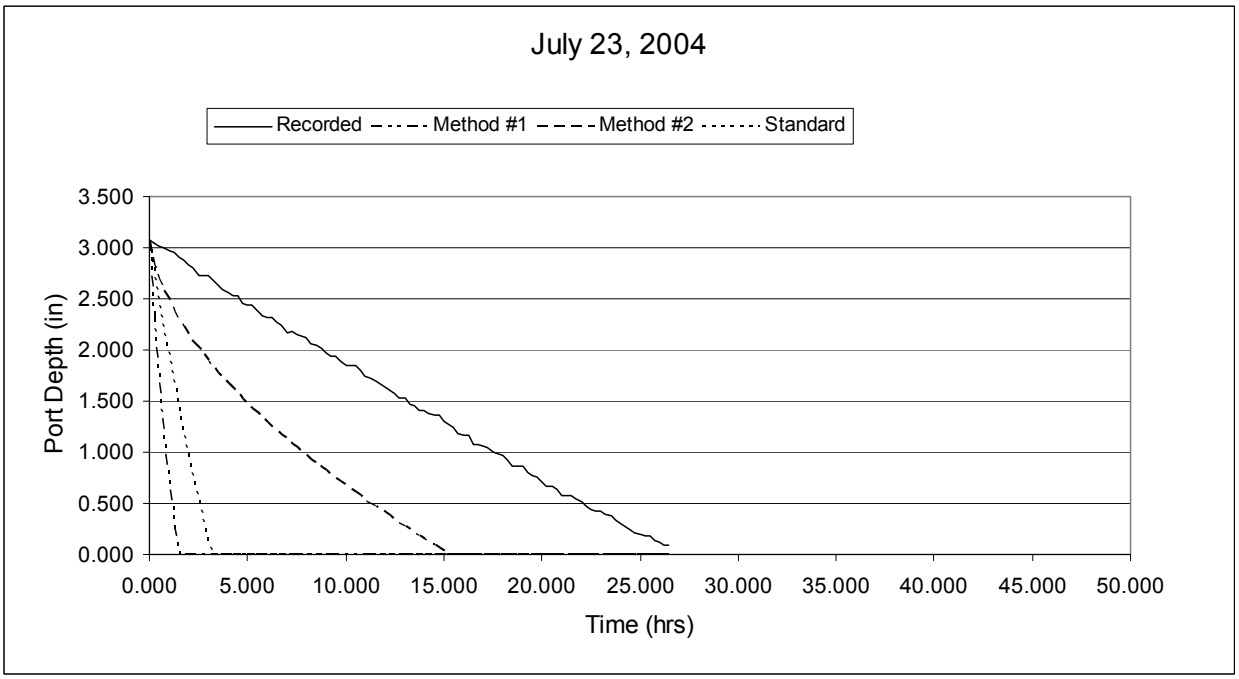
July 23, 2004
Recorded
Method #1
Method #2
Standard
Port Depth (in)
3.500
3.000
2.500
2.000
1.500
1.000
0.500
0.000
0.000
5.000
10.000
15.000
20.000
25.000
30.000
35.000
40.000
45.000
50.000
Time (hrs)

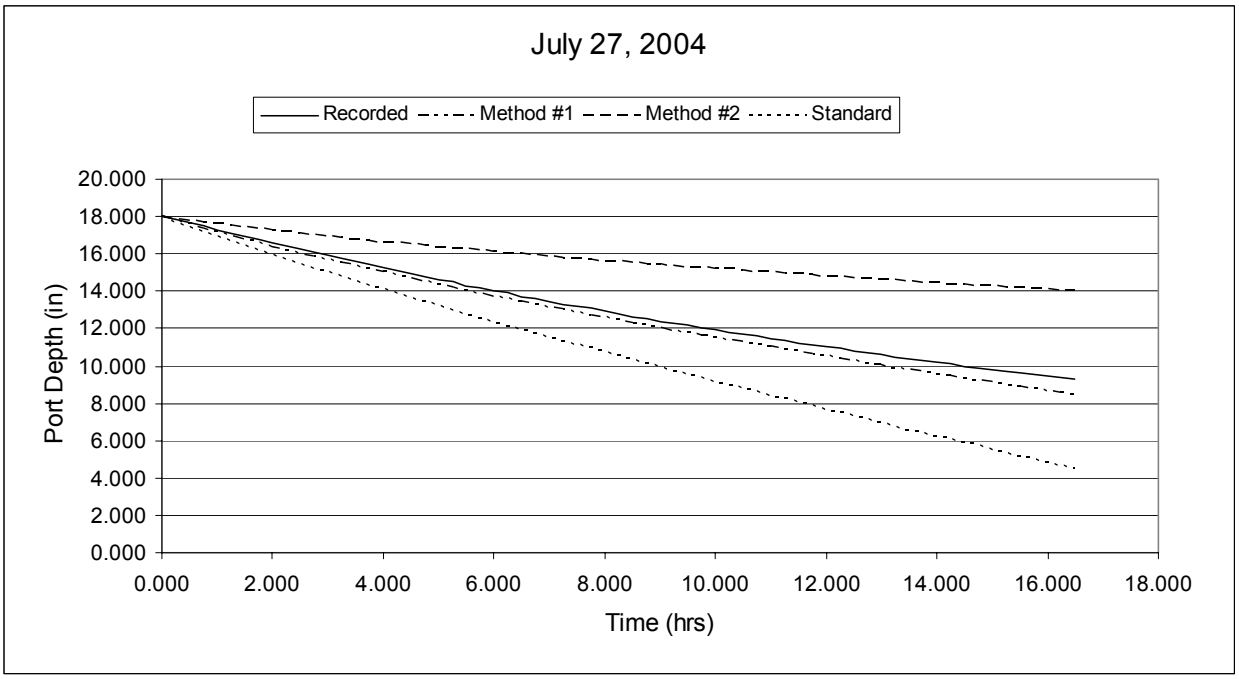
July 27, 2004
Recorded
Method #1
Method #2
Standard
Port Depth (in)
20.000
18.000
16.000
14.000
12.000
10.000
8.000
6.000
4.000
2.000
0.000
0.000
2.000
4.000
6.000
8.000
10.000
12.000
14.000
16.000
18.000
Time (hrs)

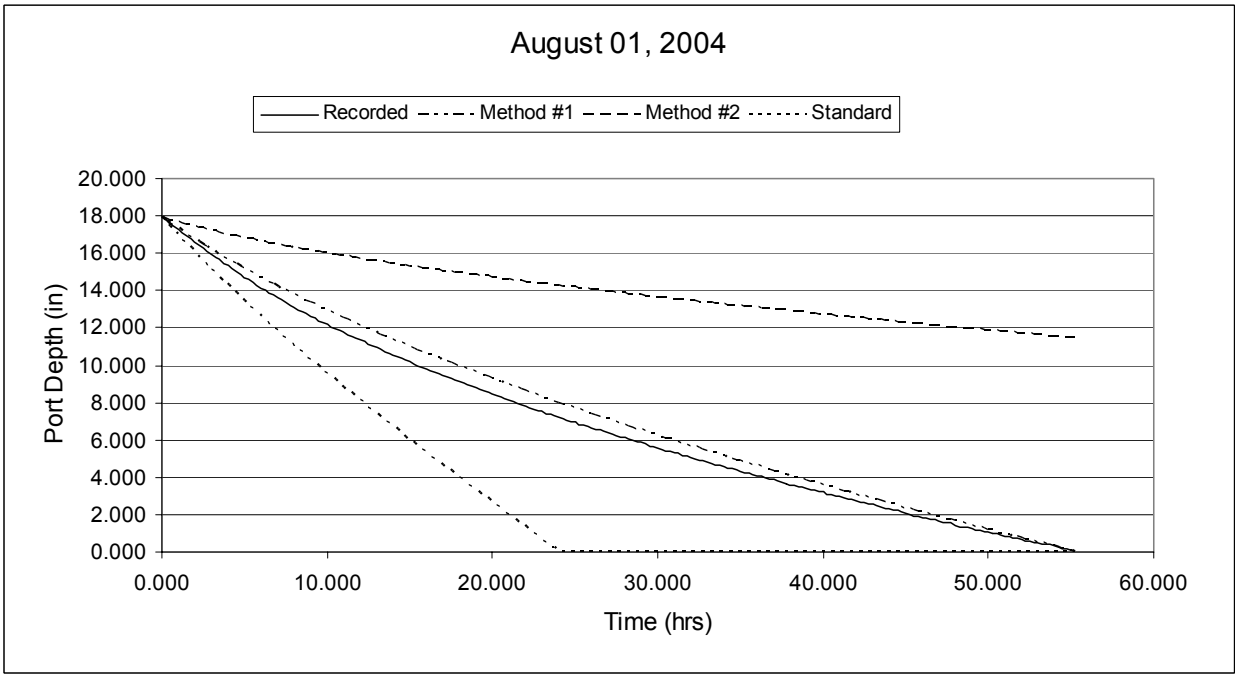
August 01, 2004
Recorded
Method #1
Method #2
Standard
Port Depth (in)
20.000
18.000
16.000
14.000
12.000
10.000
8.000
6.000
4.000
2.000
0.000
0.000
10.000
20.000
30.000
40.000
50.000
60.000
Time (hrs)

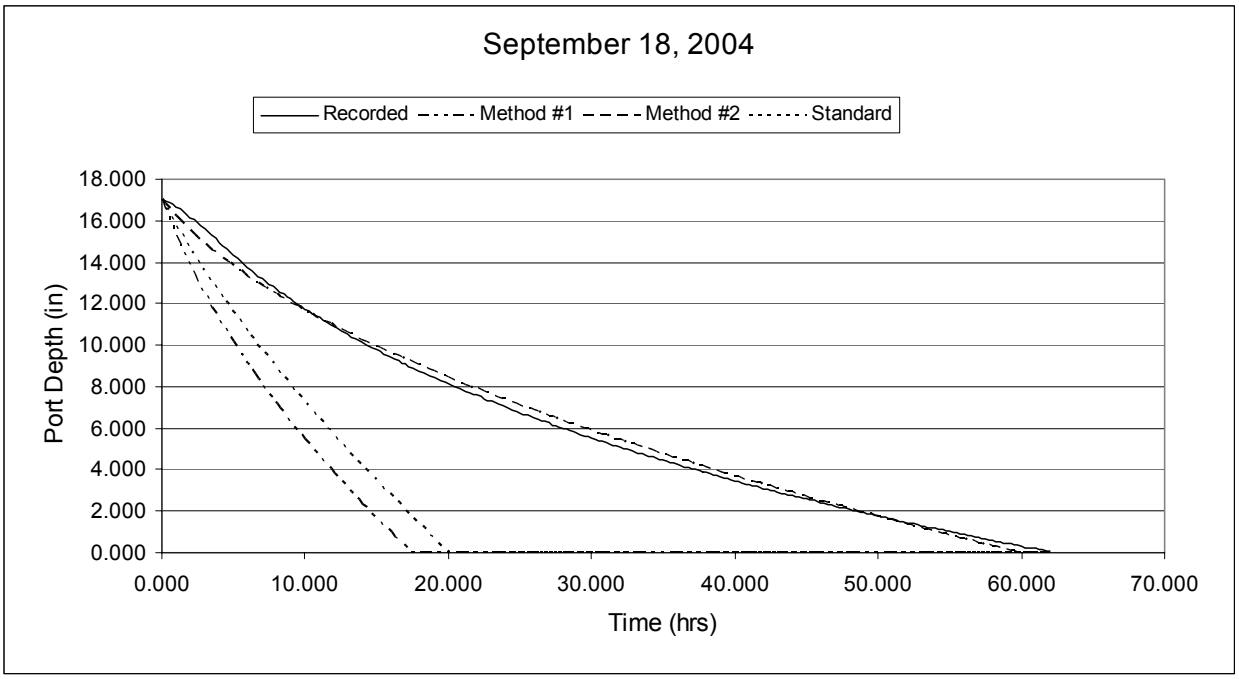
September 18, 2004
Recorded
Method #1
Method #2
Standard
Port Depth (in)
18.000
16.000
14.000
12.000
10.000
8.000
6.000
4.000
2.000
0.000
0.000
10.000
20.000
30.000
40.000
50.000
60.000
70.000
Time (hrs)

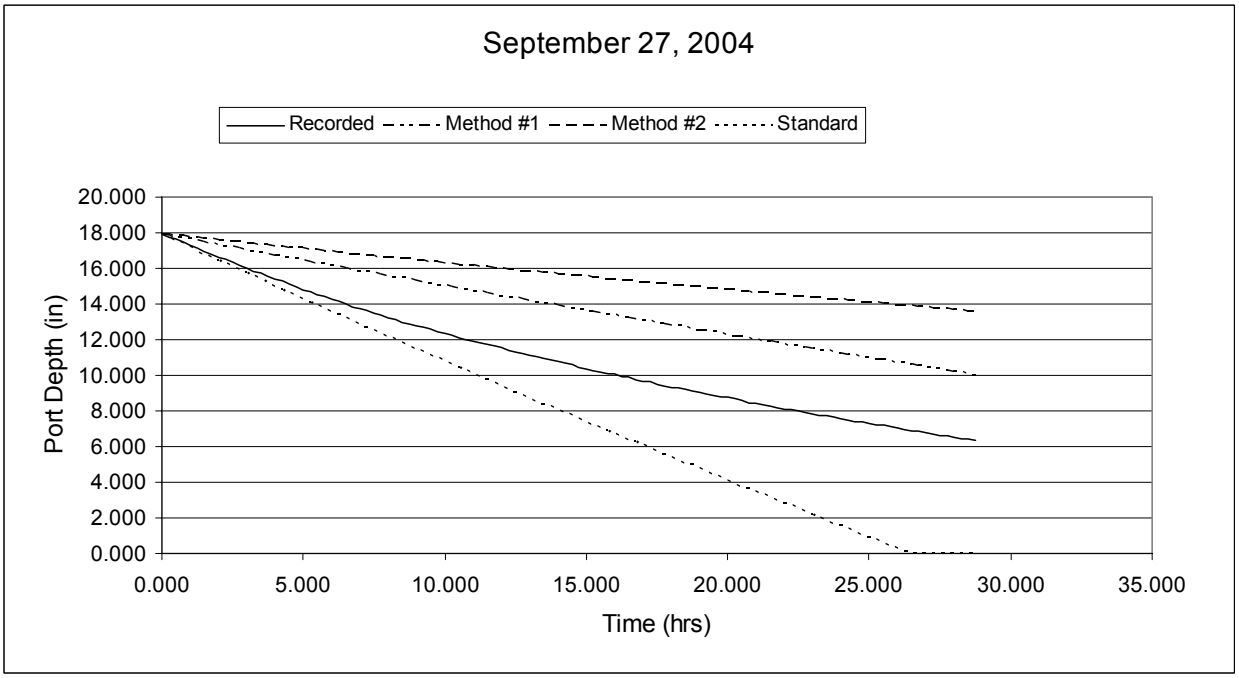
September 27, 2004
Recorded
Method #1
Method #2
Standard
Port Depth (in)
20.000
18.000
16.000
14.000
12.000
10.000
8.000
6.000
4.000
2.000
0.000
0.000
5.000
10.000
15.000
20.000
25.000
30.000
35.000
Time (hrs)

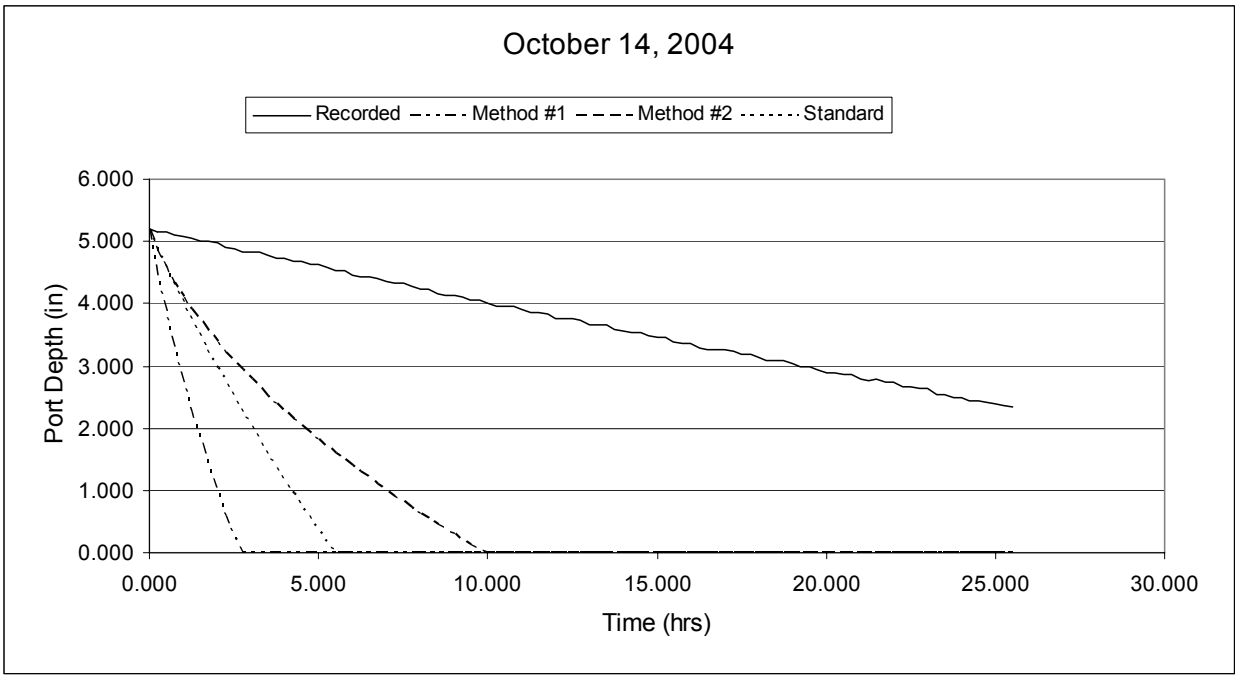
October 14, 2004
Recorded
Method #1
Method #2
Standard
6.000
5.000
4.000
3.000
2.000
1.000
0.000
Port Depth (in)
0.000
5.000
10.000
15.000
20.000
25.000
30.000
Time (hrs)

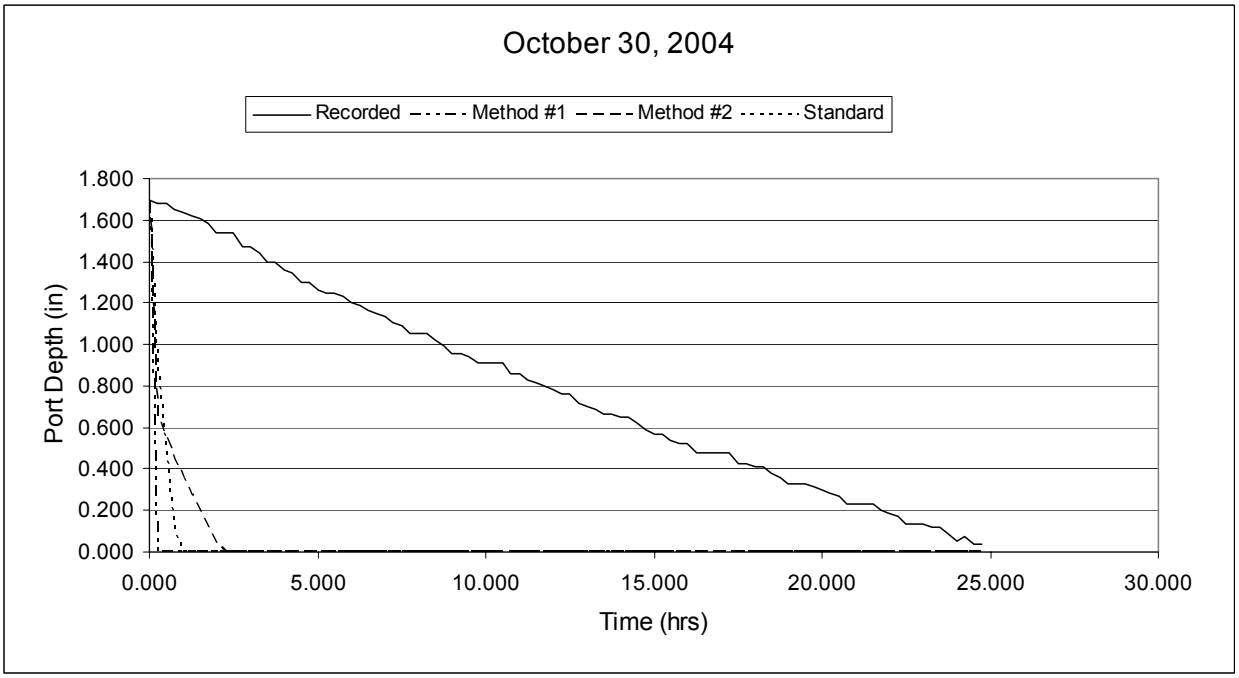
October 30, 2004
Recorded
Method #1
Method #2
Standard
1.800
1.600
1.400
1.200
1.000
0.800
0.600
0.400
0.200
0.000
Port Depth (in)
0.000
5.000
10.000
15.000
20.000
25.000
30.000
Time (hrs)

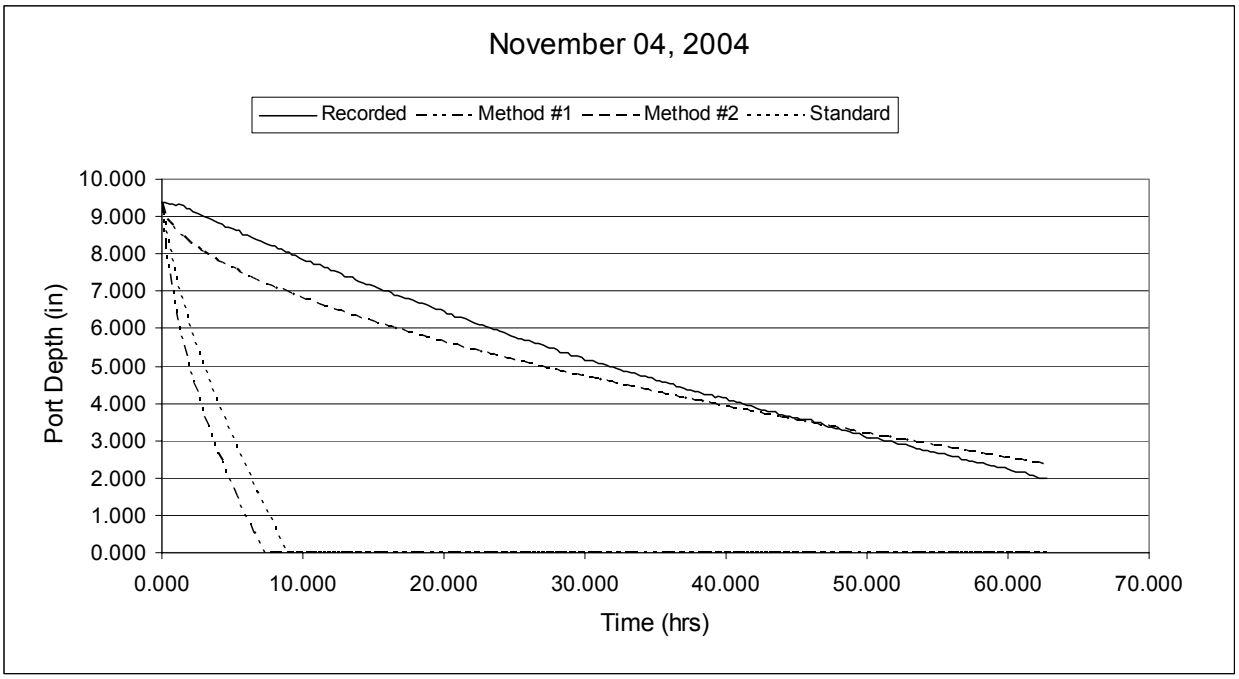
November 04, 2004
Recorded
Method #1
Method #2
Standard
Port Depth (in)
10.000
9.000
8.000
7.000
6.000
5.000
4.000
3.000
2.000
1.000
0.000
0.000
10.000
20.000
30.000
40.000
50.000
60.000
70.000
Time (hrs)

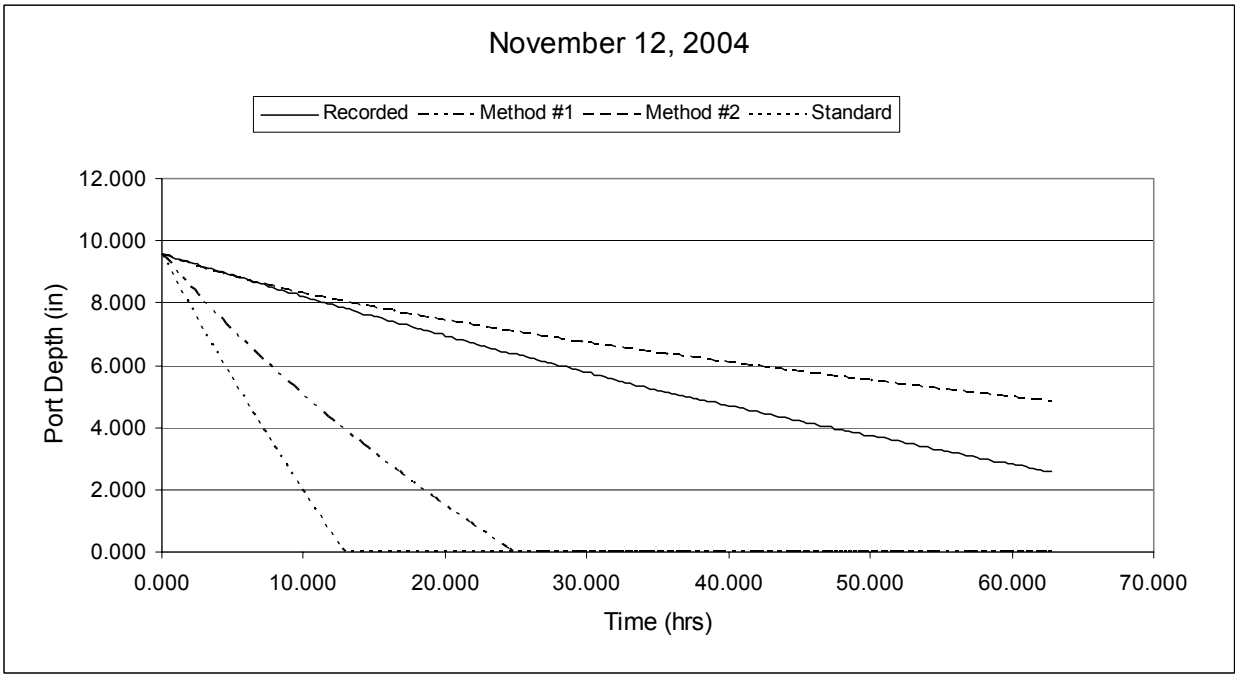
November 12, 2004
Recorded
Method #1
Method #2
Standard
Port Depth (in)
12.000
10.000
8.000
6.000
4.000
2.000
0.000
0.000
10.000
20.000
30.000
40.000
50.000
60.000
70.000
Time (hrs)

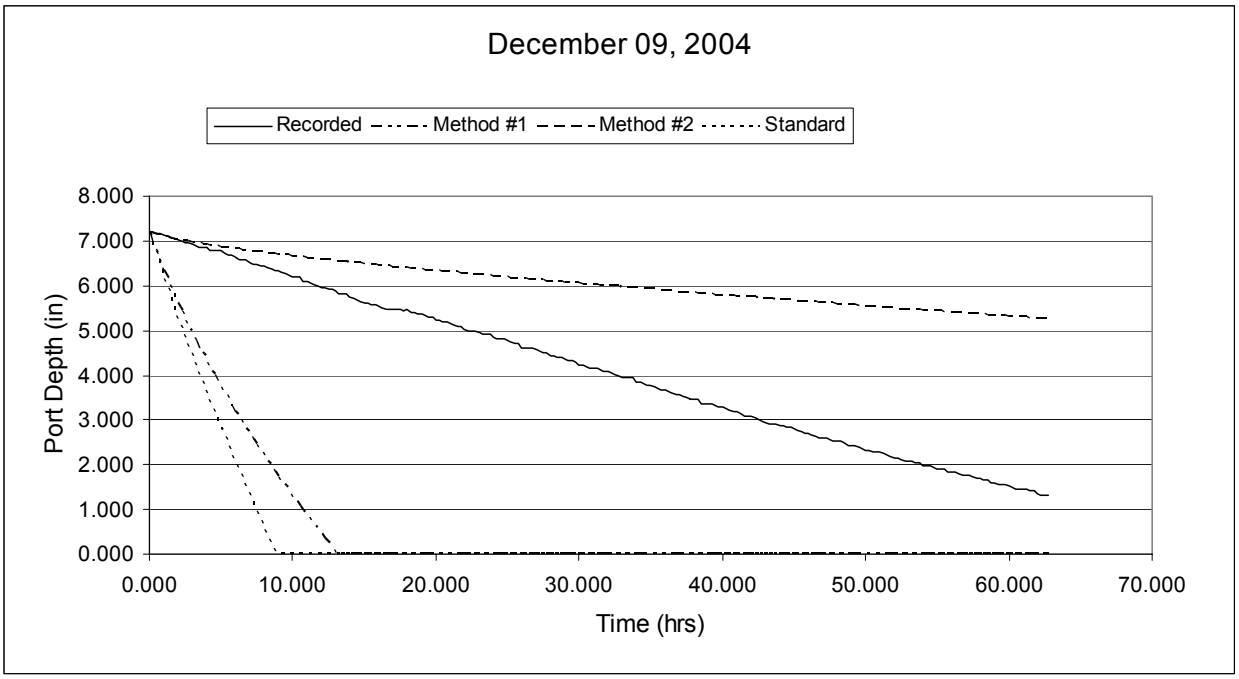
December 09, 2004
Recorded
Method #1
Method #2
Standard
Port Depth (in)
8.000
7.000
6.000
5.000
4.000
3.000
2.000
1.000
0.000
0.000
10.000
20.000
30.000
40.000
50.000
60.000
70.000
Time (hrs)

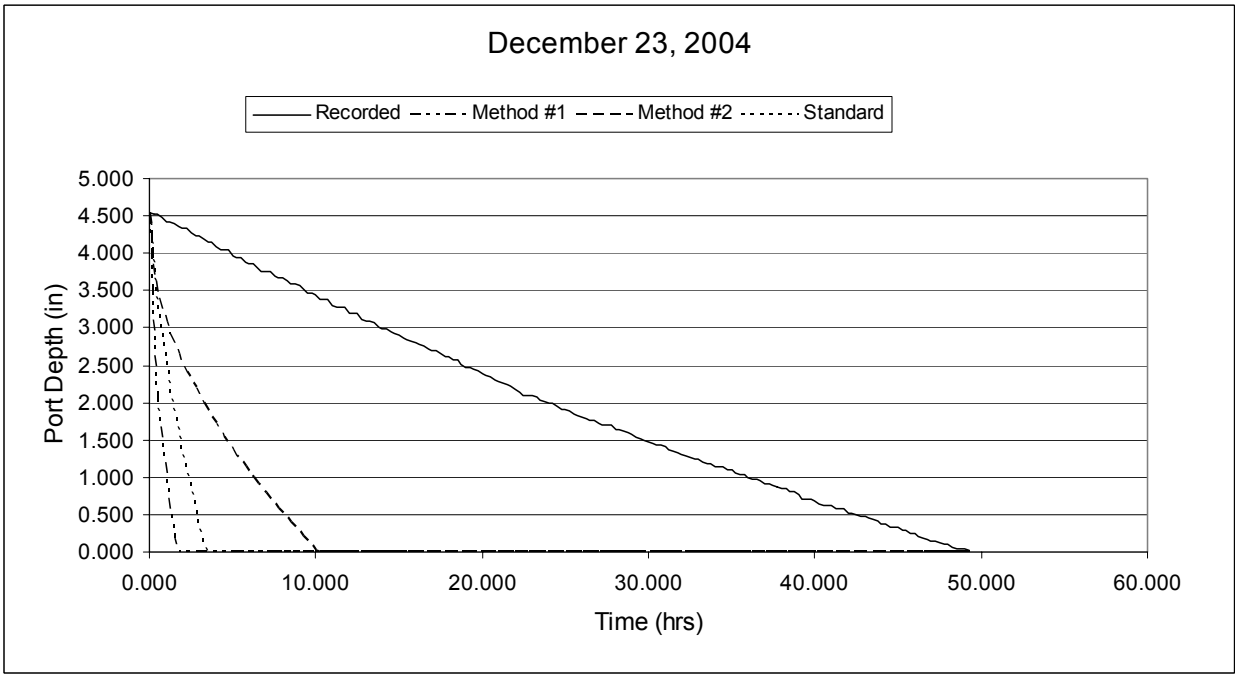
December 23, 2004
Recorded
Method #1
Method #2
Standard
Port Depth (in)
5.000
4.500
4.000
3.500
3.000
2.500
2.000
1.500
1.000
0.500
0.000
0.000
10.000
20.000
30.000
40.000
50.000
60.000
Time (hrs)

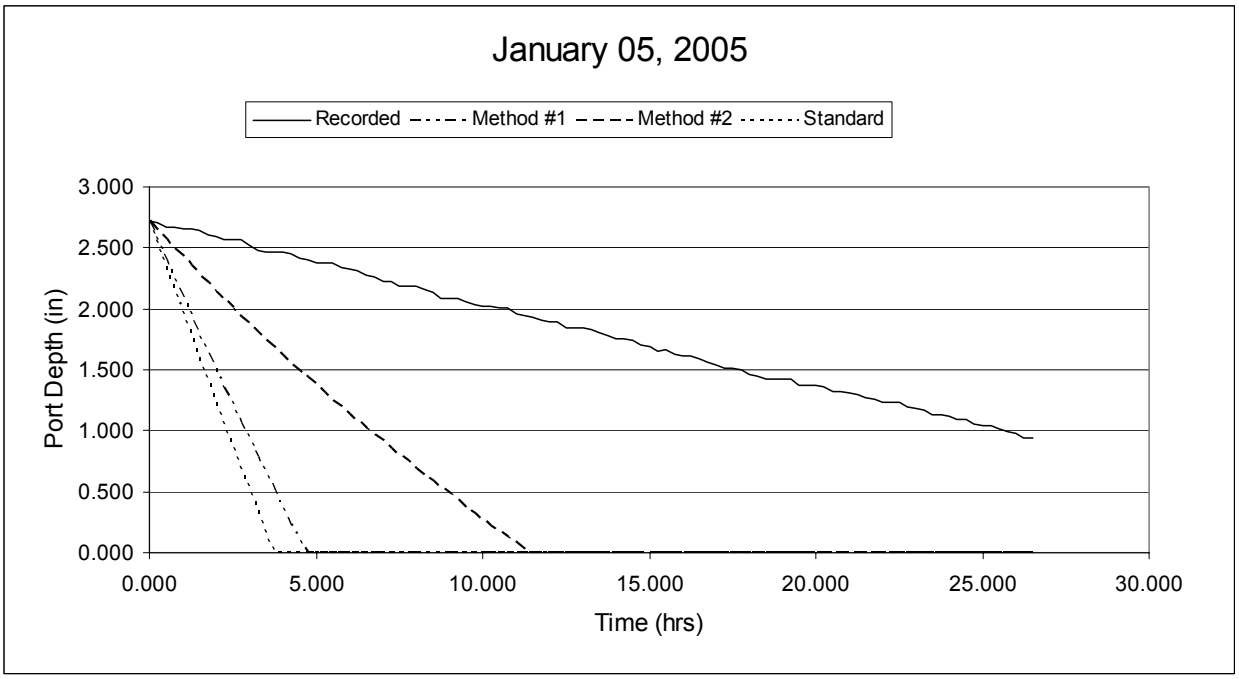
January 05, 2005
Recorded
Method #1
Method #2
Standard
Port Depth (in)
3.000
2.500
2.000
1.500
1.000
0.500
0.000
0.000
5.000
10.000
15.000
20.000
25.000
30.000
Time (hrs)

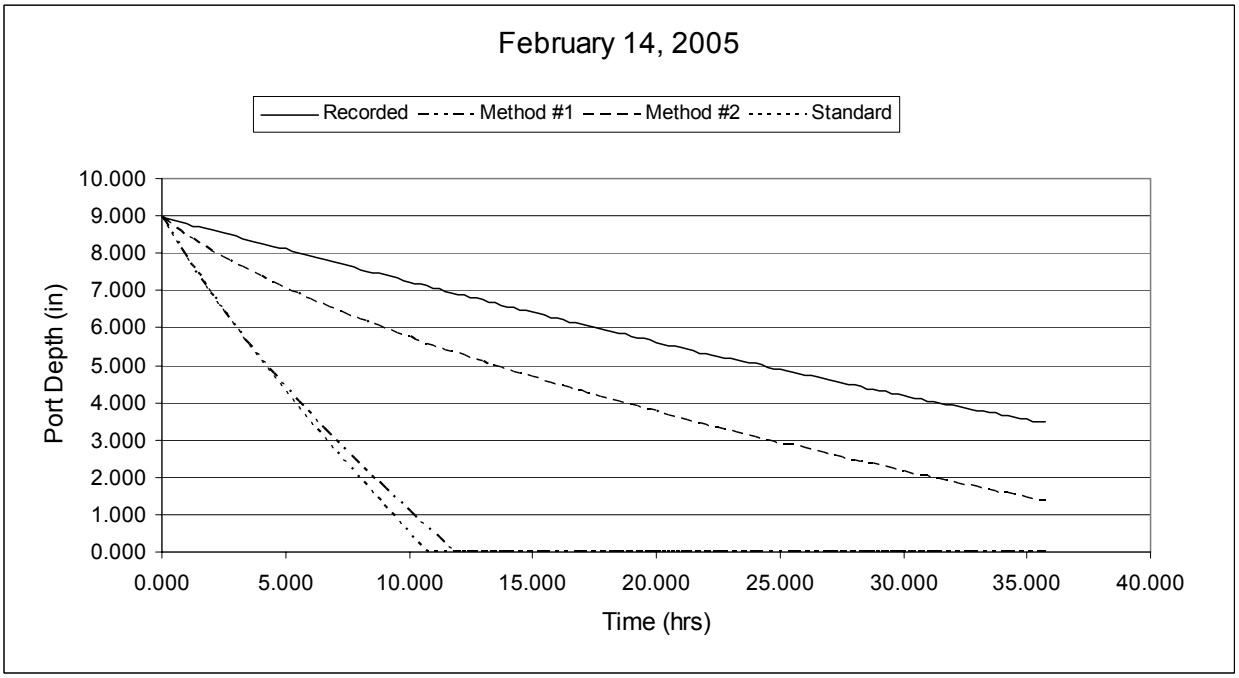
February 14, 2005
Recorded
Method #1
Method #2
Standard
Port Depth (in)
10.000
9.000
8.000
7.000
6.000
5.000
4.000
3.000
2.000
1.000
0.000
0.000
5.000
10.000
15.000
20.000
25.000
30.000
35.000
40.000
Time (hrs)

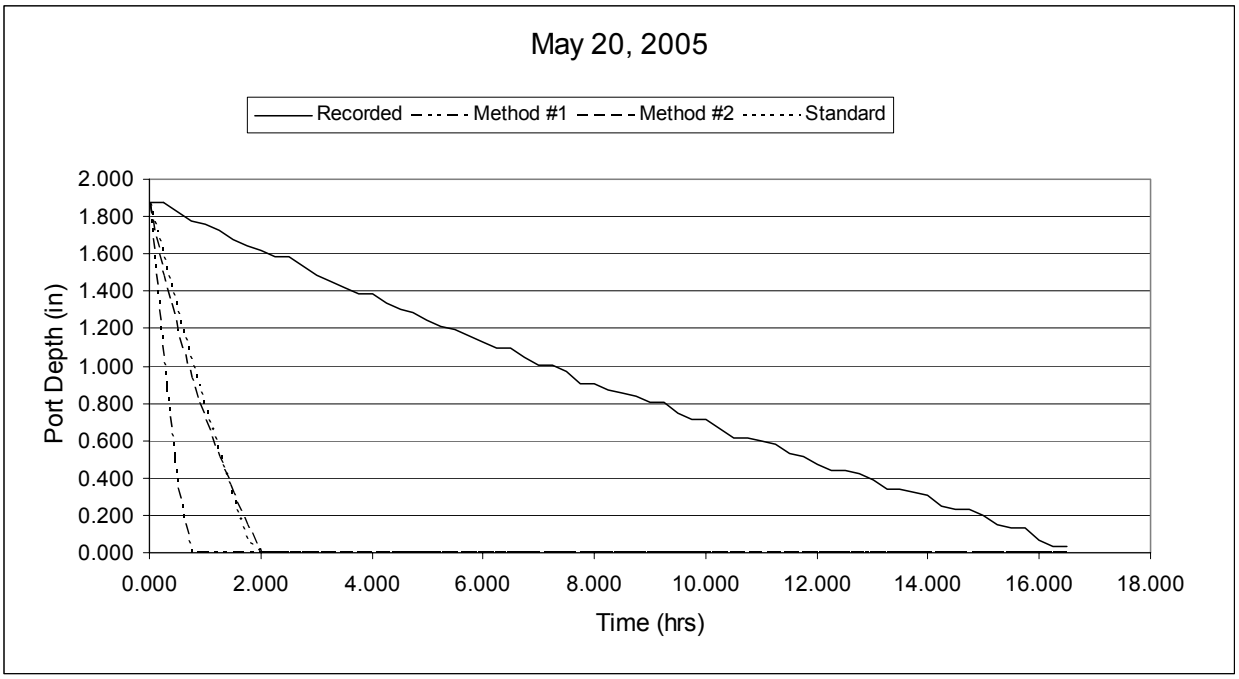
May 20, 2005
Recorded
Method #1
Method #2
Standard
Port Depth (in)
2.000
1.800
1.600
1.400
1.200
1.000
0.800
0.600
0.400
0.200
0.000
0.000
2.000
4.000
6.000
8.000
10.000
12.000
14.000
16.000
18.000
Time (hrs)

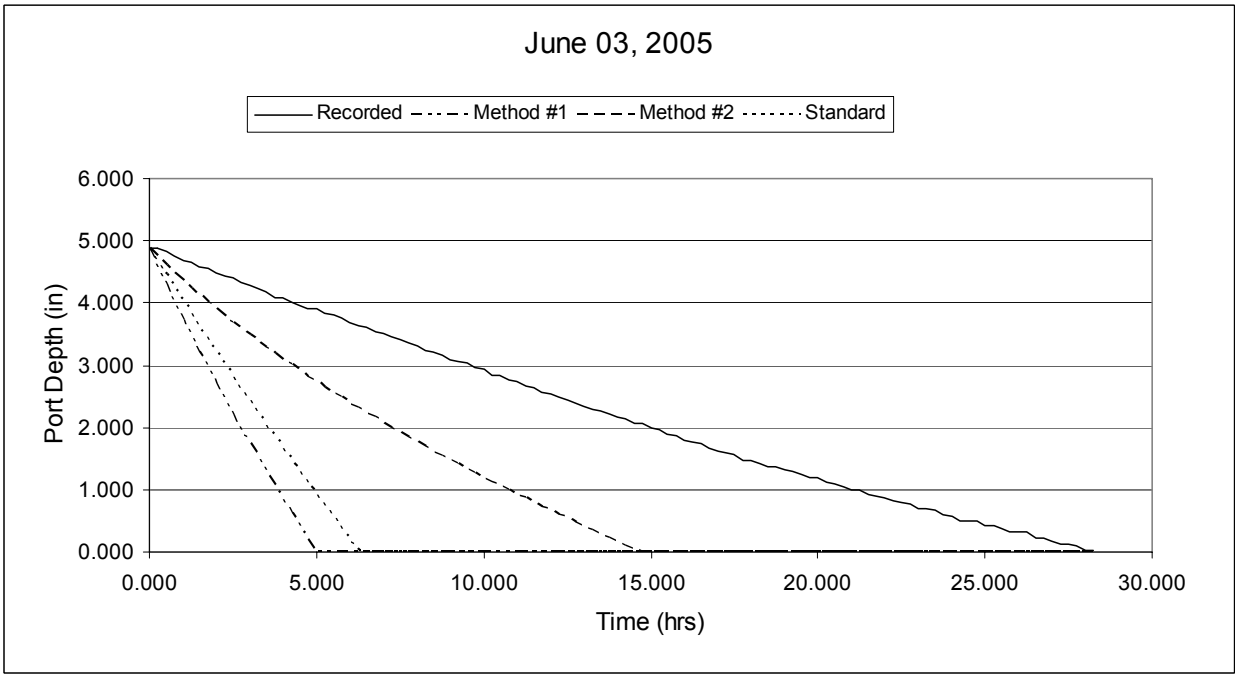
June 03, 2005
Recorded
Method #1
Method #2
Standard
Port Depth (in)
6.000
5.000
4.000
3.000
2.000
1.000
0.000
0.000
5.000
10.000
15.000
20.000
25.000
30.000
Time (hrs)

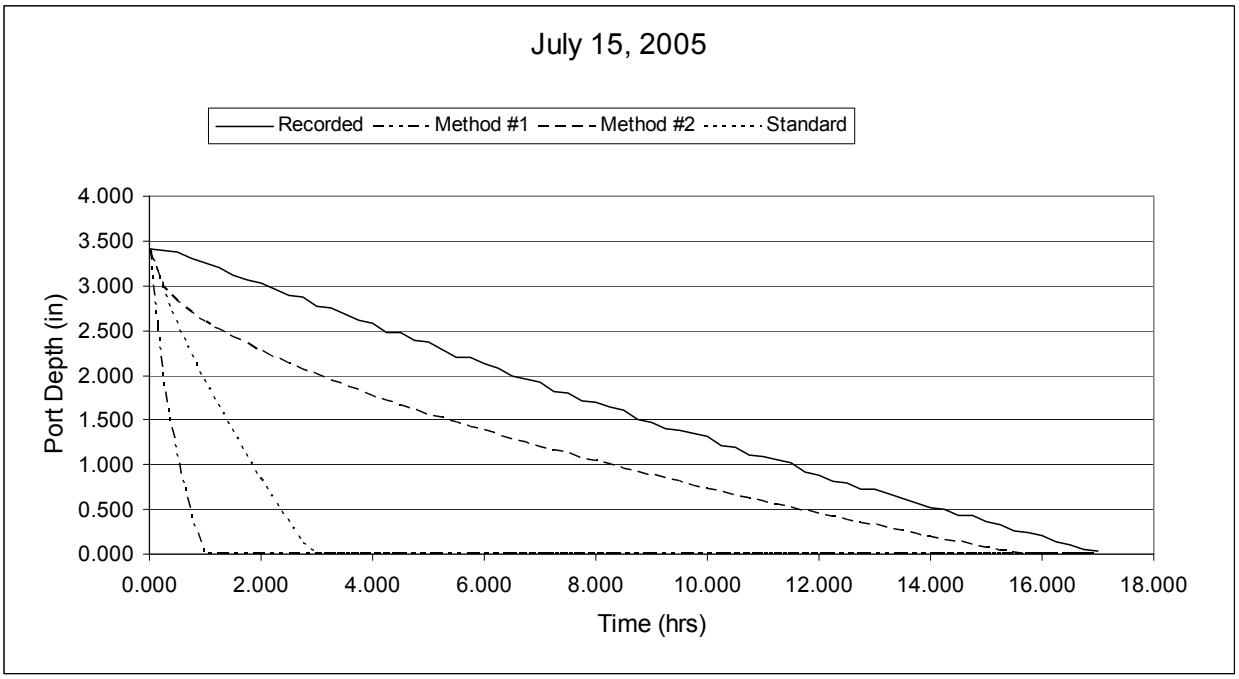
July 15, 2005
Recorded
Method #1
Method #2
Standard
Port Depth (in)
4.000
3.500
3.000
2.500
2.000
1.500
1.000
0.500
0.000
0.000
2.000
4.000
6.000
8.000
10.000
12.000
14.000
16.000
18.000
Time (hrs)

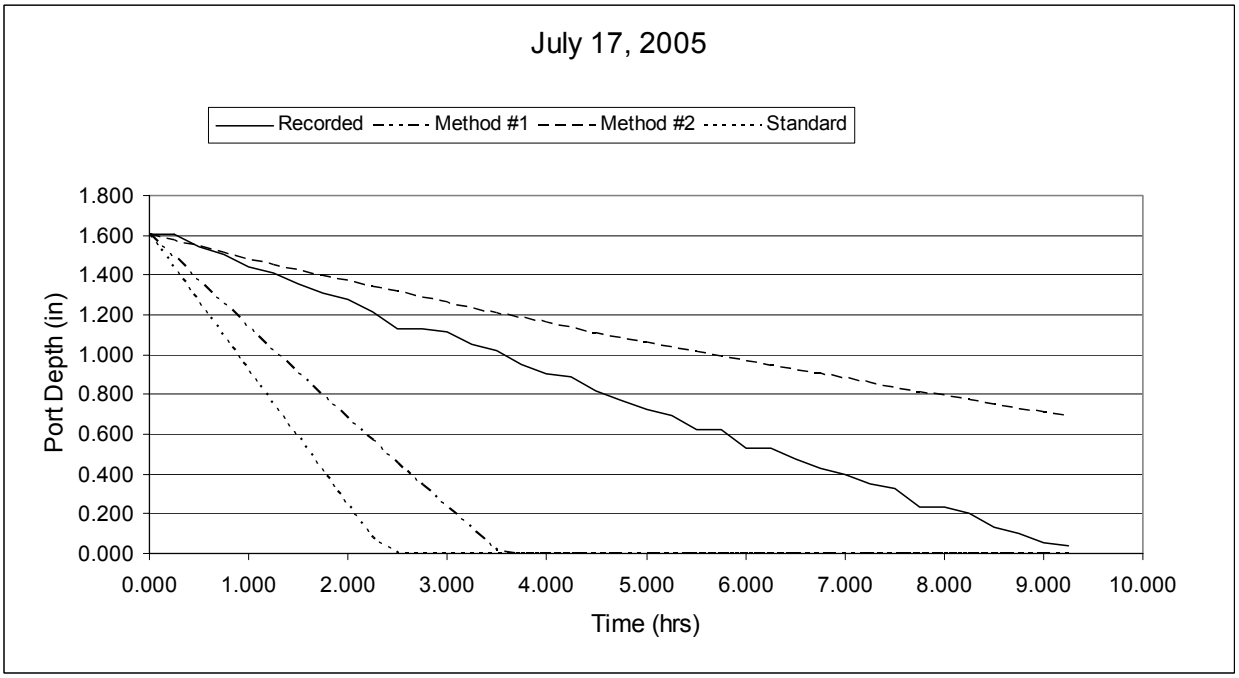
July 17, 2005
Recorded
Method #1
Method #2
Standard
Port Depth (in)
1.800
1.600
1.400
1.200
1.000
0.800
0.600
0.400
0.200
0.000
0.000
1.000
2.000
3.000
4.000
5.000
6.000
7.000
8.000
9.000
10.000
Time (hrs)

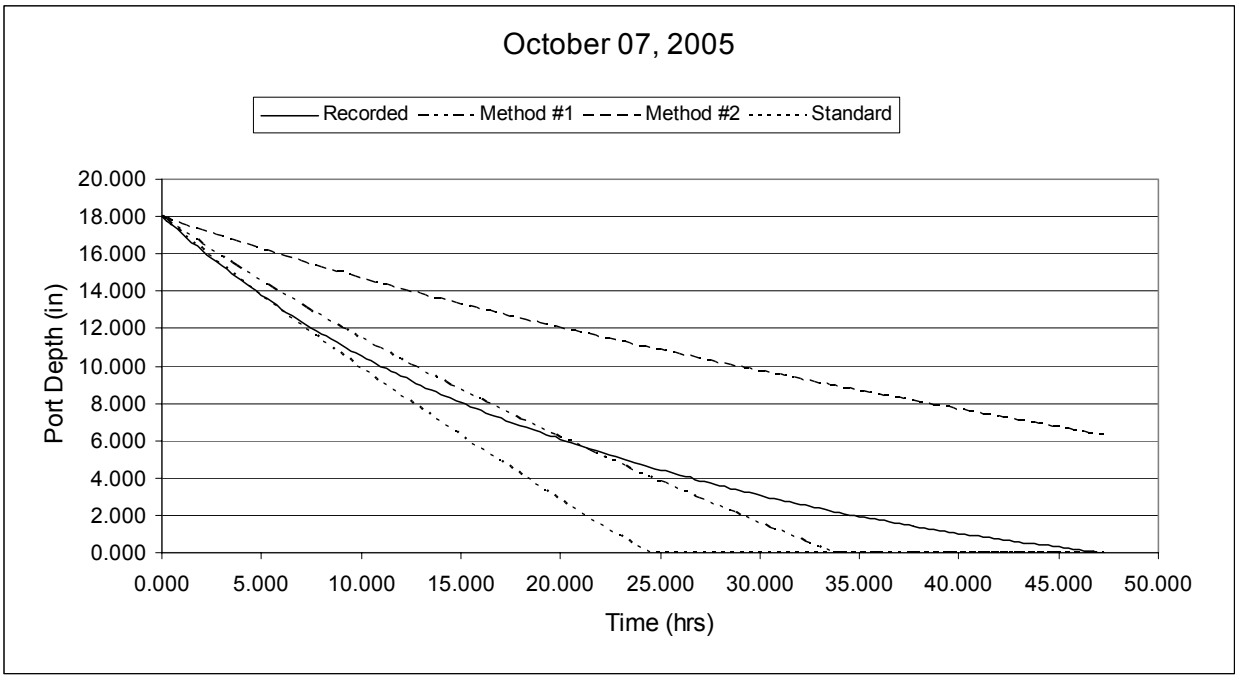
October 07, 2005
Recorded
Method #1
Method #2
Standard
Port Depth (in)
20.000
18.000
16.000
14.000
12.000
10.000
8.000
6.000
4.000
2.000
0.000
0.000
5.000
10.000
15.000
20.000
25.000
30.000
35.000
40.000
45.000
50.000
Time (hrs)

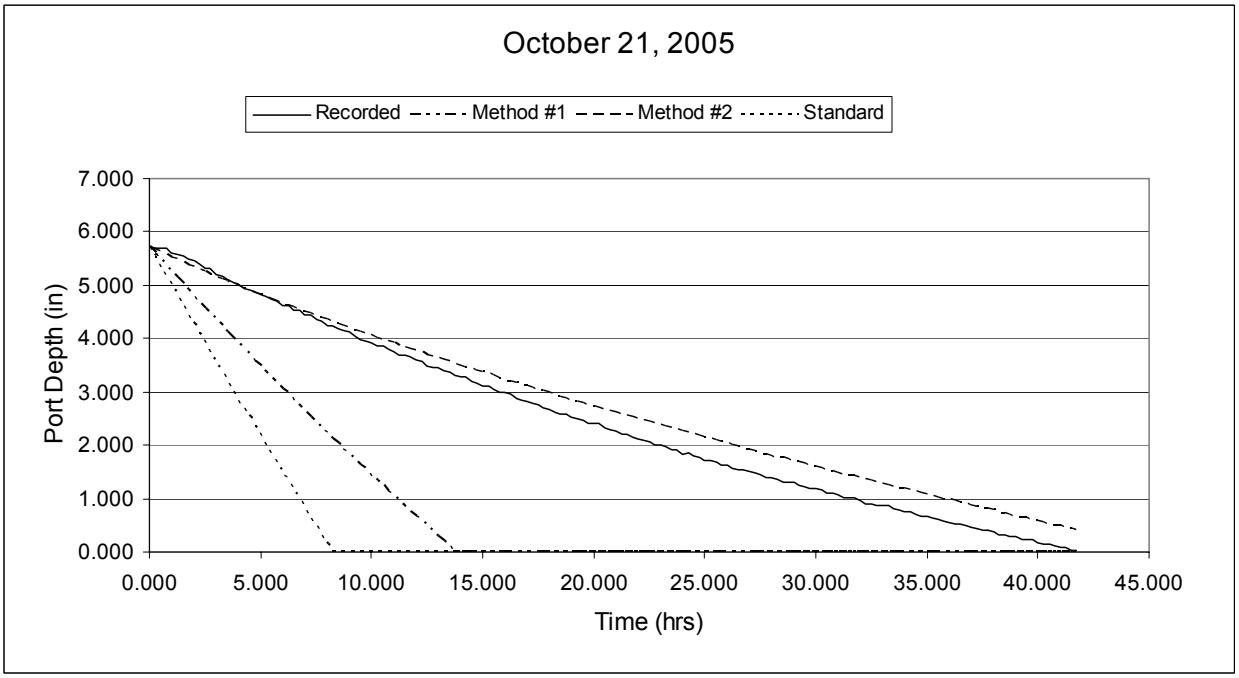
October 21, 2005
Recorded
Method #1
Method #2
Standard
Port Depth (in)
7.000
6.000
5.000
4.000
3.000
2.000
1.000
0.000
0.000
5.000
10.000
15.000
20.000
25.000
30.000
35.000
40.000
45.000
Time (hrs)

Appendix G

Sensitivity Analysis Results: Initial Wetting Front Depth

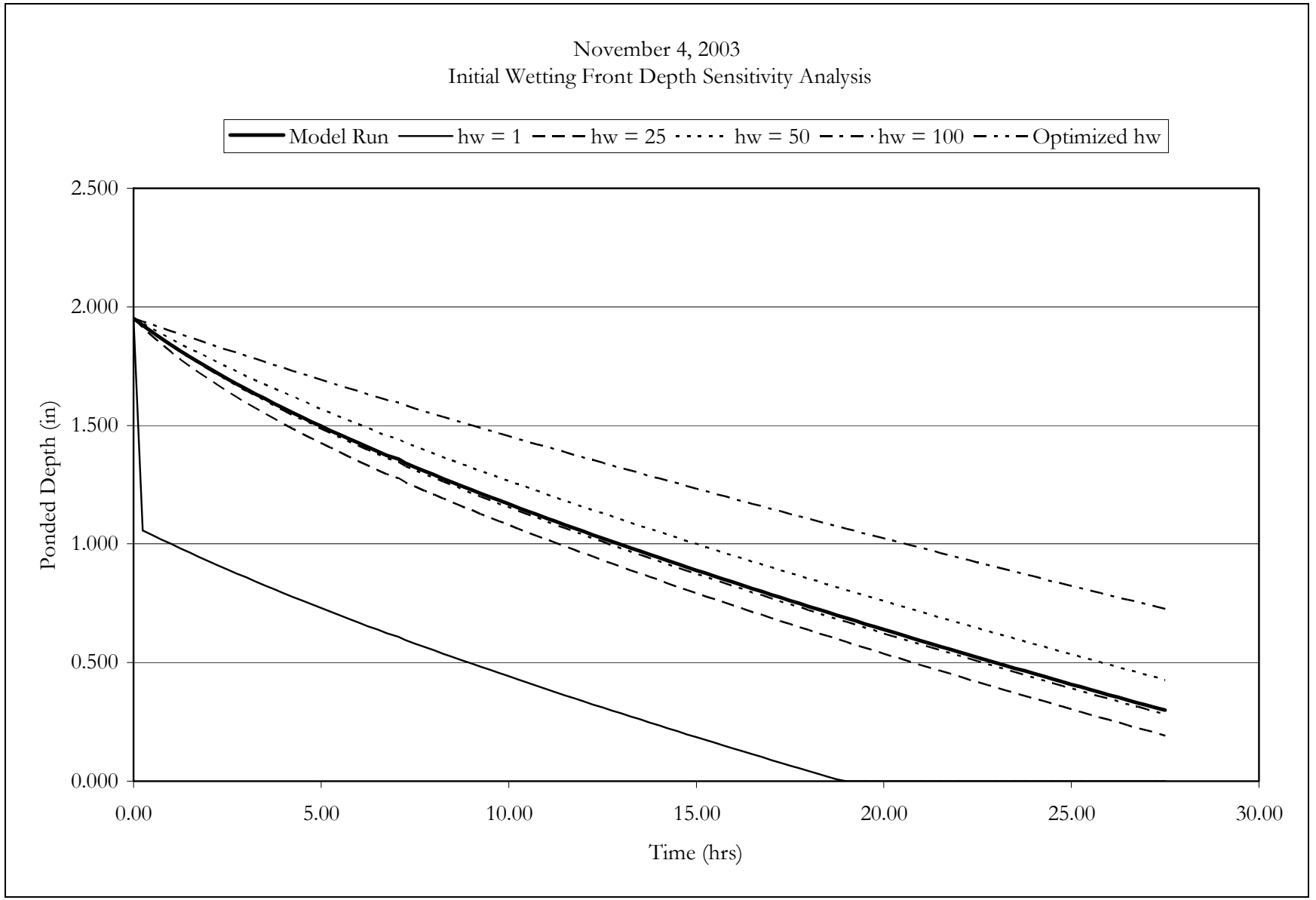
November 4, 2003
Initial Wetting Front Depth Sensitivity Analysis
Model Run
hw = 1
hw = 25
hw = 50
hw = 100
Optimized hw
2.500
2.000
1.500
1.000
0.500
0.000
Ponded Depth (in)
0.00
5.00
10.00
15.00
20.00
25.00
30.00
Time (hrs)

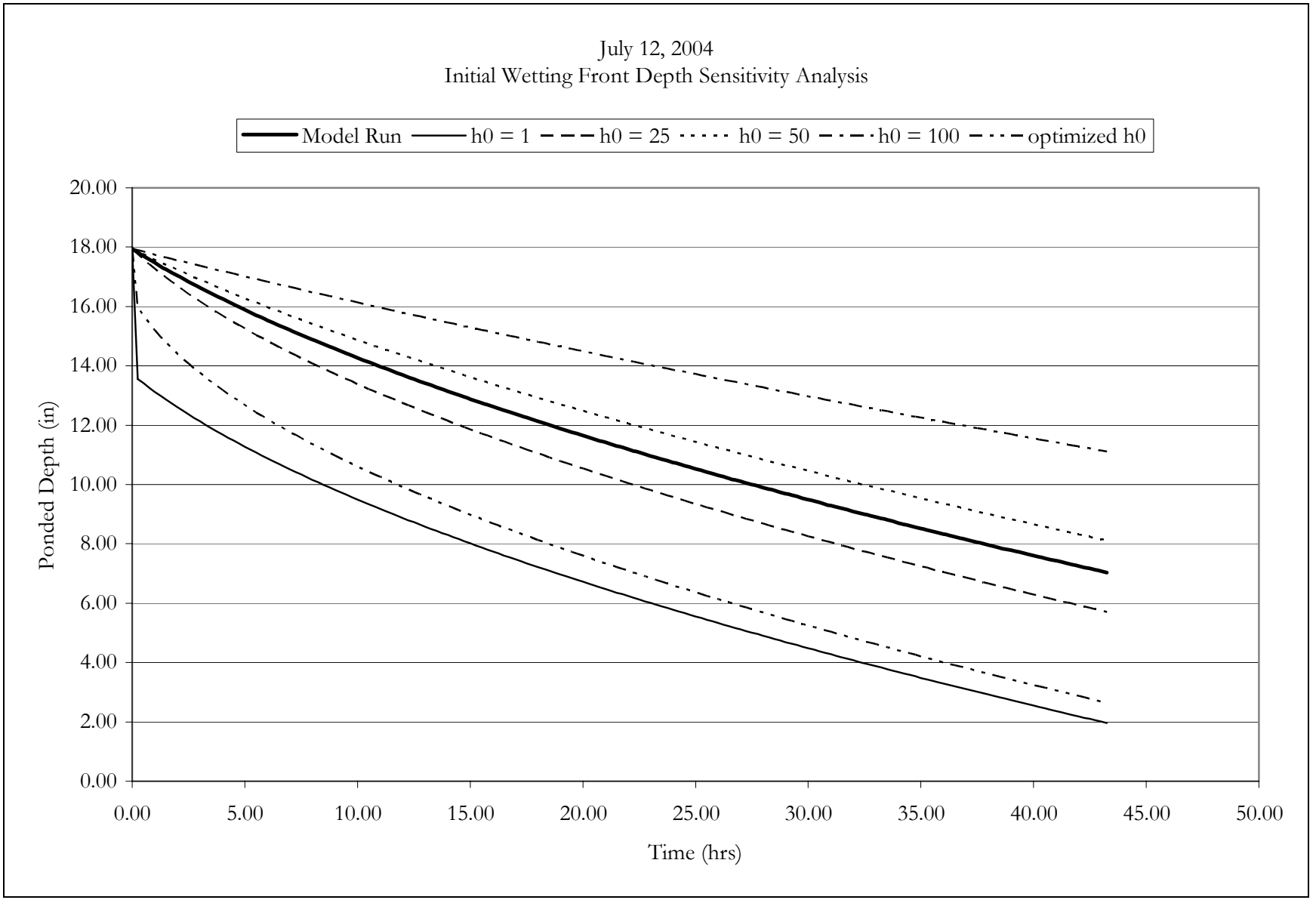
July 12, 2004
Initial Wetting Front Depth Sensitivity Analysis
Model Run
h0 = 1
h0 = 25
h0 = 50
h0 = 100
optimized h0
Ponded Depth (in)
20.00
18.00
16.00
14.00
12.00
10.00
8.00
6.00
4.00
2.00
0.00
0.00
5.00
10.00
15.00
20.00
25.00
30.00
35.00
40.00
45.00
50.00
Time (hrs)

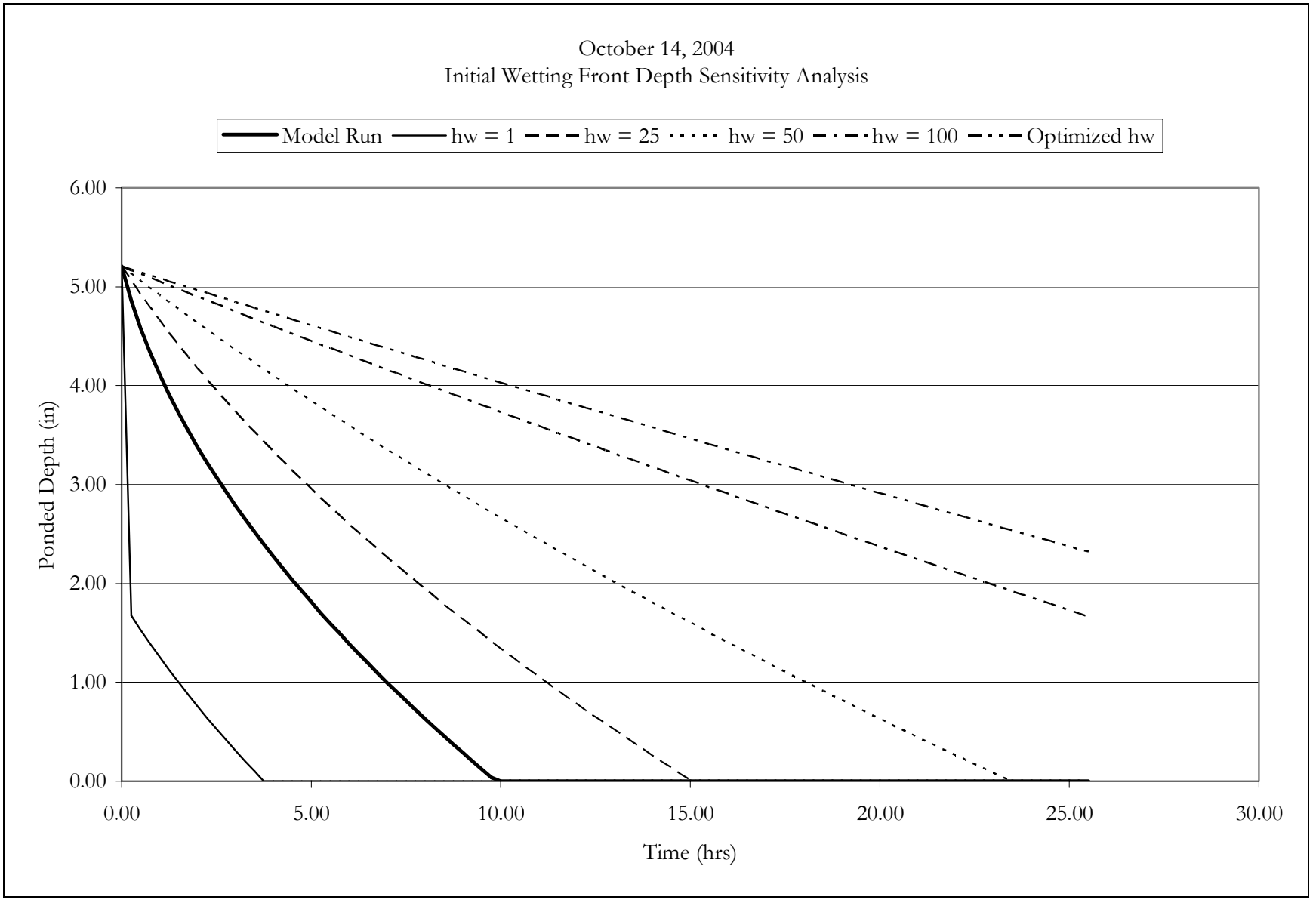
October 14, 2004
Initial Wetting Front Depth Sensitivity Analysis
Model Run
hw = 1
hw = 25
hw = 50
hw = 100
Optimized hw
Ponded Depth (in)
6.00
5.00
4.00
3.00
2.00
1.00
0.00
0.00
5.00
10.00
15.00
20.00
25.00
30.00
Time (hrs)

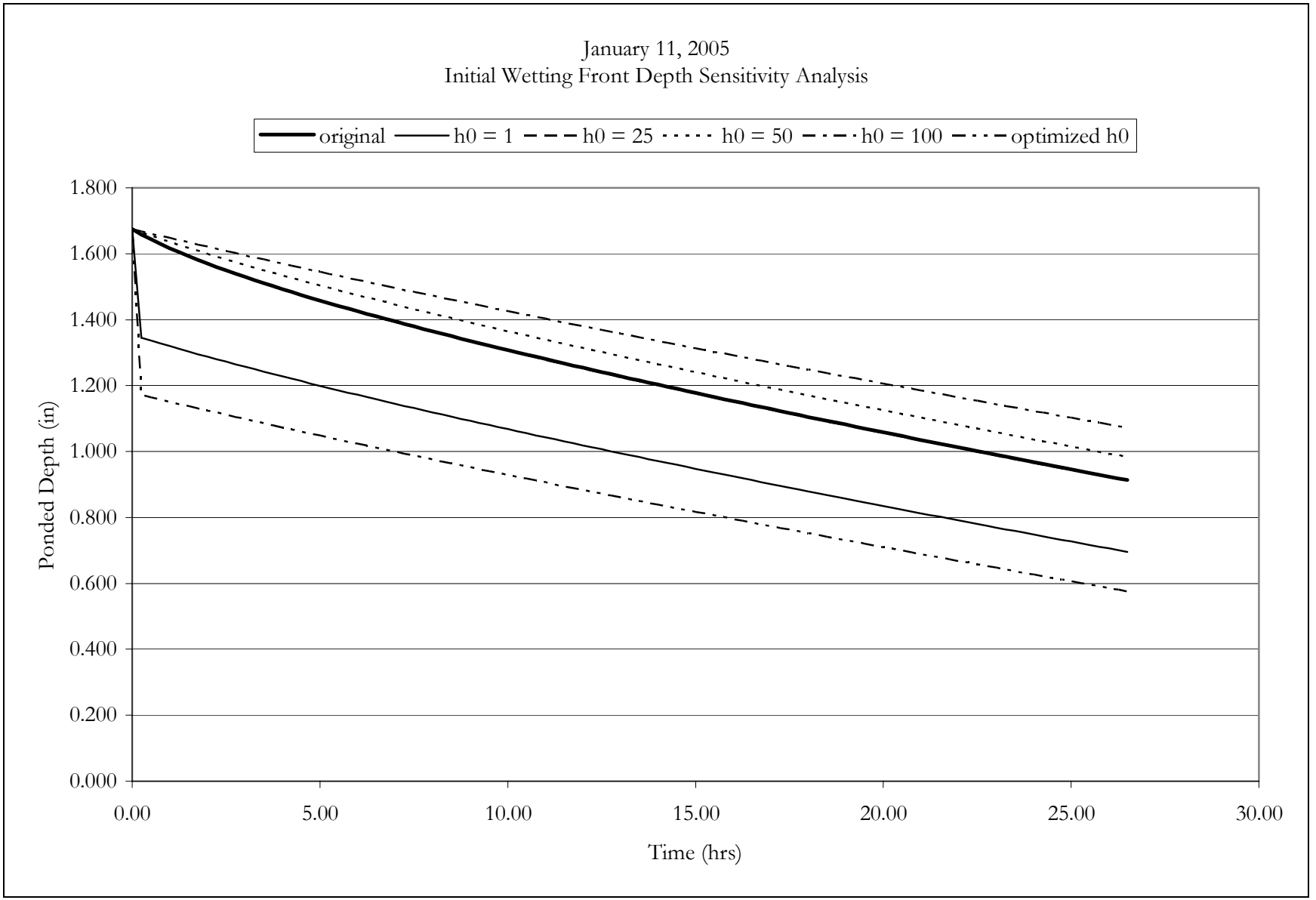
January 11, 2005
Initial Wetting Front Depth Sensitivity Analysis
original
h0 = 1
h0 = 25
h0 = 50
h0 = 100
optimized h0
Ponded Depth (in)
1.800
1.600
1.400
1.200
1.000
0.800
0.600
0.400
0.200
0.000
0.00
5.00
10.00
15.00
20.00
25.00
30.00
Time (hrs)

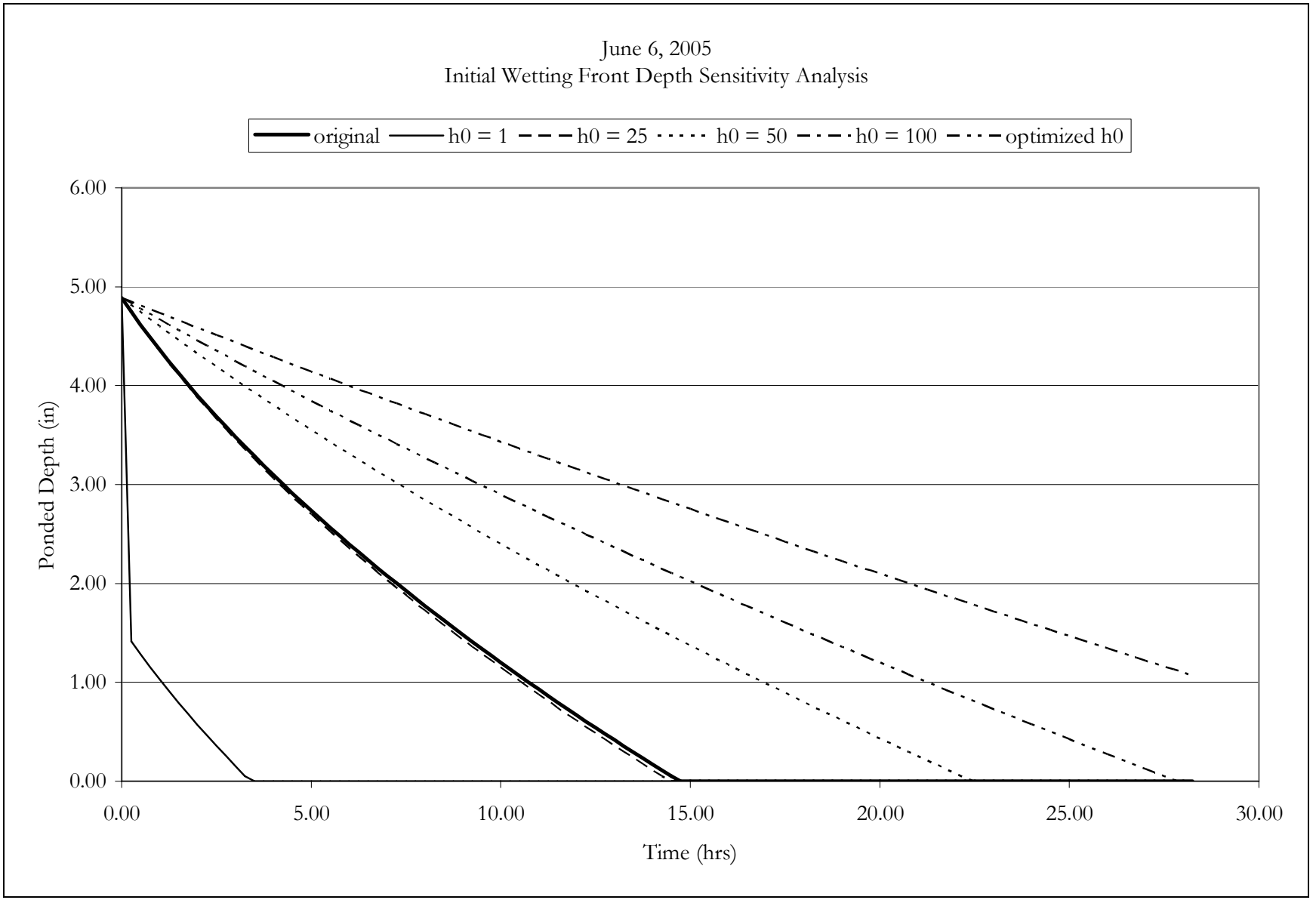
June 6, 2005
Initial Wetting Front Depth Sensitivity Analysis
original
h0 = 1
h0 = 25
h0 = 50
h0 = 100
optimized h0
Ponded Depth (in)
6.00
5.00
4.00
3.00
2.00
1.00
0.00
0.00
5.00
10.00
15.00
20.00
25.00
30.00
Time (hrs)

Appendix H

Sensitivity Analysis Results: Saturated Hydraulic Conductivity

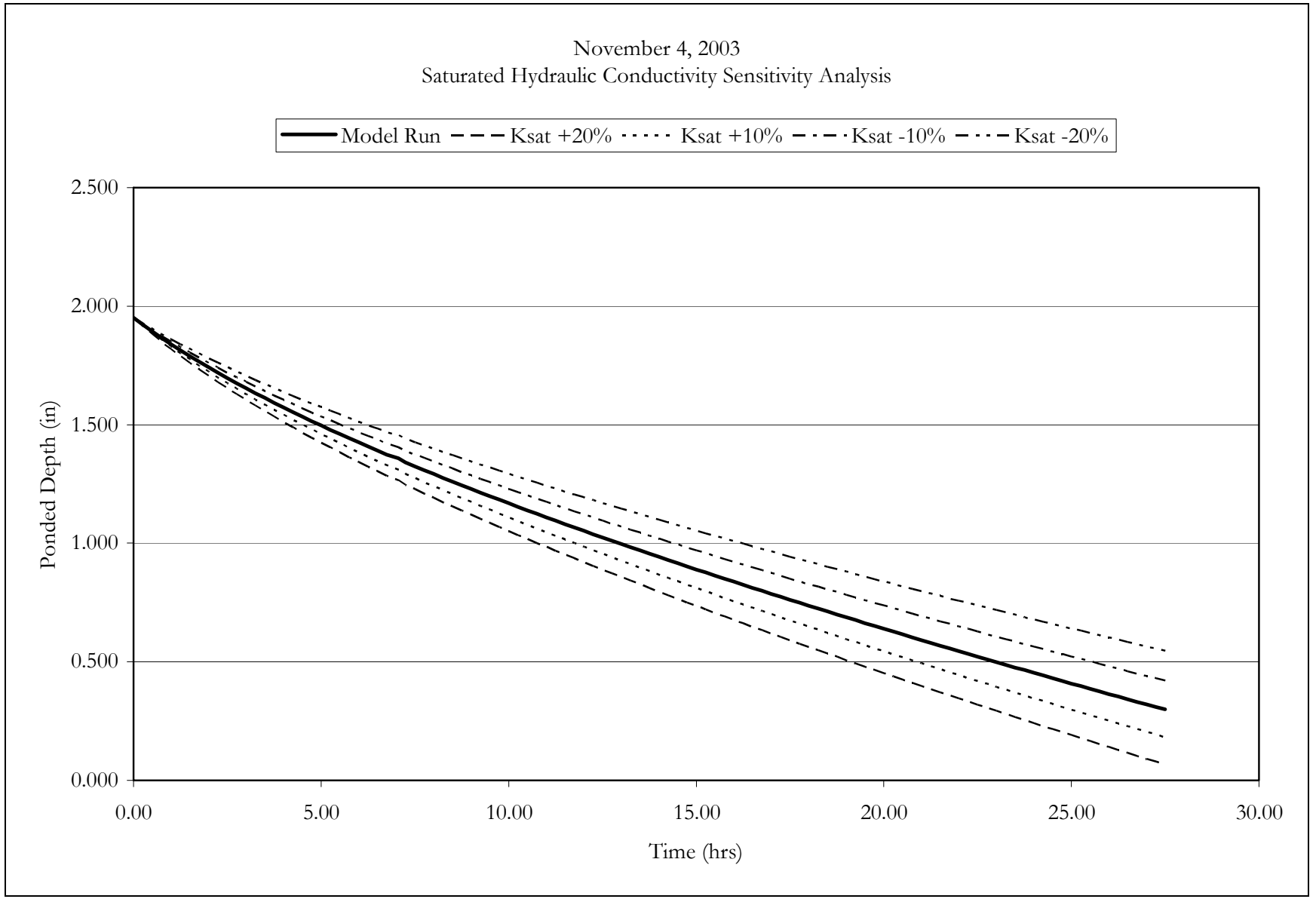
November 4, 2003
Saturated Hydraulic Conductivity Sensitivity Analysis
Model Run
Ksat +20%
Ksat +10%
Ksat -10%
Ksat -20%
Ponded Depth (in)
2.500
2.000
1.500
1.000
0.500
0.000
0.00
5.00
10.00
15.00
20.00
25.00
30.00
Time (hrs)

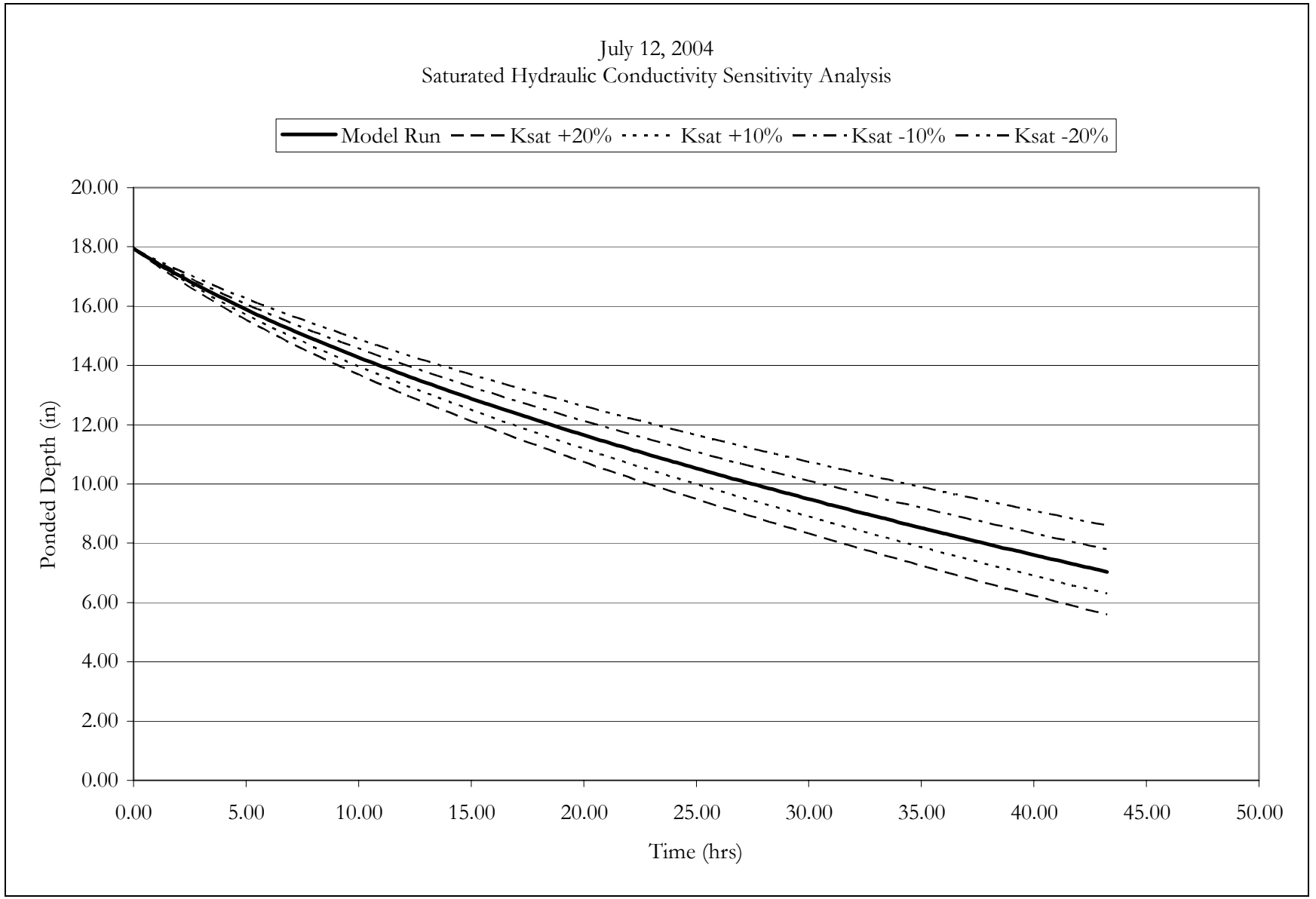
July 12, 2004
Saturated Hydraulic Conductivity Sensitivity Analysis
Model Run
Ksat +20%
Ksat +10%
Ksat -10%
Ksat -20%
Ponded Depth (in)
20.00
18.00
16.00
14.00
12.00
10.00
8.00
6.00
4.00
2.00
0.00
0.00
5.00
10.00
15.00
20.00
25.00
30.00
35.00
40.00
45.00
50.00
Time (hrs)

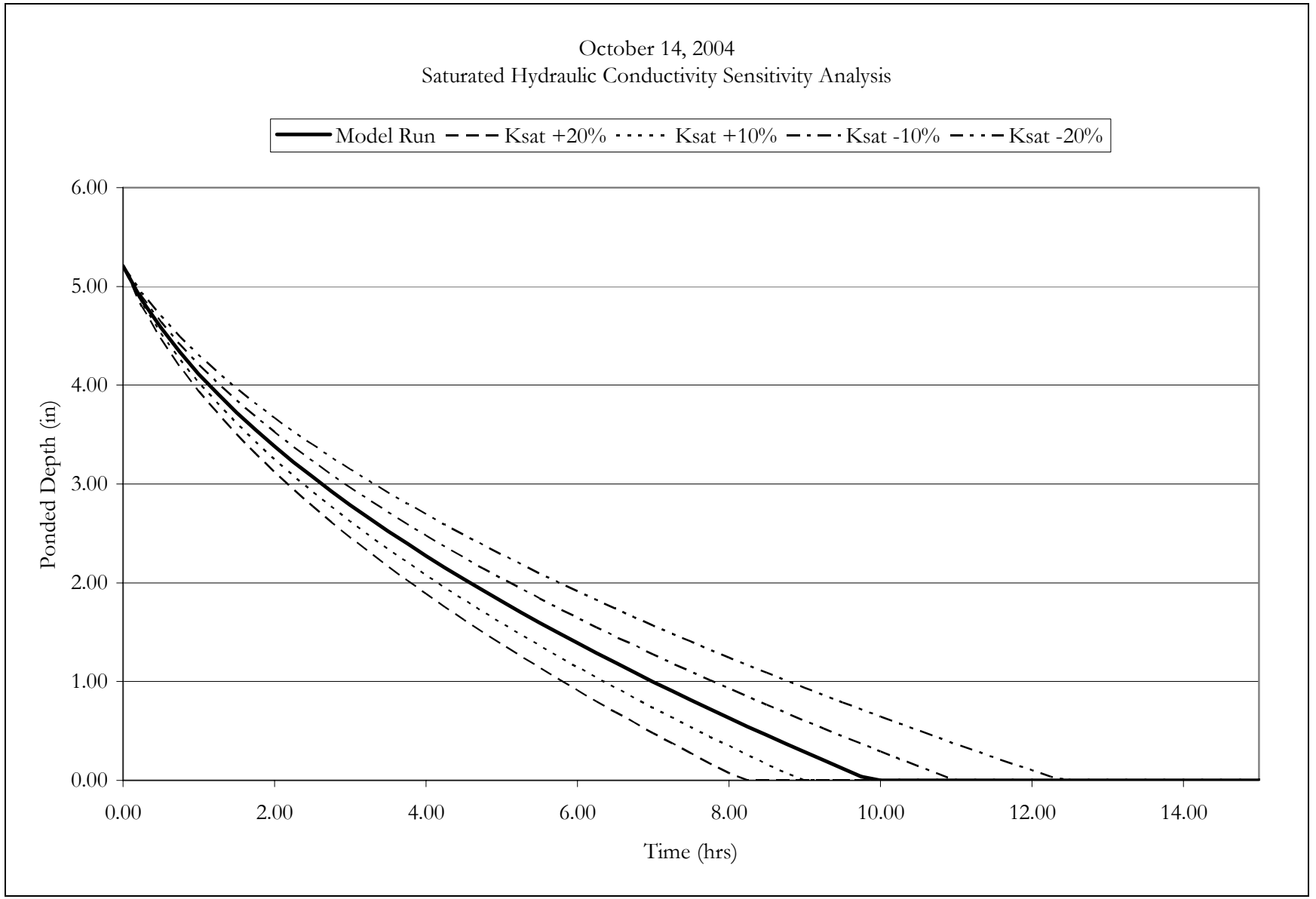
October 14, 2004
Saturated Hydraulic Conductivity Sensitivity Analysis
Model Run
Ksat +20%
Ksat +10%
Ksat -10%
Ksat -20%
Ponded Depth (in)
6.00
5.00
4.00
3.00
2.00
1.00
0.00
0.00
2.00
4.00
6.00
8.00
10.00
12.00
14.00
Time (hrs)

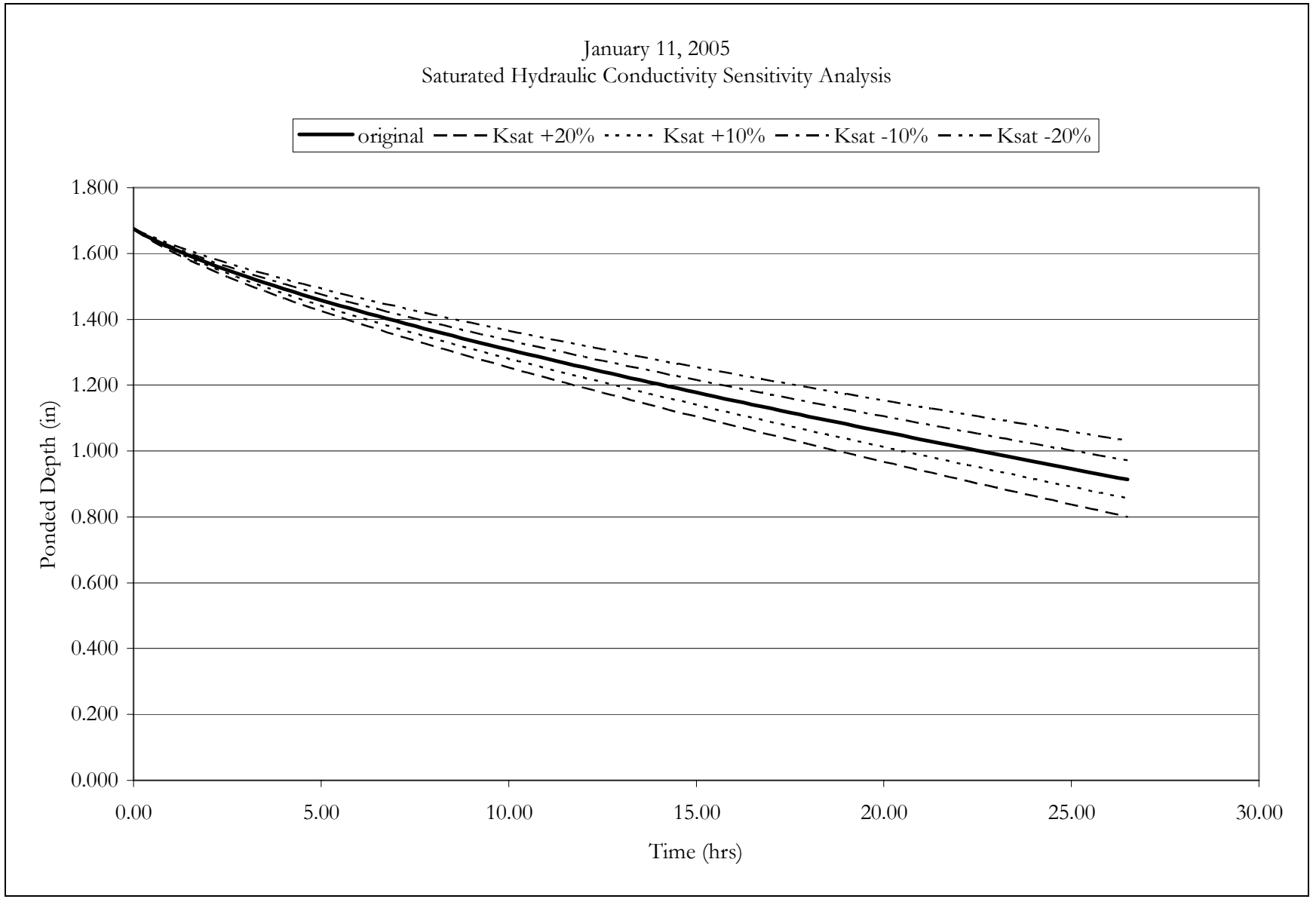
January 11, 2005
Saturated Hydraulic Conductivity Sensitivity Analysis
original
Ksat +20%
Ksat +10%
Ksat -10%
Ksat -20%
Ponded Depth (in)
1.800
1.600
1.400
1.200
1.000
0.800
0.600
0.400
0.200
0.000
0.00
5.00
10.00
15.00
20.00
25.00
30.00
Time (hrs)

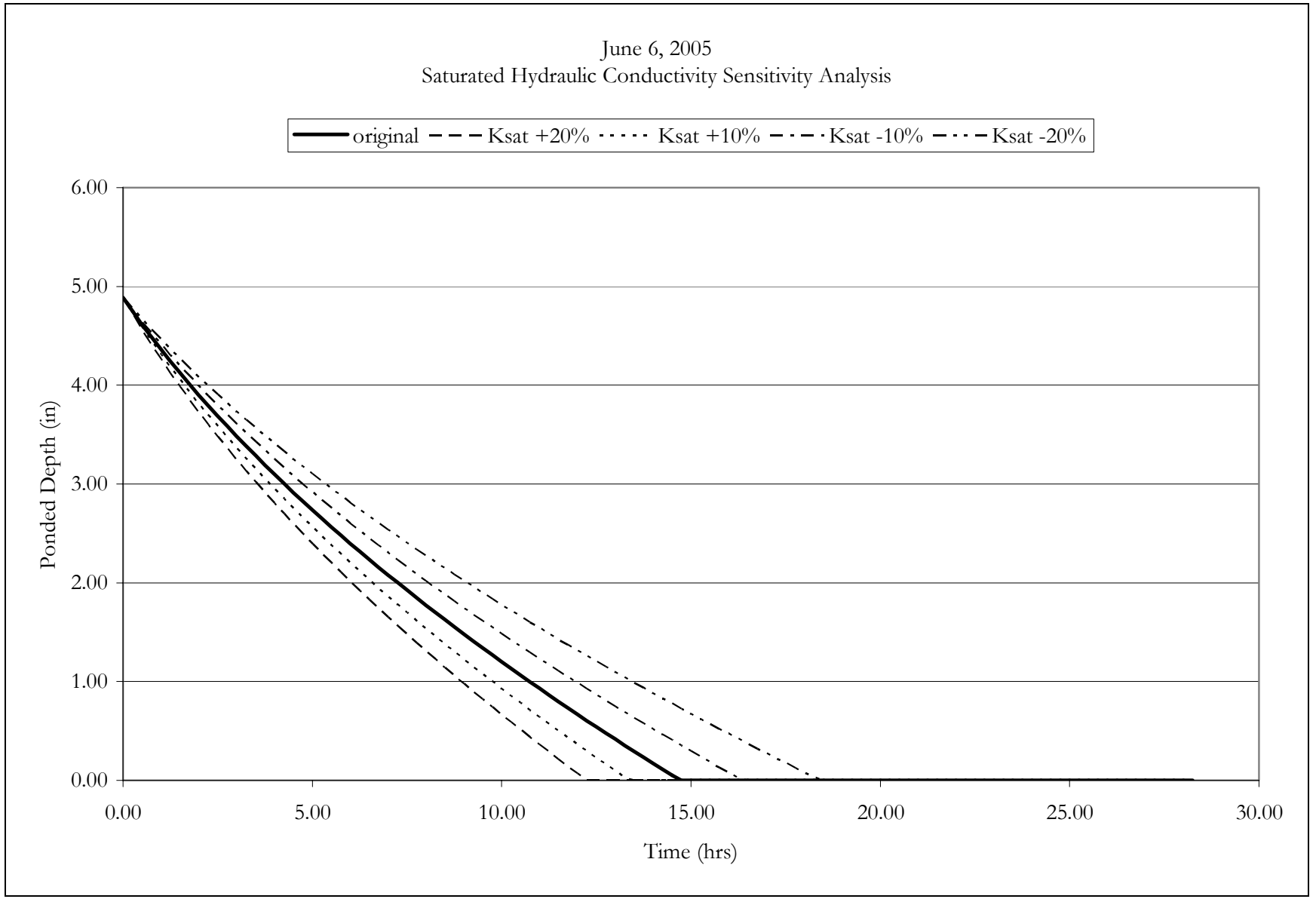
June 6, 2005
Saturated Hydraulic Conductivity Sensitivity Analysis
original
Ksat +20%
Ksat +10%
Ksat -10%
Ksat -20%
Ponded Depth (in)
6.00
5.00
4.00
3.00
2.00
1.00
0.00
0.00
5.00
10.00
15.00
20.00
25.00
30.00
Time (hrs)